

Distribution Agreement

In presenting this thesis or dissertation as a partial fulfillment of the requirements for an advanced degree from Emory University, I hereby grant to Emory University and its agents the non-exclusive license to archive, make accessible, and display my thesis or dissertation in whole or in part in all forms of media, now or hereafter known, including display on the world wide web. I understand that I may select some access restrictions as part of the online submission of this thesis or dissertation. I retain all ownership rights to the copyright of the thesis or dissertation. I also retain the right to use in future works (such as articles or books) all or part of this thesis or dissertation.

Signature:

Matthew Zimmerman

Date

Innate Immune Antagonism of Flavivirus Infection and the Impact of Preexisting
Flavivirus Antibody Responses on Secondary ZIKV Infection in the Human Placenta

By

Matthew G. Zimmerman
Doctor of Philosophy

Graduate Division of Biological and Biomedical Science
Microbiology and Molecular Genetics

Mehul S. Suthar
Advisor

Arash Grakoui
Committee Member

Jacob Kohlmeier
Committee Member

Paul Rota
Committee Member

Bernardo Mainou
Committee Member

Accepted:

Lisa A. Tedesco, Ph.D.
Dean of the James T. Laney School of Graduate Studies

Date

**Innate Immune Antagonism of Flavivirus Infection and the
Impact of Preexisting Flavivirus Antibody Responses
on Secondary ZIKV Infection in the Human Placenta**

By

Matthew G. Zimmerman
B.A., Colgate University, 2011

Advisor: Mehul S. Suthar, Ph.D.

An abstract of
A dissertation submitted to the Faculty of the
James T. Laney School of Graduate Studies of Emory University
in partial fulfillment of the requirements for the degree of
Doctor of Philosophy
in Graduate Division of Biological and Biomedical Science,
Microbiology and Molecular Genetics
2020

Abstract

Innate Immune Antagonism of Flavivirus Infection and the Impact of Preexisting Anti-Flavivirus Antibodies on Secondary ZIKV Infection in the Human Placenta

By Matthew G. Zimmerman

Humoral immunity is an essential component of the protective immune response to flavivirus infection however, the role of immunological cross-reactivity and the consequences to secondary flavivirus infection outcome remain controversial. Since its introduction to Brazil in 2015, Zika virus (ZIKV), has caused an epidemic of fetal congenital malformations within the Americas due to its unique ability to infect the human placenta and invade the fetal compartment. Because ZIKV is a mosquito-borne flavivirus with a high degree of sequence and structural homology to Dengue virus (DENV), the role of immunological cross-reactivity in ZIKV and DENV infections and its effects on vertical transmission of ZIKV from mother to child through the placenta has also been of great concern. In this dissertation, we demonstrate that viral immune complexes generated from cross-reactive DENV antibodies can enhance ZIKV infection in human placental macrophages, Hofbauer cells (HCs). We determined that this enhancement is IgG-subclass specific and likely results from increased Fc γ receptor-mediated binding and entry as well as dampening of antiviral immune responses in HCs. Using second trimester *ex vivo* human chorionic villous explants, we observed that ZIKV immune complexes can utilize the neonatal Fc receptor (FcRn)-mediated IgG transport system to traffic across the immunologically privileged syncytiotrophoblast layer of the placenta and target HCs within the villous core. Using both DENV- and ZIKV-immune sera, we also observed that ZIKV-specific IgM in early convalescent sera had a substantial impact on IgG-mediated transcytosis of ZIKV across the placental barrier. Finally, using a systems biology based approach, explored the ability of West Nile virus (WNV) and ZIKV to inhibit phosphorylation of STAT5, a previously undescribed target of viral antagonism, and downregulate STAT5-target genes downstream of RIG-I stimulation, type I interferon (IFN), and IL-4, but not GM-CSF, signaling in human monocyte-derived dendritic cells. We also found that blockade of STAT5 phosphorylation was specific to WNV and ZIKV, with no inhibition occurring during DENV1-4 or YFV-17D infection. Altogether, these findings implicate complex mechanisms of ZIKV entry into the placenta and innate immune antagonism that could greatly influence the development of flavivirus antivirals, vaccine design, and strategies for vaccine administration.

Acknowledgements

Mehul, for accepting me into your lab family, your steadfast support, our invigorating and enthusiasm for great science. Thank you for trusting me with the placental immunity arm of your lab and providing such amazing and multi-faceted PhD experience.

Past and present Suthar lab members, for lending a helpful hand, nurturing my growth in lab, and always providing a lasting camaraderie throughout the years

To my friends and Atlanta family, for providing much needed joy and respite in my life, for always lending your emotional support, and being absolute staples in my life.

To B.B., Dante, Tumbleweed, Mickey, and Bobo, for all the sloppy kisses, excited barks, loud meowing, sweet purring, and belly rubs that have brought me so much joy.

To my uncle, Kimball, for your everlasting love and memories. I miss you dearly.

To my dad, Eddie, for your love and instilling me with a good sense of humor essential for getting through tough times.

To my stepfather, Bud, for introducing me to the exciting world of medicine, but, most importantly, for your unfaltering support and love.

To my mom, Cyndi, for the late-night childhood conversations on “the worst diseases ever,” for believing in me even when my path was not so clear, and for being the most dedicated and loving mother I could ask for.

To my fiancé, Drew, for your unwavering love, for staying by my side through the laughter and the tears, for keeping me grounded, and sharing your life with me. In this incredible adventure of my life, you are my greatest treasure.

Table of Contents

Chapter 1: Introduction	12
Introduction to Pathogenic Flaviviruses	13
Innate Immune Responses against Flavivirus Infection	16
Human Antibody Responses to DENV and ZIKV	19
Cross-reactive antibody responses between DENV and ZIKV: Protective vs. Pathogenic	23
DENV and ZIKV disease severity in flavivirus-naïve individuals	26
Cross reactive antibodies in animal models of systemic ZIKV ADE	27
Introduction to the human placenta	28
Hofbauer Cells: Key Regulators within the Placenta	30
Innate Immunity at the Placental Barrier	32
Passing the TORCH: Mechanisms of ZIKV Entry into the Placenta	33
ZIKV Infection of the Human Placenta	34
Chapter 2: Cross-reactive dengue virus antibodies augment Zika virus infection of human placental macrophages	40
Introduction	41
Results	44
Discussion	53
Materials and Methods	77
Chapter 3: Anti-Zika virus IgM Inhibits Translocation and Enhancement of Zika virus Infection within the Human Placenta	87
Introduction	88
Results	93
Discussion	96
Materials and Methods	107
Chapter 4: STAT5: A Target of Antagonism by Neurotropic Flaviviruses	111
Introduction	112
Results	115
Discussion	122
Materials and Methods	135

Chapter 5: Discussion	140
Summary of WNV and ZIKV antagonism of STAT5 findings	141
Viral factors affecting STAT5 activation.....	142
Potential STAT5 Antagonism in other Target Tissues	143
Summary of Placental ZIKV Infection Findings.....	145
New Paradigm: Viral transcytosis using the placental FcRn pathway?.....	146
The Reciprocity of Immune Enhancement between ZIKV and DENV	149
Vertical Transmission of other Flaviviruses	151
The Many Flavors of ZIKV Vaccines	154
Monoclonal Antibodies as Therapeutics and Vaccine Adjuvants	156
The Spread of ZIKV and Potential for Reemergence	158
Concluding Thoughts and Questions	161
 Works Cited	 163

List of Figures and Tables

Chapter 1: Introduction	12
Figure 1-1: Sites of viral tropism during ZIKV infection	36
Figure 1-2: Differences in barrier structure and antibody translocation between human and mouse placentae.....	38
Chapter 2: Cross-reactive dengue virus antibodies augment Zika virus infection of human placental macrophages	40
Figure 2-1: Cross-reactive DENV monoclonal antibodies (mAbs) enhance ZIKV infection of human placental macrophages	58
Figure 2-2: Infection with ZIKV in the presence of mAb 33.3A06 results in increased viral binding and entry of HCs	60
Figure 2-3: HCs infected with DENV mAb:ZIKV immune complexes result in blunted type I and type III IFN antiviral responses	61
Figure 2-4: Type I IFN, but not type III IFN, restricts ZIKV infection of HCs	63
Figure 2-5: Enhanced ZIKV infection of HCs is modulated in an IgG subclass-dependent manner	64
Figure 2-6: IgG1 and IgG3 subclasses preferentially enhance ZIKV infection of human placental explants	65
Figure 2-7: Targeting FcRn reduces ZIKV infection of human placental explants.....	67
Supplemental Figure 2-1: HCs are modestly activated upon infection with DENV mAb:ZIKV immune complexes	68
Supplemental Figure 2-2: DENV mAb:ZIKV immune complexes enter HCs through an endosomal pathway	70
Supplemental Figure 2-3: HCs infected with DENV mAb:ZIKV immune complexes fail to secrete pro-inflammatory cytokines.....	71
Supplemental Figure 2-4: Cross-reactive DENV monoclonal antibodies enhance ZIKV infection of human placental explants	72
Supplemental Figure 2-5: FcRn facilitates enhanced infection of human placental explants	73
Supplemental Table 2-1: Cytokine levels in the supernatants of non-ADE and ADE-ZIKV infected HCs at 24 hpi.....	75
Supplemental Table 2-2: ZIKV specific primers and probes for strand-specific qPCR	76
Chapter 3: Anti-Zika virus IgM Inhibits Translocation and Enhancement of Zika virus Infection within the Human Placenta	87
Figure 3-1: Primary DENV3, primary ZIKV, and secondary ZIKV immune sera enhance ZIKV infection in human chorionic villous explants.....	102
Figure 3-2: Early convalescent ZIKV sera, but not DENV3 sera, inhibit ADE of ZIKV infection in human chorionic villous explants.....	103

Figure 3-3: IgM-depleted early convalescent ZIKV sera enhances ZIKV infection in chorionic villous explants	105
Chapter 4: STAT5: A Target of Antagonism by Neurotropic Flaviviruses	111
Figure 4-1: Systems biology reveals STAT5 as a regulatory node of antiviral DC responses	127
Figure 4-2: WNV actively blocks STAT5 phosphorylation and expression of STAT5 target genes.....	129
Figure 4-3: WNV and ZIKV inhibit STAT5 phosphorylation in a pathway-dependent manner	131
Figure 4-4: WNV and ZIKV antagonize STAT5 phosphorylation in the absence of IFN signaling.....	132
Figure 4-5: DENV1-4 and YFV-17D do not antagonize STAT5 phosphorylation at similar infection levels as WNV	133
Figure 4-6: ZIKV, but not WNV, blocks TYK2 or JAK1 activation to compromise STAT5 phosphorylation	134

Chapter 1: Introduction

*Contains content originally published as a review in *Cell Host and Microbe*: Zimmerman MG, Wrammert J, Suthar MS. Cross-Reactive Antibodies during Zika Virus Infection: Protection, Pathogenesis, and Placental Seeding. *Cell Host Microbe*. 2020;27(1):14–24.

It has been modified in part for this dissertation.

Introduction to Pathogenic Flaviviruses

The *Flaviviridae* family of positive-sense RNA viruses comprises a diverse group of arthropod-borne viruses, including dengue virus (DENV), West Nile virus (WNV), Japanese encephalitis virus (JEV), and Zika virus (ZIKV), and yellow fever virus (YFV), and tick-borne encephalitis virus (TBEV), which are responsible for a wide variety of severe clinical diseases in humans. Upon infection, the ~11kb flavivirus positive-sense RNA genome is directly translated into a single polyprotein and post-translationally cleaved by viral and host proteases to generate three structural proteins, capsid (C), pre-membrane/membrane (prM/M), and envelope (E) and seven nonstructural proteins, NS1, NS2a, NS2b, NS3, NS4a, NS4b, and NS5. The non-structural proteins function as the replication complex to synthesize viral RNA as well as perform auxiliary functions to antagonize host innate immune signaling pathways. The structural genes comprise the viral particle, of which E and prM proteins allow for attachment to cellular receptors, facilitating viral fusion and entry into the host cell.

WNV, a member of the JEV serocomplex of flaviviruses, has become endemic to North America and remains the leading cause of arthropod-borne viral encephalitis. Since its introduction to New York in 1999, WNV has infected over 3 million people, causing severe neurologic disease in over 13,000 (Petersen et al., 2013). WNV is maintained in nature through a sylvatic cycle between its primary arthropod vector, the *Culex spp.* mosquitos, and avian hosts. Due to lower viral loads and the transient viremic state during WNV infection, mammals, including humans, serve as dead-end hosts to WNV (Suthar et al., 2013). Infection with WNV is primarily asymptomatic with 20-40% of patients exhibiting flu-like symptoms including fever, malaise, myalgias, skin rash, lymphadenopathy, and diarrhea. Approximately 1% of WNV-infected patients will develop WNV neuroinvasive disease, a potentially fatal combination of syndromes characterized by meningitis,

encephalitis, and/or acute flaccid paralysis (Kramer et al., 2007). Physical sequelae, including neurologic muscle weakness, fatigue, and myalgia, in addition to cognitive and psychological sequelae, including depression, memory loss, and difficulty concentrating, have been shown to persist for up to 8 years after viral clearance of WNV neuroinvasive disease (Patel et al., 2015). Outside of supportive care, no vaccines or treatments exist for humans infected with WNV.

DENV is a self-limiting, acute viral infection responsible for approximately 50-100 million apparent and 300 million inapparent infections per year. DENV exists as four genetically distinct serotypes (DENV1-4) that co-circulate within endemic regions, including the tropics of Central and South America, sub-Saharan Africa, India, and Southeast Asia (Bhatt et al., 2013). Recent reports have detailed the increasing geographic distribution of DENV with the emergence of established autochthonous cases in the Mediterranean countries of Europe as well as the southern United States, including Florida and Texas (Fredericks and Fernandez-Sesma, 2014; Gossner et al., 2018). The major vectors for transmission of DENV are *Aedes aegypti* and *Aedes albopictus*, biting mosquitoes that live in tropical or subtropical regions near dense human populations (Carrington and Simmons, 2014). Primary DENV infections are generally asymptomatic or subclinical and provide lifelong immunity to subsequent infections with the homologous serotype. However, secondary infection with heterologous DENV serotypes can manifest as “severe dengue,” a collection of serious sequelae caused by increased capillary permeability shortly after defervescence. This can lead to severe hemorrhage, hypovolemic shock, and end-organ damage with fatal outcomes occurring in 20% of those without supportive medical care (Guzman and Harris, 2015). Symptomatic dengue fever and severe DENV infections can also lead to long-lasting arthralgias, arthropathies, and memory loss at least two years following acute illness (Garcia et al., 2011).

ZIKV has recently emerged in the Americas and continues to be a significant public health concern in many regions co-endemic with DENV. Like DENV, ZIKV is primarily transmitted by infected *Aedes spp.* mosquitoes; however, ZIKV can also be transmitted between persons through sexual contact or blood transfusion (Brasil et al., 2016a; de Araujo et al., 2018; Nogueira et al., 2018). While the majority of ZIKV infections in adults are asymptomatic (~80%), symptomatic cases can present with mild febrile illness characterized by headache, rash, fever and conjunctivitis, sometimes with severe neurological sequelae (Brasil et al., 2016a). ZIKV exhibits a diverse tropism, infiltrating numerous immunologically privileged regions within the body. These include the male and female reproductive organs, adult and fetal central nervous systems, peripheral nervous system, urinary tract, as well as the structural and neurologic portions of the eye (**Figure 1**) (Carroll et al., 2017; Figueiredo et al., 2019; Miner and Diamond, 2017; Oh et al., 2017; Retallack et al., 2016; Tabata et al., 2016). The most devastating complications of ZIKV occur during infection of the placenta and vertical transmission to the developing fetus, leading to adverse pregnancy outcomes including spontaneous abortion and fetal brain abnormalities. Approximately 30% of congenitally infected fetuses exhibit morphological abnormalities by ultrasound (e.g. microcephaly or brain calcifications) whereas the vast majority exhibit no overt clinical manifestations at birth (Brasil et al., 2016a). While microcephaly is associated with direct infection of neural stem and progenitor cells (Miner and Diamond, 2016), neonates with normal head circumference at birth may exhibit neurodevelopmental abnormalities during the first year of life (Heald-Sargent and Muller, 2017; Kapogiannis et al., 2017; Mulkey et al., 2018). Indeed, recent reports of infants with congenital ZIKV infection revealed neurodevelopmental abnormalities in the absence of overt microcephaly, including vision loss, epilepsy and delays in age-appropriate developmental skills (Cardoso et al., 2019; Lopes Moreira et al., 2018; Rice et al., 2018; Wheeler et al., 2018).

Innate Immune Responses against Flavivirus Infection

During arboviral transmission through mosquito vectors, flaviviruses are known to target skin-resident myeloid cells such as Langerhans cells, dermal dendritic cells (DCs), and macrophages (Castanha et al., 2020; Schmid and Harris, 2014; Suthar et al., 2013). Activated DCs traffic to skin-draining lymph nodes and result in viremia in the host. In turn, this allows the virus to gain access to organs that support virus replication (e.g. spleen, brain, placenta). Activation of DCs is initiated through intracellular recognition of pathogen-associated molecular patterns (PAMPs) by innate immune sensing molecules like RIG-I like receptors (RLRs) and Toll-like receptors (TLRs) followed by a robust type I and type III IFN and inflammatory cytokine responses (Quicke and Suthar, 2013; Suthar et al., 2013). RLRs are double-stranded viral RNA sensors residing the cytosol that include retinoic acid inducible gene-I (RIG-I), melanoma differentiation association gene 5 (MDA5), and laboratory of genetics and physiology 2 (LGP2) (Chow et al., 2018). RIG-I and MDA5 have similar structures with a repressor C-terminal domain (CTD), a DExD/H helicase with high affinity to double-stranded RNA, and N-terminal caspase activation and recruitment domains (CARDs). LGP2, which does not have CARD domains, is thought to act as an accessory regulator of RIG-I and MDA5 signaling, showing both inhibitory and activating action, respectively. (Bruns et al., 2014; Loo and Gale, 2011; Quicke et al., 2019). RIG-I recognizes short double-stranded RNA with 5' di- or tri-phosphate overhangs or single-stranded RNA with 5' triphosphate ends and poly-U/UC or AU sequences (Goubau et al., 2014; Saito et al., 2008; Schnell et al., 2012). MDA5, on the other hand, detects long double-stranded RNA. Upon recognition of replicating viral RNA, K63-ubiquitination of the RD changes RIG-I to an "open" conformation, oligomerization of the RLR, and K63-ubiquitination of the CARD domains (Chow et al., 2018). Post-translational modification of the CARD domain allows RIG-I to bind to the CARD domain on the adaptor

protein mitochondrial antiviral signaling (MAVS) protein to initiate downstream type I/III IFN responses through interferon regulatory factor 3 (IRF3) and proinflammatory cytokine expression through NF- κ B. TLRs also play a pivotal role in mitigating viral replication and spread. TLR3, TLR7, and TLR8 are the primary TLRs for sensing RNA viruses and are located within endosomal compartments (Quicke and Suthar, 2013). TLR3 recognizes long dsRNA and signals through the TIR domain-containing adaptor protein inducing IFN β (TRIF), leading to activation of both IRF3 and NF- κ B. TLR7 and TLR8 both recognize ssRNA and activate IRF3, IRF5, IR7, and NF- κ B through myeloid differentiation primary response protein 88 (MyD88).

Once the IRF proteins have been activated, high levels of type I and type III IFN are expressed and secreted by the infected cell. IFN α and IFN β are the primary type I IFNs secreted during viral infection, and they signal through the type I IFN receptor (IFNAR), a heterodimer comprised of one IFNAR1 and one IFNAR2 chain (Schneider et al., 2014). IFNAR is expressed ubiquitously throughout the body and induces a rapid, robust inflammatory response essential for restricting flavivirus infection (Bowen et al., 2017b; Grant et al., 2016; Keller et al., 2006; Lazear et al., 2016; Lazear et al., 2013; Morrison et al., 2013; Pinto et al., 2014; Quicke and Suthar, 2013; Suthar et al., 2012a; Suthar et al., 2013; Suthar et al., 2010; Zust et al., 2014). Type III IFN (IFN λ 1-4 in humans), the most recent addition to the IFN family, binds to a heterodimer created by the IFNLR1 and IL-10R β chains. Unlike IFNAR, IFNLR is predominantly expressed on specialized epithelial and endothelial cells surfaces at anatomic barriers (e.g. blood-brain barrier, placenta) and initiates a less inflammatory reaction compared to type I IFN (Lazear et al., 2019). Type III IFN has been shown to mitigate ZIKV infection in pregnant mouse model systems as well as protect the placental barrier from ZIKV infection (Bayer et al., 2016; Corry et al., 2017; Jagger et al., 2017). Tight junctions in the blood-brain barrier are also

strengthened upon stimulation with IFN λ , reducing WNV entry into the brain parenchyma (Lazear et al., 2015a). Upon type I and type III IFN binding, transphosphorylation of JAK1 and TYK2, specific Janus kinases (JAK) bound at the cytoplasmic tails of IFNAR1 and IFNAR2, occurs. JAK kinases come in four varieties, JAK1, JAK2, JAK3, and TYK2 and are specific to each subunit of type I and type III IFN receptors (e.g. TYK2 binds IFNAR1, JAK1 binds IFNAR2) (Schneider et al., 2014). Phosphorylation of the JAK kinases results in binding at the Src homology 2 (SH2) domains on signal transducer and activator of transcription (STAT) proteins, in this case, phosphorylation of specific tyrosine residues on STAT1 and STAT2 (Lazear et al., 2019). Phosphorylated STAT1 and STAT2 then form a heterodimer which binds to IRF9, forming the ISGF3 transcription complex and upregulating numerous ISG-encoded antiviral effector genes.

Type I IFN responses are essential for restricting flavivirus infection, thus, flaviviruses have developed clever mechanisms to inhibit type I IFN signaling. One route of IFN blockade is through inhibition at the receptor or JAK kinase level. Best and colleagues demonstrated that WNV NS5 can inhibit prolidase, a protein implicated in regulating IFNAR accumulation, maturation, and proper ISG expression, in human fibroblasts (Lubick et al., 2015). WNV has also been shown to inhibit STAT1 and STAT2 phosphorylation as well as JAK1 and TYK2 phosphorylation in A549 cells. Disparate results were seen in WNV moDCs where only pSTAT1 was inhibited and no effect on JAK1 or TYK2 phosphorylation was observed in infected Vero cells. (Zimmerman et al., 2019b). Binding of WNV to Tyro3/Axl/Mer (TAM) tyrosine kinases also inhibit type I IFN signaling through upregulation of suppressor of cytokine signaling 1 and 3 (SOCS1/3) and help establish productive infection in murine bone-marrow derived dendritic cells (Bhattacharyya et al., 2013). ZIKV was also found to actively inhibit type I IFN stimulated JAK1 and TYK2 phosphorylation in Vero cells (Zimmerman et al., 2019b). In a separate

mechanism, the ZIKV NS2b/NS3 protease was shown to cause moderate proteasomal degradation of JAK1 in A549 cells (Wu et al., 2017)

Flaviviruses can also inhibit STAT signaling downstream of the JAK kinase phosphorylation. Blockade of STAT1 and STAT2 phosphorylation has been observed in pathogenic WNV strains (NY99, TX02) in A549 human lung adenocarcinoma cell lines compared to the non-pathogenic Madagascar strain (Suthar et al., 2012a). WNV NS4A and NS4B can also block activation of STAT1 signaling and downstream binding to interferon stimulated response elements ISREs, a finding conserved amongst YFV and DENV (Munoz-Jordan et al., 2005). DENV and ZIKV NS5, through two different cellular mechanisms, cause proteasomal degradation of human, but not mouse, STAT2 downstream of type I IFN signaling (Grant et al., 2016; Morrison et al., 2013). Bowen et al. demonstrated that ZIKV actively inhibits STAT1 and STAT2 phosphorylation in human monocyte-derived dendritic cells (Bowen et al., 2017b). Although IFN λ is important in viral inhibition, the viral immune evasion mechanisms specific to type III IFN signaling are currently understudied. Regardless, type I and type III IFN utilize the same JAK kinases and STAT proteins in their respective signaling cascades, so viral antagonism of JAK kinases and STAT proteins likely affects both IFN pathways. The sheer number of evolved viral evasion strategies against the type I/III IFN signaling makes it clear that innate immune functionality is necessary for early viral inhibition, allowing for the development of effective adaptive immune responses against the virus

Human antibody responses to DENV and ZIKV

During viral replication, the flavivirus envelope region undergoes numerous structural and conformational changes to produce both immature and mature virions. Formation of immature viral particles containing the nucleocapsid, lipid membrane, E, and

prM occurs within the endoplasmic reticulum lumen. These immature particles have 60 distinct spikes on their surface comprised from a trimer of prM-E heterodimers. Flaviviruses are next shuttled to the trans-Golgi network, and through furin-mediated cleavage at pH 6.0, prM is released from the immature viral particle, allowing the 180 E-protein monomers to form 90 E-protein dimers. These E-protein dimers have three distinct regions, the amino-domain E domain I (EDI), the fusogenic peptide-containing EDII, and the carboxy-terminal EDIII which mediates viral binding to target cells (Hasan et al., 2018). Because of the outward orientation of the prM spikes on immature virions and E dimers on mature viral particles, flavivirus-infected hosts generate antibody (Ab) responses targeting these proteins to neutralize the virus.

Rapid generation of anti-flavivirus IgM antibodies characterize the late acute and early convalescent phase of infection, approximately 4-11 days after onset of symptoms, and begin to decline 15 days post-viral clearance (Paz-Bailey et al., 2019; Prince and Matud, 2011). As IgM levels peak during early convalescence, anti-flavivirus IgG, which comprise the long-lasting memory response to flavivirus infection, can be detected 8-14 days post-onset (Hoen et al., 2019; Vazquez et al., 2007). Primary infection with DENV generates a small, but potentially neutralizing Ab response targeting EDI, EDII, and EDIII, the original DENV serotype and broad, but minimally neutralizing, cross-reactive Ab response to heterologous serotypes (Beltramello et al., 2010; Lai et al., 2008). EDI/EDII-specific Abs, including ones targeting the immunodominant EDII fusion loop, comprise a majority of the cross-reactive response but display poor neutralizing activity while the EDIII-specific Abs, although lower in quantity, show superior neutralization activity (Beltramello et al., 2010; Flipse and Smit, 2015; Lai et al., 2008). These cross-reactive, poorly neutralizing DENV Abs produced by primary DENV infection have been implicated in antibody-dependent enhancement (ADE) and severe dengue cases during secondary

DENV infection (Guzman and Harris, 2015). Highly neutralizing Abs were found to target the complex quaternary epitopes spanning the EDI-EDII hinge domain and EDIII of adjacent E protein dimers (Beltramello et al., 2010; de Alwis et al., 2012). Depletion of E-protein specific antibodies from primary DENV-2 and DENV-3-immune sera with whole DENV-2 and DENV-3 virions, not recombinant E protein coated beads, eliminated the neutralization capacity towards the same DENV serotype (de Alwis et al., 2012). Unlike primary DENV infections, secondary and tertiary DENV infection typically provides long-lasting immunity to subsequent infection with homotypic and heterotypic serotypes through the generation of both potentially neutralizing type-specific and cross-reactive antibodies (Collins et al., 2017; Patel et al., 2017). Cross-reactive antibodies targeting prM, an epitope exposed on immature DENV virions, also comprise a significant amount of the non-neutralizing, broadly cross-reactive antibody response to primary dengue infection, increasing dramatically upon secondary dengue infection (Beltramello et al., 2010; de Alwis et al., 2011; Dejnirattisai et al., 2010; Lai et al., 2008; Rodenhuis-Zybert et al., 2015). Anti-prM antibodies, due to their low neutralization activity and broad cross-reactivity across DENV serotypes, have been implicated in enhancement of dengue virus infection (Dejnirattisai et al., 2010).

Analysis of immune sera from ZIKV-infected patients has shown similar neutralization across African, Asian, and South American ZIKV strains, suggesting that, in contrast to DENV, only a single serotype of ZIKV exists (Dowd et al., 2016). Primary ZIKV infection elicits a broadly cross-reactive, lowly-neutralizing antibody response to EDI and EDII of ZIKV and DENV1-4 E proteins. In contrast, EDIII-specific and quaternary epitope-binding antibodies showed high levels of ZIKV neutralization with minimal binding to DENV1-4 (Stettler et al., 2016). Collins et al. corroborated this work by showing that antibodies from primary ZIKV infection can bind monomeric soluble ZIKV EDI and EDIII

with minimal neutralization of DENV1-4 (Collins et al., 2019). In addition, similar to DENV, depletion of recombinant E protein-specific antibodies did not significantly reduce neutralization capacity of the patient sera, suggesting that ZIKV-specific neutralizing antibodies also target complex quaternary E protein epitopes (Collins et al., 2019; Stettler et al., 2016).

The ZIKV and DENV E proteins are highly similar, sharing ~54% amino acid sequence homology, which results in antibody cross-reactivity with sera from early convalescent serum from dengue-infected patients (Priyamvada et al., 2016b; Sirohi et al., 2016). Because of the structural similarities between ZIKV and DENV and their co-circulation within similar endemic regions, understanding how previous DENV immunity can shape the ZIKV-specific antibody response is of paramount interest. Collins et al. found that DENV infection, while exhibiting broad DENV serocomplex cross-reactivity and increasing neutralization with subsequent DENV1-4 infections, does not establish durable neutralizing levels of antibodies cross-reactive with ZIKV during late convalescence (>6 months after most recent infection) (Collins et al., 2017). Conversely, ZIKV infection in DENV-experienced patients caused high levels of activation of cross-reactive memory B cell responses targeting DENV during early convalescence which waned to primarily ZIKV-specific antibody responses by late convalescence (Andrade et al., 2019). The duration and degree of cross-reactive antibody responses to DENV was related to the number of previous DENV1-4 exposures prior to secondary ZIKV infection. Although DENV infection may not produce long-lasting cross-reactive antibodies to ZIKV, previous DENV infection can influence the antibody response to secondary ZIKV infection. Rogers et al. demonstrated that the initial plasmablast response in DENV-experienced ZIKV infected patients showed high levels of DENV cross-neutralization and low neutralization of ZIKV, suggestive of an expansion of memory B cells influenced by original antigenic sin

(Rogers et al., 2017). However, by late convalescence, potent clonal expansion and somatic hypermutation of highly neutralizing ZIKV-specific antibodies were observed in the DENV-experienced ZIKV-infected donors compared to those who were DENV-naïve, a finding comparable to that seen in secondary DENV infections. A longitudinal study using a pediatric Nicaraguan cohort also demonstrated that previous DENV immunity minimally shaped the overall breadth and specificity of ZIKV-specific memory B cell responses (Andrade et al., 2019).

Cross-reactive antibody responses between DENV and ZIKV: Protective vs Pathogenic

The influence of previous flavivirus immunity on flavivirus pathogenesis was first described in 1977 by Scott Halstead following the observation that DENV4-immune serum and serum from infants of DENV2-infected mothers enhanced *in vitro* DENV infection in cultured blood leukocytes (Halstead and O'Rourke, 1977; Marchette et al., 1979). Halstead also discovered that rhesus macaques injected with anti-DENV2 serum previous to DENV infection consistently exhibited higher viral loads (Halstead, 1979). Observations in DENV2-immune mothers in Thailand also demonstrated that severe dengue disease seen in Thai infants correlated to the DENV2-specific antibody titers received from their mothers (Kliks et al., 1988). Both of these *in vivo* studies were instrumental in the early understanding of ADE of flavivirus infection. ADE occurs when sub-neutralizing levels of cross-reactive antibodies bind to structurally similar viruses, allowing for enhanced viral entry into normally less-permissive FcγR-bearing myeloid cells, including monocytes, macrophages, and dendritic cells.

Enhanced viral infection in the setting of ADE has been proposed to occur through either “external” or “internal” mechanisms in relation to the host cell. External ADE is

defined as the increased binding and entry of virions through endocytosis of immune complexes bound to FcγRs on myeloid cells, resulting in dramatically increased infection (Halstead, 2014). Further research into mechanisms of ADE have also shown that binding of viral immune complexes to FcγRs can cause simultaneous downstream modulation of inflammatory immune responses as well as secretion of anti-inflammatory cytokines, a process termed “intrinsic” ADE. Binding of DENV immune complexes on THP-1 monocytes increases IL-10 transcription and translation, decreased IL-12, IFN γ , and TNF α production, and increased SOCS expression (Chareonsirisuthigul et al., 2007; Ubol et al., 2010). In addition, downregulation of key components of the RIG-I signaling pathway were also observed including decreases in MAVS and phospho-IRF3 expression (Ubol et al., 2010). Through both external and internal mechanisms of ADE, viral burden in infected cells is greatly augmented and is considered the primary cause of the increased inflammation and devastating symptoms of severe dengue disease (Halstead, 2003).

Numerous epidemiologic studies have assessed whether pre-existing DENV antibodies facilitate the manifestation of either apparent dengue infection or severe dengue disease during secondary heterotypic DENV infection. Early prospective cohort studies in Thailand identified a correlation with age (>10 years), not DENV seropositivity, that distinguished apparent (symptomatic) vs. inapparent (asymptomatic or subclinical) infections. However, 12.5% (7 of 56) of children with secondary DENV infections and 0% (0 of 47) with primary DENV infection were hospitalized with dengue hemorrhagic fever (Burke et al., 1988). Another pediatric cohort in Sri Lanka also reported that patients with pre-existing monotypic neutralizing DENV antibodies were more likely to develop apparent dengue fever over those with heterotypic cross-reactive neutralizing antibodies (Corbett et al., 2015). In a large retrospective serologic study in Santiago de Cuba, distinct chronologic DENV epidemics paired with thorough viral surveillance demonstrated that 92.1% (4,608 of 5,003) patients presenting with overt dengue fever and 98.5% (191 of

193) patients that developed severe dengue disease during the 1997 DENV-2 epidemic were seropositive for DENV-1 antibodies (Guzman et al., 2000). More recently, a large prospective study in a Nicaraguan pediatric cohort suggests that previous dengue immunity, particularly within the 1:20 to 1:80 titer range, results in higher risk of severe dengue hemorrhagic fever/dengue shock syndrome (DHF/DSS) as a result of ADE (Katzelnick et al., 2017). A recent meta-analysis pooling data from numerous cohort and cluster studies corroborated these epidemiologic findings, determining that DENV immune status directly affects the clinical outcomes during secondary DENV infection greater than one year after initial infection (Clapham et al., 2017). Phase III safety and efficacy studies on Sanofi Pasteur's Dengvaxia, a live-attenuated tetravalent yellow fever chimeric DENV vaccine, have also demonstrated that vaccinated seronegative children have a higher relative risk of acquiring severe dengue infection. Conversely, dengue seropositive children who received the vaccine showed lower incidence rates of hospitalization and decreased disease severity caused by secondary DENV infection (Sridhar et al., 2018). However, it remains poorly understood how Dengvaxia-induced cross-reactive antibody responses affect subsequent infection with ZIKV and other co-circulating flaviviruses.

Utilizing the same Nicaraguan pediatric cohort mentioned earlier, Gordon and colleagues observed that previous dengue immunity protected against symptomatic ZIKV infection, but did not mitigate the risk of primary ZIKV infection (Gordon et al., 2019). Pre-existing dengue immunity has been postulated to influence the incidence of congenital Zika syndrome (CZS) or spontaneous abortion during ZIKV infection in pregnant mothers. Serologic analysis of a Brazilian cohort of pregnant women revealed that 50% (7 of 14) DENV-IgG negative women and 43.8% (43 of 98) DENV-IgG positive women had abnormal birth outcomes (Halai et al., 2017a). Another study reported that increased ZIKV-specific neutralizing antibody titers, not differences in DENV EDIII-specific antibody titers, were found in ZIKV-infected pregnant women with confirmed CZS when compared

to case controls (Robbiani et al., 2019). Generalized linear model analysis determining factors differentiating CZS cases and controls showed that multi-typic dengue immunity (neutralizing antibodies to ≥ 2 DENV serotypes) were protective against CZS (Pedroso et al., 2019). Additional prospective studies that stratify pregnant patients based on monotypic and heterotypic DENV infection as well as DENV antibody titers are necessary to fully grasp the impact of cross-reactive DENV antibodies on vertical transmission and adverse pregnancy outcomes in ZIKV-infected pregnant mothers.

DENV and ZIKV disease severity in flavivirus-naive individuals

The presence of sub-neutralizing levels of DENV cross-reactive antibodies inducing ADE of infection is considered the primary mechanism behind severe dengue disease in patients with secondary DENV infections. However, primary DENV infection can develop into apparent dengue fever or severe dengue disease in flavivirus seronegative individuals. European traveler studies found that adult patients without prior flavivirus immunity correlated with severe DENV disease (34%; 8 of 22) or spontaneous bleeding (29%; 5 of 17) upon acquiring primary DENV infection (Wichmann et al., 2007). A prospective Thai cohort reported that 23% of patients with primary DENV infection developed dengue hemorrhagic fever compared to 53% of those with secondary DENV infections (Vaughn et al., 2000). Notably, a large majority of cases (31 of 32) which manifested as severe dengue were caused by primary infection with DENV-1 and DENV-3. However, during a prospective Cuban cohort study during a DENV-2 outbreak in 1997, a small frequency of patients (2 of 193) with primary DENV infection developed severe dengue symptoms. While humoral immune status between cohorts remains the chief hypothesis, the discrepancies in apparent infection/severe dengue rates between cohorts

have been attributed to genetic variation between different ethnicities, HLA-allele polymorphisms, cohort age ranges, and nutritional status (Coffey et al., 2009).

Due to the recent emergence of ZIKV as well as the co-circulation of ZIKV and DENV in endemic countries, prospective epidemiologic studies assessing the possible connections amid congenital Zika syndrome (CZS) and flavivirus-naïve or DENV-seropositive pregnant mothers remains limited. During the height of the Brazilian ZIKV epidemic from 2016-2017, 94 pregnant women who gave birth to infants with or without microcephaly were tested for ZIKV infection as well as presence of preexisting DENV immunity. Approximately 16% (5 of 30) of the microcephalic cases had confirmed primary ZIKV infection while 63% (19 of 30) had confirmed previous DENV and ZIKV plaque reduction neutralization test (PRNT) titers, indicating that previous DENV immunity is not a prerequisite for ZIKV entry into the fetal compartment (de Araujo et al., 2016). Another study from Brazil corroborated these findings by observing even higher rates among dengue-IgG negative, ZIKV-infected pregnant women (50%; 7 of 14) present with abnormal birth outcomes compared to DENV-IgG positive cases (43.8%; 43 of 98) (Halai et al., 2017a). However, additional prospective epidemiologic studies as well as *ex vivo* or animal model experimentation are needed to fully dissect the complex risk factors and pathways through which ZIKV can seed and infect the fetal compartment.

Cross reactive antibodies in animal models of systemic ZIKV ADE

Mouse and non-human primate (NHP) model systems have been utilized to study the influence of DENV humoral immunity on ZIKV pathogenesis and severity of infection. Due to the inability of ZIKV to evade murine type I IFN signaling, particularly STAT2-mediated innate immunity, deletion of murine *Stat2* or insertion of human *STAT2* are necessary for studying ZIKV pathogenesis in mouse systems (Gorman et al., 2018; Grant

et al., 2016). Passive immunization provided by human DENV and WNV convalescent serum followed by ZIKV challenge caused enhancement of ZIKV replication in multiple target organs and increased mortality in pregnant and non-pregnant *Stat2*^{-/-} mice (Bardina et al., 2017; Brown et al., 2019). Conversely, when immunocompetent 129Sv/ev mice were pre-treated with DENV cross-reactive monoclonal antibodies (mAbs) and challenged with ZIKV, no enhanced disease was demonstrated (Stettler et al., 2016). A caveat to these studies is the use of human serum and purified IgG within mice to induce ADE of ZIKV infection. Murine cells also do not express FcγRIIa, FcγRIIc, or FcγRIIIa, all of which are found in human cells and can participate in binding Fc regions of viral immune complexes, allowing for ADE (Bruhns, 2012). Past studies have also affirmed that human IgG binds less efficiently to murine FcγRs, but, later studies have shown that human IgG binding to murine FcγRs is comparable to murine IgG (Langerak et al., 2019). Given these limitations, the impact of ADE in contributing to worsened ZIKV disease severity remains unclear.

Introduction to the human placenta

Established by the 3rd week of gestation, the human placenta is the sole physical and immunologic barrier between the maternal and fetal bloodstreams. For the duration of pregnancy, it is responsible for transporting nutrients, solutes, and waste between the mother and developing fetus (Coyne and Lazear, 2016). The functional unit of the human placenta are chorionic villi, tree-like structures anchored to the maternal decidua or floating within the intervillous space. These villi are primarily hemomonochorial with an apical syncytiotrophoblast (STB) layer overlaying a basolateral progenitor cytotrophoblast (CTB) layer. STBs are terminally-differentiated cells that form a completely fused syncytium which comprises the first barrier of defense for the placenta against invading pathogens

(Arora et al., 2017). Beneath the STB and CTB layers lies the villous stroma which contains numerous cell types, including stromal fibroblasts, villous macrophages (Hofbauer cells (HCs)), and fetal endothelial cells comprising the fetal vasculature. During the first trimester, extravillous trophoblasts (EVTs), which invade the decidua and anchor villi, form plugs on the maternal spiral arteries, inhibiting the oxygen-rich maternal blood from entering the intervillous space. Without maternal blood during the first trimester, the villi are instead bathed in uterine secretions that are phagocytosed by STBs to provide nutrition to the fetus (**Figure 2A**). Signifying the beginning of the second trimester, the EVT plug dissolves and the flow of blood from the spiral arteries into the intervillous space is uninhibited, bathing the chorionic villi in maternal blood (Ander et al., 2019).

At the start of the second trimester, maternal IgG appears in the intervillous space within the maternal blood and transcytoses across the STB layer into the villous stroma using the neonatal Fc receptor (FcRn), providing passive immunity to the developing fetus equal to the mother's IgG levels by birth (**Figure 2B**) (Palmeira et al., 2012; Simister and Story, 1997). FcRn is a heterodimer formed by the MHC-class I like α heavy chain, encoded by the *FCGRT* gene, and β 2-microglobulin light chain. Crystallographic data also suggests that FcRn binds IgG at a 1:1 or 2:1 stoichiometry at the CH2-CH3 hinge region in the Fc portion of IgG (Martin et al., 2001). Monomeric antibodies or immune complexes (ICs) are likely internalized at the apical side of polarized epithelial cells through fluid-phase pinocytosis and transported into early endosomes containing FcRn. The low pH environment (pH ~6.0) of the early endosomes allows efficient binding of antibodies and ICs to FcRn, which signals the endosome to traffic and release the endosomal contents at the basolateral side (Pyzik et al., 2015). Once the immune complexes pass through the basolateral side of the STB barrier, HCs, which express Fc γ RI (CD64), Fc γ RII (CD32), and Fc γ RIII (CD16), can bind IgG immune complexes with high affinity (Simister and Story, 1997). In addition, villous endothelial cells lining the fetal blood vessels

preferentially express FcγRIIb2, an Fc receptor implicated in immune complex transport into the fetal vascular lumen (Lyden et al., 2001).

Hofbauer Cells: Key Regulators within the Placenta

Hofbauer cells (HCs) are fetal-derived tissue-resident macrophages specific to the chorionic villous stroma of the placenta. The exact origin of HCs is still largely debated, but they are proposed to arise from villous mesenchymal stem cells as early as 18 days post-implantation, steadily rise in number through the second trimester, and remain until birth (Ingman et al., 2010; Reyes and Golos, 2018). Later in gestation, it is hypothesized that HCs are recruited from circulating fetal monocytes, particularly during placental insult and active secretion of MCP-1 by placental fibroblasts (Toti et al., 2011). HCs assume several unique responsibilities in the placenta ranging from placental homeostasis, placental growth, to stimulating vasculogenesis and angiogenesis. *In vitro* and immunohistochemical studies have determined that paracrine signaling from HCs can stimulate trophoblastic proliferation and fusion into STBs. These paracrine signals also modulate the levels of β-human chorionic gonadotropin (β-hCG) and human placental lactogen (hPL) secreted by trophoblasts (Cervar et al., 1999; Khan et al., 2000). HCs also express high levels of Sprouty proteins in close proximity to trophoblasts which assist in development of chorionic villous branching (Anteby et al., 2005). HCs also reside closely to the fetal vasculature at early gestational timepoints, suggesting their potential role in angiogenic growth (Seval et al., 2007). Indeed, VEGF, an important angiogenic growth factor, is highly expressed in HCs starting in the 5th week of pregnancy, supporting the differentiation of endothelial cell precursors and early vasculature from angioblastic stem cells in the villous stroma (Demir et al., 2004; Demir et al., 2007). Finally, HCs can act as immune surveyors within the villous stroma through phagocytosis of immune complexes that cross the STB layer.

Immunologic insult to the placenta can have devastating effects to the growth and development of the fetus, thus, it is evolutionarily advantageous to restrict robust immune responses in the villous stroma. HCs express classic M2 immunomodulatory macrophage markers including the CD206 mannose receptor, CD163 scavenger receptor, and CD209 (DC-SIGN) and have been shown to secrete IL-10 and TGF- β (Reyes and Golos, 2018; Reyes et al., 2017; Schliefssteiner et al., 2017). Epigenetic studies have also shown hypermethylation of markers of inflammatory M1 macrophage such as TLR9, IL1B, and IL12RB2 and hypomethylation of M2 macrophage markers CCL2, CCL3, CCL14, and CD209 (Kim et al., 2012). Macrophages can exhibit high levels of plasticity, shifting from M1 to M2 depending on the microenvironment milieu. However, HCs maintain a predominantly immunomodulatory phenotype despite expressing phenotypic markers and secreting cytokines associated with both M1 and M2 macrophages during placental insult. Gestational diabetes mellitus (GDM), which causes a low-grade inflammatory environment within the placenta, did not alter TGF- β and VEGF secretion and increased expression of M2 markers, CD206, C209, and CD163. Alternatively, HCs from GDM patients also showed increased expression of M1 markers, CD86 and CD40, with slight increases in IL-1 β and IL-6 (Schliefssteiner et al., 2017). ZIKV-infected HCs also displayed minimal pro-inflammatory cytokine secretion and expression of costimulatory markers, CD80, CD86, and CD40, despite high levels of ZIKV infection (Quicke et al., 2016b; Zimmerman et al., 2018). While the mostly immunomodulatory functions of HCs provide a highly suitable environment for placental growth, repair, and angiogenesis, HCs are very permissive to viral infections such as ZIKV, RSV, HIV-1, and potentially hCMV, and can act as reservoirs for incoming viral infections in the placenta (Bokun et al., 2019; Johnson and Chakraborty, 2012; Maidji et al., 2006; Quicke et al., 2016a; Zimmerman et al., 2018).

Innate Immunity at the Placental Barrier

As the first line of defense between the mother and the fetus, the placenta has a variety of innate immunologic mechanisms to protect the fetus from invading pathogens circulating in the maternal blood. Unlike many other epithelial cell types, STBs lack intracellular junctions, eliminating paracellular routes of entry into the fetal compartment (Robbins and Bakardjiev, 2012). Due to its complex actin polymer network and high levels of elasticity, the STB layer easily maintains its around floating chorionic villi, restricting direct invasion and cell-to-cell spread of *Listeria monocytogenes* infection (Robbins et al., 2010; Zeldovich et al., 2013). Placental sections from human placenta infected with CMV *in utero* and *in vitro* showed minimal infection in the STB layer with a majority of CMV proteins expressing within the CTB layer and villous core (Fisher et al., 2000). Primary human trophoblasts and JEG-3 cells, a human choriocarcinoma cell line, have been shown to restrict *Toxoplasma gondii* infection when actively fused into a functional STB layer in three-dimensional culture systems (Ander et al., 2018; McConkey et al., 2016). In addition, STBs, alongside their own resilience against viral infections, provide robust antiviral resistance to adjacent cells from, including CMV, VSV, poliovirus, varicella zoster, HSV-1, HIV-1, and rubella virus as shown through paracrine signaling of exosomes containing antiviral miRNA to primary human trophoblasts and non-trophoblastic human cell lines (Bayer et al., 2015; Delorme-Axford et al., 2013). STBs also prevent ZIKV from crossing the STB layer through constitutive secretion and autocrine signaling of type III IFN; however, whether type III IFN affects neighboring placental cells is currently unknown (Bayer et al., 2016). Pregnant mice treated with anti-IFNAR antibodies also displayed protection from ZIKV infection when type III IFN was administered after formation of the chorioallantoic placenta at D9.5, underpinning the importance of type III IFN in placental antiviral defenses (Jagger et al., 2017). Ten Toll-like receptors (TLRs) are encoded within villous CTBs with TLR-3 showing the highest levels of mRNA in the placenta (Koga et al.,

2014; Pudney et al., 2016). TLR-2, TLR-3, TLR-4, TLR-5, and TLR-9 are expressed primarily within CTBs and HCs with TLR organization in the CTB layer shifting from highly organized to dispersed from the first to second trimester. Despite its robust antiviral and antimicrobial defenses, the STB layer showed minimal expression of TLRs (Pudney et al., 2016).

Passing the TORCH: Mechanisms of ZIKV Entry into the Placenta

Despite the strong immunologic and biophysical defense mechanisms of the trophoblast layers of the placenta, once the STB layer is breached, there is little immunologic resistance to infection. Evolutionarily, large immune responses within the villous stroma, while eliminating the pathogen, can have detrimental effects on the developing fetus (Yockey et al., 2018). Because of the limited resistance beyond the STB layer, TORCH pathogens, an acronym for *T. gondii*, other (*L. monocytogenes*, *Treponema pallidum*, enteroviruses, parvoviruses, HIV, varicella zoster virus (VZV)), rubella virus, CMV, HSV-1/2 and the newest member, ZIKV, have developed clever strategies to bypass placental defenses (Coyne and Lazear, 2016). ZIKV has been hypothesized to bypass the highly antiviral STB layer and seed the fetal compartment via infection of invading EVT_s, cells that anchor the villi into the decidua and have no basolateral STB layer. In addition, *in vitro* infection of amniotic epithelial cells suggests that ZIKV may infiltrate the fetal space via a paraplacental route through the amniochorion (Tabata et al., 2018; Tabata et al., 2016). Viral shedding of ZIKV from both vaginal and seminal secretions as well as documented sexual transmission of ZIKV suggests that ZIKV can also ascend the female reproductive tract to potentially infect the fetus (D'Ortenzio et al., 2016; Mead et al., 2018; Reyes et al., 2019). Studies in rhesus macaques have shown that vaginal inoculation with ZIKV preferentially causes ascending infection of the female reproductive tract with delayed, but robust, viremia and dissemination (Carroll et al., 2017). Intravaginal

infection of wild-type pregnant mice with ZIKV caused productive infection in the reproductive tract and viral NS1 was detected in the brains of infected fetuses, however, this did not affect the overall health of the fetus (Yockey et al., 2016). Subneutralizing levels of CMV-specific or dengue cross-reactive antibodies can also generate immune complexes with CMV and ZIKV, respectively, and traffic the virions across the STB layer through FcRn-mediated transport (Brown et al., 2019; Maidji et al., 2006; Rathore et al., 2019; Zimmerman et al., 2018).

ZIKV Infection of the Human Placenta

ZIKV is quite unique amongst pathogenic flaviviruses due to its ability to efficiently cross the placental barrier and teratogenicity upon infection of the fetus. During ZIKV infection *in vivo*, histopathologic findings show ZIKV antigen expression and extensive damage within the chorionic villi, including edema, placental infarctions, stromal calcifications, HC hypercellularity, and sclerosis (Hirsch et al., 2018; Martines et al., 2016). Despite these pathologic findings, other groups have reported minimal inflammation coupled with HC hypercellularity in the placenta during second and third-trimester ZIKV infection *in vivo* (Rosenberg et al., 2017). We and others have also demonstrated that, once the STB layer has been circumvented, ZIKV preferentially targets and productively infects HCs within the villous stroma (Bhatnagar et al., 2017; Jurado et al., 2016; Quicke et al., 2016b; Tabata et al., 2016; Zimmerman et al., 2018). In one study, ZIKV RNA was isolated from placental tissues in 75% of women who experienced adverse pregnancy outcomes, and ZIKV replicating negative-sense RNA was found localized to HCs in 50% of the women with positive ZIKV RT-PCR results. ZIKV was also found to persist in the placenta for over 200 days post maternal onset of symptoms (Bhatnagar et al., 2017). Emerging epidemiological observations estimate that between 20-50% of pregnant women with possible ZIKV exposure had detectable ZIKV RNA in the placenta

(Reagan-Steiner et al., 2017). Recent studies from our group and others have also determined that cross-reactive dengue virus (DENV) antibodies can bind to ZIKV and greatly enhance ZIKV infection in both HCs and mid-gestation chorionic villous explant tissues (Hermanns et al., 2018; Priyamvada et al., 2016b; Zimmerman et al., 2018). Because DENV and ZIKV are co-endemic and pregnant women living in these areas are often seropositive for DENV, the degree to which cross-reactive antibody responses affect ZIKV pathogenesis, especially within the placenta, remains incompletely understood.

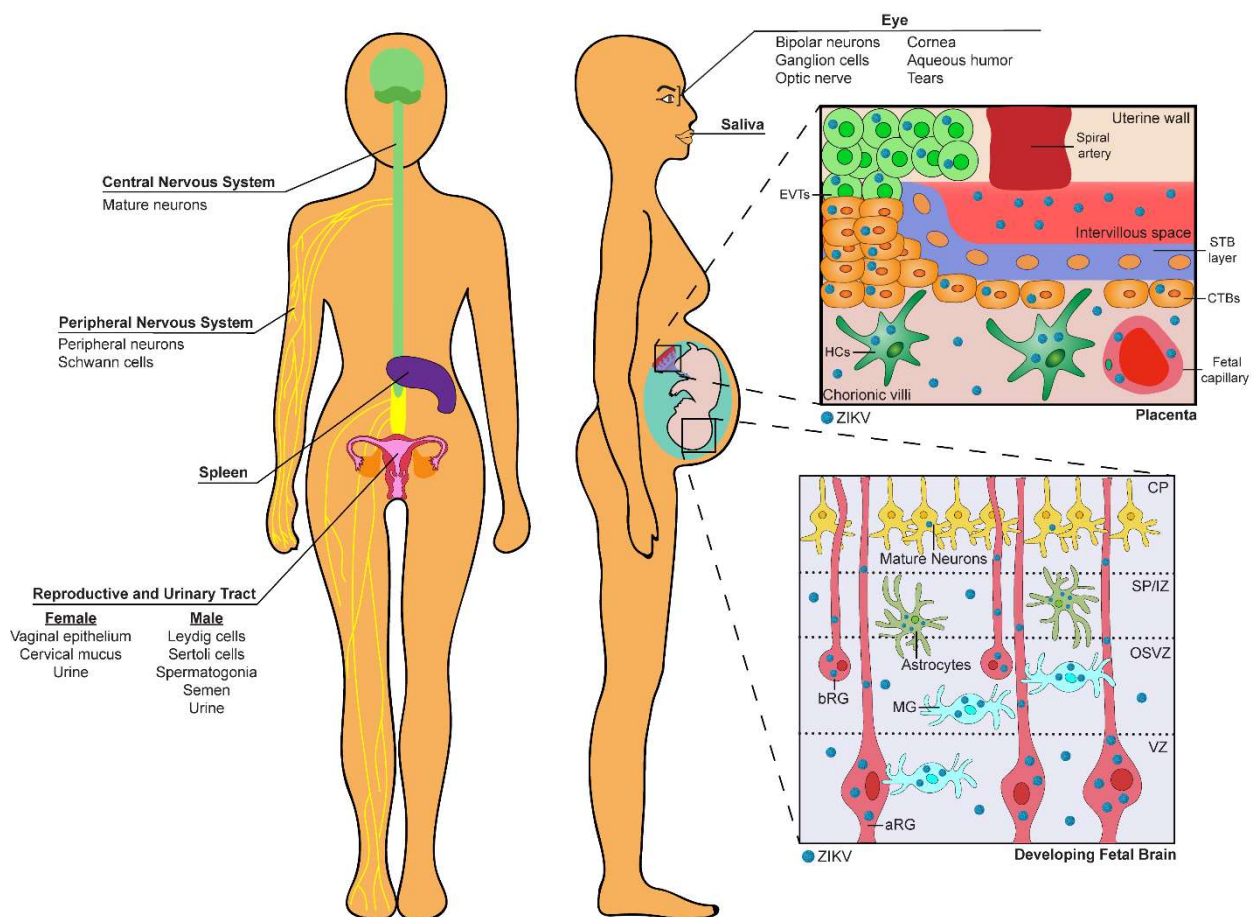


Figure 1. Sites of viral tropism during ZIKV infection. Human and mouse studies have identified ZIKV infection of mature neurons of the adult brain as well as peripheral neurons and myelinating Schwann cells of the peripheral nervous system. ZIKV can also infect primary human cortical samples within numerous cells types of the developing fetal brain: in the apical radial glia (aRG) progenitor cells of the ventricular zone (VZ); microglia (MG), astrocytes, and basal radial glia (bRG) of the outer subventricular zone (OSVZ) and subcortical plate (SP). Limited ZIKV infection has also been detected in mature neurons of the cortical plate (CP). ZIKV can also be detected in the vaginal epithelium and cervical mucus. Notably, ZIKV infection of the placenta was found in invading villous trophoblasts, cytotrophoblasts, Hofbauer cells, and fetal endothelial cells in human placental cell culture

and *ex vivo* chorionic villous explant studies. ZIKV was also found in Leydig cells and Sertoli cells of the male gonads as well as spermatogonia and semen in male subjects. ZIKV has been detected within the urine and saliva of non-human primates and humans. ZIKV also infects the retinal (bipolar neurons, ganglion cells, optic nerve) structures of the eye in mice and was found in the aqueous humor and tears in humans. ZIKV infection has also been identified within the spleen.

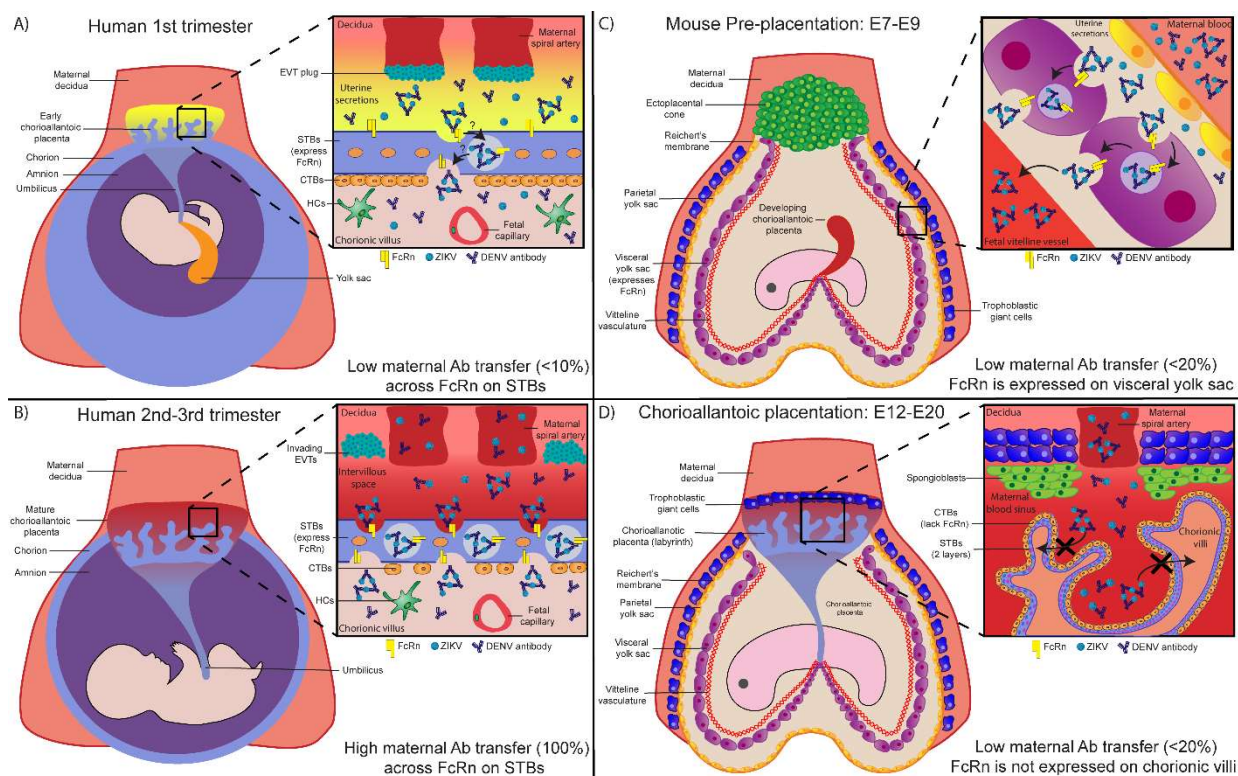


Figure 2. Differences in barrier structure and antibody translocation between human and mouse placentae.

A) By the third week of gestation, the human chorioallantoic placenta has invaded the maternal decidua and established the chorionic villous system for nutrient exchange. The chorionic villi are composed of a fused syncytiotrophoblast (STB) layer with underlying progenitor cytotrophoblasts (CTBs) that can regenerate the STB layer or develop into extravillous trophoblasts (EVTs). At this point in pregnancy, EVT plugs the maternal spiral arteries, hindering maternal blood from contacting the chorionic villi. Instead, the chorionic villi are bathed in uterine secretions to provide nutrition. Unlike the second and third trimesters, transfer of maternal IgG across the STB layer into the villous stroma is low (<10% maternofetal transfer efficiency) **B)** Dissolution of the EVT plugs and flooding of the intervillous space with maternal blood signifies the start of the second trimester. At approximately the 13th week of gestation until

term, maternal IgG and immune complexes readily bind to the neonatal Fc receptor on the STB surface and are transcytosed into the villous stroma with 100% maternofetal transfer efficiency. Once in the villous stroma, these antibodies and complexes can be phagocytosed by resident Hofbauer cells (HCs) or taken up fetal endothelial cells to enter the fetal circulation. **C)** In contrast to humans, the mouse has two different placentae throughout gestation. Around embryonic age 7-9 (E7-9), the mouse is surrounded by trophoblastic giant cells and the vitelline yolk sac (VYS) placenta. The VYS placenta is comprised of an outer endodermal cell layer with a mesodermal vitelline vasculature network underneath. The VYS endodermal cell layer expresses FcRn and allows for modest levels of passive antibody transfer from the uterine secretions to the developing fetal mouse (<20% maternofetal transfer efficiency). At this point, the labyrinthine chorioallantoic placenta is not fully established **D)** Around E12, the enveloping trophoblastic giant cells now divert blood through the spongiotrophoblast layer into the fully formed labyrinthine chorioallantoic placenta, containing interwoven villous structures perfused with maternal blood. Distinct from humans, the chorionic villi of the mouse trichorioallantoic placenta contain an outermost CTB layer with two inner STBs layer. In contrast to the VYS placenta, neither the CTB nor STB layers express FcRn and cannot transfer maternal antibodies to the fetus.

Chapter 2: Cross-reactive dengue virus antibodies augment Zika virus infection of human placental macrophages

Matthew G. Zimmerman^{1,2,†}, Kendra M. Quicke^{1,2,†}, Justin T. O'Neal^{1,2}, Nitin Arora³, Deepa Machiah^{2,4}, Lalita Priyamvada^{1,2}, Robert C. Kauffman^{1,2}, Emery Register^{1,2}, Oluwaseyi Adekunle^{1,2}, Dominika Swieboda¹, Erica L. Johnson¹, Sarah Cordes^{3,6}, Lisa Haddad³, Rana Chakraborty¹, Carolyn B. Coyne^{3,5}, Jens Wrammert^{1,2}, Mehul S. Suthar^{1,2,*}

¹Department of Pediatrics, Division of Infectious Disease, Emory University School of Medicine, Atlanta, GA 30322, USA.

²Emory Vaccine Center, Yerkes National Primate Research Center, Atlanta, GA 30329, USA.

³Department of Pediatrics, University of Pittsburgh School of Medicine, Pittsburgh, PA 15224, USA.

⁴Molecular Pathology Core Lab, Yerkes National Primate Research Center, Atlanta, GA 30329, USA.

⁵Center for Microbial Pathogenesis, Children's Hospital of Pittsburgh of UPMC (University of Pittsburgh Medical Center), Pittsburgh, PA 15224, USA.

⁶Department of Gynecology and Obstetrics, Emory University, School of Medicine, Atlanta, Georgia 30322, USA.

*Lead contact: msuthar@emory.edu (M.S.S)

†These authors contributed equally to this work.

Introduction

Zika virus (ZIKV) is a mosquito-borne flavivirus responsible for continuing epidemics of fetal congenital malformations within the Americas since its introduction to Brazil in 2015 (de Oliveira et al., 2017; Melo et al., 2017; Rasmussen et al., 2016). Symptoms include a self-limiting febrile illness accompanied by rash, conjunctivitis, arthralgias, myalgias, and fatigue; however, 80% of ZIKV infections are asymptomatic in healthy individuals (Lazear and Diamond, 2016). ZIKV is primarily transmitted through bites from infected *Aedes* mosquitos but can also be transmitted through sexual contact and blood transfusion (Lazear and Diamond, 2016). Notably, vertical transmission of ZIKV from mother to child *in utero* has been implicated in the rise of congenital microcephaly among neonates in ZIKV-endemic regions (Coyne and Lazear, 2016). Additionally, recent studies have discovered some infants with normal head circumference developed post-natal onset microcephaly, eye abnormalities, joint disorders, and sensorineural hearing loss following congenital ZIKV infection (Delaney et al., 2018; Fitzgerald et al., 2018; van der Linden et al., 2016). These studies demonstrate that congenital ZIKV infection has wide-ranging effects on infected fetuses, emphasizing the importance of understanding the mechanisms of vertical transmission.

The placenta acts as the sole physical and immunologic barrier between the maternal and fetal blood supply and is responsible for efficient gas, nutrient, and waste exchange during pregnancy (Coyne and Lazear, 2016). In humans, the placenta is composed of anchoring chorionic villi, which penetrate the uterine wall, as well as floating chorionic villi that are bathed in maternal blood pooling in the intervillous space (Arora et al., 2017). We and others have shown that ZIKV productively infects Hofbauer cells (HCs) and, to a lesser extent, cytotrophoblasts (CTBs) (Jurado et al., 2016; Quicke et al., 2016b; Tabata et al., 2016). Following viral seeding of the placenta, ZIKV primarily infects HCs

and persists within the placenta and fetal brain throughout pregnancy (Bhatnagar et al., 2017). However, the mechanisms of transplacental transmission of ZIKV and seeding of the placenta are not well understood. Syncytiotrophoblasts (STBs) maintain resistance to ZIKV infection through the constitutive secretion of IFN- λ , a type III IFN known for providing immunologic protection at anatomic barriers (e.g. blood-brain barrier, placenta, epithelial surfaces) during viral infection (Bayer et al., 2016; Lazear et al., 2015a; Lazear et al., 2015b). In mice, the IFN- λ -dependent antiviral response correlates with gestational age, specifically the development of the mature trophoblast barrier at later stages of pregnancy (Jagger et al., 2017). The inability of ZIKV to directly infect STBs suggests alternative routes for ZIKV transplacental transmission.

The emergence of ZIKV in the Americas overlaps with the regional distribution of dengue virus (DENV) seroprevalence, a related flavivirus that infects 50-100 million people per year (Bhatt et al., 2013). Numerous studies have shown that DENV antibodies can cross-react with ZIKV, which differs from DENV by 41-46% in the envelope protein, resulting in enhanced ZIKV infection in Fc γ R-expressing cells (Dejnirattisai et al., 2016; Paul et al., 2016; Priyamvada et al., 2016b). To provide passive immunity to the developing fetus, transport of maternal IgG across the placenta starts by the 12th week of gestation and sharply increases between the second and third trimesters (Simister, 1998; Simister and Story, 1997). Furthermore, in DENV-seropositive pregnant mothers, DENV-specific IgG can be found at higher titers within the cord sera compared to the maternal serum by term birth (Castanha et al., 2016). However, it is not clear what role DENV-induced cross-reactive antibodies play in facilitating transplacental transmission of ZIKV.

Here, we evaluate the impact of cross-reactive DENV antibodies on ZIKV infection of the placenta. We demonstrate that the presence of DENV monoclonal antibodies (mAbs) increased ZIKV infection from approximately 10% to over 80% of HCs in culture. Despite enhanced ZIKV infection, we observed blunted type I IFN induction, antiviral gene

expression, HC activation and pro-inflammatory cytokine production. We found that exogenous type I, but not type III IFN, significantly restricted ZIKV replication within ZIKV- and immune complex-infected HCs. Using mAbs with the identical binding site cloned onto different IgG Fc scaffolds, we determined that ZIKV complexed with IgG1 and IgG3 resulted in higher infection of HCs compared to IgG2 and IgG4. Finally, we found that immune-complexed ZIKV was more efficient at infecting human placental explant tissue than non-complexed virus. Additionally, ZIKV infection of HCs and human placental explants are enhanced in an IgG subclass-dependent manner and targeting FcRn reduced ZIKV replication in human placental explants. Collectively, these findings support a mechanism by which cross-reactive DENV antibodies may facilitate viral vertical transmission across the placental barrier and enhancement of ZIKV infection in HCs.

Results

Cross-reactive DENV antibodies enhance ZIKV infection of HCs. The envelope (E) proteins between DENV and ZIKV are structurally similar, resulting in the generation of cross-reactive antibodies (Priyamvada et al., 2016b; Sirohi et al., 2016). Thus, we determined whether DENV cross-reactive antibodies can enhance ZIKV infection of HCs. Primary HCs were isolated from full-term placenta and infected with ZIKV (PRVABC59) alone or complexed with anti-DENV2 mAbs (IgG1 subclass). We evaluated four DENV2 mAbs, which vary in ZIKV binding and neutralization (Priyamvada et al., 2016b), along with a non-specific control mAb originally isolated from a patient with acute influenza infection (Wrarmert et al., 2011) (**Figure 1A**). The three ZIKV cross-reactive DENV mAbs robustly enhanced ZIKV infection with >70% of cells infected at the highest mAb concentration (10 $\mu\text{g}/\text{mL}$) as compared to cells infected with ZIKV alone at a MOI of 1 (4%) or 10 (21%; **Figure 1B**). We found the most dramatic enhancement of ZIKV infection in HCs treated with the 33.3A06 mAb at 10 $\mu\text{g}/\text{mL}$ (83.5%) as compared to the 31.3F03 (76.3%) and 33.3F05 (75.7%) mAbs. As previously reported, the non-cross-reactive 33.3E04 mAb and the non-specific control mAb (influenza virus EM4CO4 mAb) failed to enhance ZIKV infection (Priyamvada et al., 2016b). We also performed 33.3A06 antibody titrations in HCs from three additional donors and observed a dose-dependent decrease in ZIKV infection, beginning at 1.6×10^{-2} $\mu\text{g}/\text{mL}$ and reaching similar levels as ZIKV infection alone (MOI 1) by 1.28×10^{-4} $\mu\text{g}/\text{mL}$ mAb (**Figure 1C**). We also observed the highest levels of infectious virus in the supernatants under conditions where ZIKV immune complexes were generated with 4×10^{-1} to 1.6×10^{-2} $\mu\text{g}/\text{mL}$ of 33.3A06 mAb (**Figure 1D-E**). Compared to ZIKV infection alone (MOI 1 or 10) or ZIKV infection in the presence of the non-specific control mAb, we observed very little change in CD40, CD80, and CD86 upon ADE-ZIKV infection of HCs (**Figure S1A-D**). We also did not observe a substantial increase in cell death with either ZIKV infection alone or following infection with immune-

complexed ZIKV as compared to mock infected cells (**Figure S1E**). Moreover, we treated HCs with Bafilomycin A1, which is a potent inhibitor of endosomal acidification (Wang et al., 2006), and observed reduced ZIKV infection in the context of ADE and non-ADE conditions (**Figure S2**). This suggests that immune complexed-ZIKV infects HCs through an endosomal-mediated process to infect HCs. Altogether, these findings demonstrate that cross-reactive DENV antibodies augment ZIKV infection of HCs with minimal effects on cellular activation or cell death.

DENV mAb immune complexes increase ZIKV binding and entry in HCs. To date, the mechanisms of ADE during flavivirus infection remain incompletely understood; however, it is hypothesized that enhancement of viral infection can involve two different, but not mutually exclusive, mechanisms: extrinsic or intrinsic ADE (Taylor et al., 2015). Extrinsic ADE is defined as sub-neutralizing concentrations of antibody binding to a virus and subsequently increasing attachment and entry into cells expressing Fc receptors. Intrinsic ADE involves negative regulation of innate immune signaling following binding of immune complexes to surface Fc receptors, thus making the cells more permissive to viral infection (Taylor et al., 2015). To establish the mechanism of ADE of ZIKV infection in HCs, we performed viral binding and entry assays on HCs infected with ZIKV alone (MOI 1 or 10) or in the presence of cross-reactive and non-specific mAbs (**Figure 2A**). As expected, we observed a log-fold increase in viral binding and entry in HCs between ZIKV at a MOI of 1 and 10 (**Figure 2B**). In ADE-ZIKV-infected HCs, we observed significantly increased viral binding as compared to ZIKV infection of HCs in the presence of the non-specific control mAb. Similarly, we also observed a log-fold increase in viral entry in ADE-ZIKV-infected cells as compared to ZIKV alone at a MOI of 1 or in the presence of non-specific control mAb. Despite similar levels of viral entry between cells infected with ZIKV at a MOI of 10 and ADE-ZIKV-infected cells, we consistently observed higher levels of infected cells

as measured by viral E protein staining in ADE-ZIKV-infected HCs (**Figure 1**). These findings suggest that extrinsic ADE plays a significant role in enhancing ZIKV infection of HCs.

ADE of ZIKV infection induces IFN gene expression but dampens antiviral responses in HCs. We next determined whether any differences exist in the induction of innate immune responses between non-ADE- and ADE-ZIKV-infected HCs. We evaluated the expression of type I and type III IFNs following ZIKV infection of HCs. HCs infected with ZIKV alone (MOI of 1 or 10) or in the presence of the non-specific control mAb displayed robust induction of type I and III IFN mRNAs, which corresponded with increased viral RNA as compared to time-matched mock-infected controls (**Figure 3A**). Similarly, robust increases in IFN- β (630-fold), IFN- α (267-fold) and IFN- λ (209-fold) transcript expression were observed in the highest ADE-ZIKV infected HCs as compared to time-matched mock-infected controls. Notably, we failed to detect IFN- β and IFN- λ protein in the supernatants of HCs infected under any condition (non-ADE and ADE-ZIKV infected HCs; **Figure 3B**). This finding is consistent with our previous observations in ZIKV-infected HCs and moDCs, in which we failed to observe IFN- β protein in cells or in the supernatants despite robust induction of IFN- β transcripts (Bowen et al., 2017a; Quicke et al., 2016b). We did observe basal IFN- α protein in the supernatants of mock-infected cells. Notably, we observed a significant reduction in IFN- α protein in ADE-ZIKV-infected HCs as compared to HCs infected with ZIKV alone (MOI 1) or in the presence of the non-specific control mAb (**Figure 3B**). These results indicate that ZIKV infection potentially triggers transcription of type I and III IFNs, suggesting that ZIKV can block the translation/secretion of type I IFNs into the supernatant.

Next, we evaluated the effect of ADE-ZIKV infection on the induction of pro-inflammatory cytokines/chemokines. For this analysis, we performed a 25-plex cytokine/chemokine analysis on supernatants following ZIKV infection of HCs (non-ADE and ADE; **Table S1**). Infection of HCs with ZIKV at MOI 1 resulted in significant increases in MCP-1, MIP-1 α and MIP-1 β , and modest increases in IL-2R and IL-1R α over mock-infected controls (**Figure S3**). Despite high levels of infection, we observed a lack of induction of MCP-1, MIP-1 α , MIP-1 β , IL-2R and IL-1R α as well as other proinflammatory cytokines/chemokines (**Table S1**) in ADE-ZIKV-infected HCs over mock-infected cells. MCP-1 (CCL2), MIP-1 α (CCL3), and MIP-1 β (CCL4) are important for trafficking and infiltration of inflammatory myeloid cells and leukocytes to sites of flavivirus infection (Michlmayr and Lim, 2014). Notably, levels of IL-8, a cytokine canonically associated with neutrophil trafficking and degranulation but also non-inflammatory placental angiogenesis in HCs (Schliefsteiner et al., 2017), was reduced in ADE-ZIKV-infected HCs compared to mock infected controls (**Figure S3**). Furthermore, we failed to detect IL-10, which has been implicated in contributing to intrinsic ADE (Tsai et al., 2014), in either mock-infected cells or following ZIKV infection of HCs (**Table S1**).

We next measured the expression of the RIG-I-like receptors (RLRs), which play a critical role in triggering an innate immune response following ZIKV infection and antiviral effector genes that restrict ZIKV infection (Bowen et al., 2017a). At the transcript level, we observed that *DDX58* (RIG-I), *IFIH1* (MDA5), and *DHX58* (LGP2) expression were induced in HCs infected with ZIKV alone (MOI of 1 and 10) or in the presence of the non-specific control mAb as compared to time-matched mock-infected controls (**Figure 3C**). However, at the highest concentrations of 33.3A06 mAb immune-complexed ZIKV, which corresponded with robust ZIKV replication, we observed minimal induction of *DDX58* (3.4-fold), *IFIH1* (3.1-fold), and *DHX58* (2.8-fold) as compared to time-matched mock-infected controls. In a similar manner, we observed minimal induction of antiviral effector genes

IFIT1 (8.0-fold), *IFIT2* (31.4-fold), *IFIT3* (4.9-fold), *RSAD2* (5.0-fold) and *OAS1* (1.1-fold) in ADE-ZIKV-infected HCs as compared to cells infected with ZIKV alone (MOI of 1 and 10) or in the presence of the non-specific control mAb (**Figure 3C**). To determine whether ZIKV also blocks the translation of antiviral effector genes, we performed Western blot analysis on a parallel set of infected HC samples. ZIKV infection alone (MOI of 1 and 10) showed robust increases in expression of the RLRs, IFIT proteins, Viperin and OAS1 over mock-infected controls (**Figure 3D**). However, we observed a lack of RLRs and antiviral effector proteins in ADE-ZIKV-infected cells as compared to mock-infected cells. As a control, we did not observe any changes in GAPDH protein across the various conditions of infected HCs. Combined, these findings suggest that binding of ZIKV immune complexes to Fc receptors induces intrinsic ADE by triggering a negative signal within HCs that blunts antiviral effector gene expression.

Type I IFN, but not type III IFN, restricts ADE-ZIKV infection in HCs. We next determined whether type I or III IFN can restrict ADE of ZIKV infection in HCs by performing an interferon inhibition assay (Bowen et al., 2017a). In this assay, we infected HCs with ZIKV immune complexes for 1h followed by treatment with recombinant human IFN- λ 1 or IFN- β (10 IU/mL or 100 IU/mL) for 24h. We measured both ZIKV infection by intracellular viral E protein staining and infectious virus production by FFA. Following IFN- λ 1 treatment, we observed a modest, yet significant, increase in the percentage of ZIKV-infected cells as compared to untreated cells (**Figure. 4A, top**). Notably, we observed this increase in both non-ADE- and ADE-ZIKV-infected cells (**Figure 4C**). However, we did not observe an increase in infectious virus release following IFN- λ treatment (**Figure. 4A, bottom**). In contrast to IFN- λ , IFN- β treatment resulted in significant reduction in both the percentage of ZIKV infected cells and infectious virus in the supernatants (**Figure. 4B**). This reduction was consistent across non-ADE- and ADE-ZIKV-infected HCs (**Figure 4C**).

These results indicate that HCs are highly responsive to IFN- β treatment and that IFN- β inhibits ZIKV replication in HCs despite the high levels of infection seen with ADE.

IgG subclass influences infectivity of HCs during ADE. Given that our work thus far employed an IgG1 subclass mAb, we next determined whether similar levels of enhanced ZIKV infection were observed across various IgG subclasses. We performed flow cytometry analysis on HCs isolated from full-term placenta and found that these cells express CD16, CD32 and CD64, albeit to varying levels (**Figure 5A**). We observed that >98% of HCs expressed CD32 and CD64; however, <2% of cells expressed CD16. Fc γ Rs bind to the Fc portion of different IgG subclasses with varying affinities (Smith and Clatworthy, 2010); therefore we assessed the ability of ZIKV complexed with IgG1, IgG2, IgG3 and IgG4 to infect HCs. We generated a panel of mAbs containing the Fab region from the cross-reactive 33.3A06 mAb but interchanged the Fc regions with the four human IgG subclasses. We also generated a mutant form of IgG1 containing a “LALA” modification in the Fc region, which is known to substantially inhibit Fc γ RI, Fc γ RII, and Fc γ RIII binding (Beltramello et al., 2010; Hessel et al., 2007). We generated ZIKV immune complexes using this panel of mAbs and observed similar levels of infection with IgG1, IgG3, and IgG4 subclasses with substantially reduced infection with IgG2 at the highest antibody concentration (**Figure 5B**). However, at lower Ab concentrations (1.6×10^{-2} , 3.2×10^{-3} $\mu\text{g/mL}$), we observed distinct differences in viral infection using the panel of 33.3A06 IgG subclasses. IgG1 and IgG3 immune complexes displayed a higher percentage of infected cells (76.9% and 82% 4G2+ cells, respectively); IgG4 had an intermediate phenotype (64.5% 4G2+ cells), and IgG2 displayed low levels of infection (4.38% 4G2+ cells; **Figure 5B**). As previously shown, ADE of ZIKV infection is lost at the 6th-7th mAb dilutions for the entire panel of 33.3A06 mAb IgG subclasses. ZIKV immune complexes generated with the 33.3A06 IgG1-LALA mAb variant showed reduced infection

across all antibody concentrations and reached similar levels as cells infected with ZIKV alone (MOI 1) or in the presence of non-specific control mAb. This demonstrates that ADE-ZIKV occurs through an Fc receptor-dependent mechanism. Collectively, the results demonstrate that HCs express specific FcγRs that promote binding of viral immune complexes and augment ZIKV infection in an IgG subclass-specific manner.

Cross-reactive DENV mAbs enhance ZIKV infection of human mid-gestation placental explants. We next determined the ability of cross-reactive DENV mAbs to enhance ZIKV infection of human mid-gestation placental explants. For these studies, we generated ZIKV immune complexes using the panel of 33.3A06 IgG subclasses and infected second-trimester human placental villous explants with the immune complexes, ZIKV alone, or in the presence of non-specific control mAb. In explants treated with the 33.3A06 mAb immune complexes, we detected increased levels of positive- and negative-sense ZIKV RNA as compared to ZIKV infection alone or in the presence of non-specific control mAb (**Figure 6A**). Specifically, we found that infection with IgG1 and IgG3 displayed increased infection as compared to IgG4 and IgG2. We observed a mAb dose-dependent increase in ZIKV replication as ZIKV immune complexes generated with low 33.3A06 mAb concentrations (0.001 µg/mL) displayed similar levels of positive and negative-strand viral RNA as that of ZIKV alone, or in the presence of the non-specific control mAb. Additionally, we observed a log-fold increase in ZIKV RNA in the supernatants from 33.3A06 IgG1 immune complex-infected explants and a 1.5 log-fold increase with IgG3-ZIKV immune complexes as compared to the control samples (**Figure 6B**). Similarly, we found increased infectious virus in the supernatants from placental explants infected with IgG1-ZIKV immune complexes but not in the explants infected with ZIKV alone or in the presence of the non-specific control mAb (**Figure S4**). Altogether,

these data show that cross-reactive DENV mAbs, particularly IgG1 and IgG3 subclasses, enhance ZIKV infection of human placental explants.

We next performed immunohistochemical analyses on placental explants infected with the 33.3A06 ZIKV immune complex, the EM4CO4 non-specific antibody or ZIKV alone. In the explants treated with ZIKV immune complexes, we demonstrated that ZIKV E protein (red deposition) was predominantly found within cells with similar morphology and localization within the villous stroma as CD163+ HCs (green deposition; **Figure 6C**). Markedly, no ZIKV E protein was detected within the STB or CTB layers. In contrast, explants infected with ZIKV alone or in the presence of a non-specific antibody control showed no evidence of ZIKV E protein throughout the tissue.

Targeting IgG-FcRn interactions reduces ZIKV infection of human placental explants. ZIKV infection of HCs within the villous stroma coupled with the lack of STB or CTB infection in mid-gestation explants indicates that these viral immune complexes can transcytose across the trophoblast layer. During pregnancy, maternal IgG is transported across the STB layer of the chorionic villi, providing passive immunity to the developing fetus. To determine what role FcRn plays in transplacental transport of ZIKV immune complexes, we pre-treated mid-gestation placental explants with Protein A from *Staphylococcus aureus*, a protein shown to bind the CH2-CH3 domains of IgG and inhibit binding to FcRn (Deisenhofer, 1981; Raghavan et al., 1994), and subsequently infected with ZIKV complexed with the 33.3A06 IgG1 enhancing antibody. Human IgG3 is not able to bind Protein A (Jendeberg et al., 1997; Lindmark et al., 1983); therefore, as a control, we also infected placental explants with ZIKV complexed to 33.3A06 IgG3 mAbs. Using strand-specific qPCR, we observed significant dose-dependent decreases in both positive- and negative-sense ZIKV RNA with increasing concentrations of Protein A

(Figure 7A). In detail, we detected 14.3-fold and 33.3-fold decreases in positive-sense ZIKV RNA as well as 4.9-fold and 12.2-fold decreases in negative-sense ZIKV RNA in explants treated with 10 ug/ml and 100 ug/ml Protein A, respectively. Notably, explants infected with ZIKV IgG3 immune complexes showed minimal change in either positive- or negative sense ZIKV RNA in the presence of Protein A. We also found that treatment of mid-gestation explants with DVN24, a mAb that specifically targets and blocks the IgG-binding region of FcRn (Christianson et al., 2012), significantly inhibited ZIKV replication by 16.5-fold **(Figure S5A)**.

Lastly, we determined whether ADE of ZIKV infection seen in mid-gestation explants was dependent on FcγR binding. In agreement with our earlier observations in HCs *in vitro*, we observed >1.5 log-fold decreases in both positive- and negative-sense ZIKV RNA in explants infected with ZIKV bound to 33.3A06 IgG1-LALA mAbs compared to ones infected with the 33.3A06 IgG1 viral immune complexes **(Figure 7B)**. Additionally, explants infected with 33.3A06 IgG1-LALA immune complexes were analyzed by immunohistochemistry and probed for ZIKV E protein. Consistent with the lack of viral enhancement seen in HCs and explants, explants infected with 33.3A06 IgG1-LALA immune complexes did not exhibit appreciable ZIKV infection **(Figure S5B)**. Overall, this data illustrates that ZIKV infection of placental explants are enhanced by cross-reactive DENV antibodies, and ZIKV infects and replicates in HCs within the villous stroma. Moreover, these studies also suggest that ZIKV immune complexes can utilize the FcRn IgG transport system to transcytose across the STB layer to infect HCs in an FcγR-dependent fashion.

Discussion

Our findings demonstrate that cross-reactive DENV mAbs can augment ZIKV infection of HCs isolated from full-term placenta in a dose-dependent manner. Mechanistically, we determined that cross-reactive DENV mAb immune complexes enhanced viral binding to HCs and increased viral entry. However, despite the high levels of infection seen in ADE-ZIKV-infected HCs, we observed minimal upregulation of costimulatory markers and production of pro-inflammatory cytokines. Although HCs induce type I and III IFN transcript during ADE-ZIKV infection, IFN protein secretion as well as expression of key antiviral effectors were severely diminished in ADE-ZIKV-infected cells. Notably, ADE-ZIKV infection was significantly reduced upon IFN- β treatment. We also found that enhancement of ZIKV infection in HCs is dependent on the IgG-subclass of the cross-reactive antibody with the strongest enhancement observed in the presence of IgG1 and IgG3 immune complexes. Consistent with these results, we observed enhanced ZIKV infection in human mid-gestation placental explants in an IgG-subclass specific manner and obtained data suggesting that ZIKV immune complexes can transcytose across the STB layer in an FcRn-dependent manner to target HCs within the villous stroma.

Although HCs have been found to be the primary cell type infected during ZIKV infection (Bhatnagar et al., 2017; Jurado et al., 2016; Quicke et al., 2016b), a limitation of our study is the relevance of the observed immune complex-mediated increase of ZIKV infection in isolated human HCs *in vitro*. To address this, we examined the impact of cross-reactive DENV mAbs on enhancement of ZIKV infection in *ex vivo* human second-trimester placental explants. ZIKV infection of the developing fetus and subsequent ZIKV-associated congenital abnormalities can occur across all three trimesters during pregnancy (Shapiro-Mendoza et al., 2017). However, because transport of maternal IgG across the placenta is minimal during the first trimester and rises dramatically between

22-26 weeks of gestation (Palmeira et al., 2012; Simister and Story, 1997), we chose to focus our study on second-trimester human explants. Recent work has demonstrated that ZIKV replicates and persists within the placentas of ZIKV-infected women as well as the brains of the developing fetuses (Bhatnagar et al., 2017). In addition, replicative intermediate viral RNA appeared to correspond to HC staining in the placenta of ZIKV-infected women (75%; n=12) with adverse pregnancy outcomes during the first or second trimester. Given that ZIKV infection induces minimal HC death (**Supplemental Figure 1E**), ZIKV immune complexes target HCs (**Figure 6C**), and that ZIKV persists in HCs throughout pregnancy, continuous spillover of ZIKV into the fetal bloodstream could lead to continuous viral seeding of the fetus.

More recent work has shown that, in a cohort of pregnant women with possible ZIKV exposure, over half of the women with previous anti-flavivirus immunity who successfully gave birth were positive for ZIKV RNA in placental tissues (Reagan-Steiner et al., 2017). Others have shown that the presence of DENV IgG in ZIKV-infected pregnant women did not significantly increase the incidence of abnormal birth outcomes compared to DENV-IgG negative patients (Halai et al., 2017b). However, this study focused on the role of previous flavivirus immunity on adverse pregnancy outcomes, not viral seeding of the placenta. Neither of these studies categorized the flavivirus-exposed, ZIKV-infected women based on DENV IgG titers nor prevalence of individual DENV IgG subclasses. Making these differentiations could potentially increase the observed incidence of viral seeding of the placenta and adverse pregnancy outcomes during ZIKV infection in flavivirus-exposed women. Our observations suggest that viral immune complexes can bypass the STB layer through an FcRn-dependent manner and establish infection within HCs localized within the villous core in an IgG-subclass dependent manner. Altogether, our data support that previous flavivirus immunity could influence viral seeding of the placenta.

DENV infection initiates a robust IgG response with peak levels occurring a few weeks after infection and persisting for a decade or longer (Wahala and Silva, 2011). Further characterization of this IgG response has shown skewed production of IgG1 and IgG3 in individuals who develop symptomatic dengue fever (Koraka et al., 2001). It has also been shown that >100-fold increased DENV-specific IgG1 can be found within the cord blood of infants born to DENV-experienced mothers compared to DENV-specific IgG4 (Castanha et al., 2016). This correlates with our findings that increased negative-sense ZIKV RNA and infectious virus release was detected in HCs and placental explants treated with cross-reactive IgG1 and IgG3 mAbs complexed to ZIKV compared to IgG4 and IgG2 mAb subclasses (**Figure 6A-B**). Translocation of IgG across the placenta is a normal physiologic process facilitated by FcRn, a specialized Fc receptor expressed by STBs, to provide passive immunity to the developing fetus (Coyne and Lazear, 2016; Simister and Story, 1997; Simister et al., 1996; Story et al., 1994). Our results could reflect that FcRn preferentially binds immune complexes comprised of different IgG subclasses. Studies examining the kinetics of monomeric human IgG (hIgG) binding to human FcRn (hFcRn) have determined that hIgG1 binds to hFcRn with greater affinity than hIgG3, hIgG4 and hIgG2, with hIgG2 exhibiting the lowest affinity for FcRn binding (Abdiche et al., 2015; Ober et al., 2001). This correlates with our observations that the highest levels of viral enhancement were observed in IgG1 and IgG3 immune complexes.

Mechanistically, we observed that DENV mAb:ZIKV immune complexes increased viral binding and entry in HCs, a phenomenon known as “extrinsic ADE” (**Figure 2B**). Moreover, we discovered that increased ZIKV infection of HCs correlated with reduced expression of RLRs (DDX58, IFIH1, DHX58) as well as key antiviral effectors (IFIT1, IFIT2, IFIT3, OAS1, RSAD2) (**Figure 3**). This may reflect the ability of ZIKV to block type I IFN signaling through mechanisms involving inhibition of STAT phosphorylation (Bowen et al., 2017a) and/or STAT2 degradation (Grant et al., 2016). An alternative hypothesis is that

binding of cross-reactive DENV mAb immune complexes to FcγRs on HCs dampens innate immune responses through a cell autonomous process termed “intrinsic ADE.” FcγRII, which is highly expressed on HCs (**Figure 5A**), is differentiated into two subclasses, FcγRIIa and FcγRIIb, each of which express cytoplasmic Ig gene family tyrosine activation or inhibitory motifs (ITAMs and ITIMS), respectively (Smith and Clatworthy, 2010). Previous studies have demonstrated that binding DENV-Ab complexes to FcγRIIa, but not FcγRIIb, enhances DENV infection of a monocytic cell line. Modifying the ITAM to an ITIM domain on FcγRIIa ablated enhanced DENV infection (Boonnak et al., 2013). However, the downstream effects of switching the ITAM and ITIM domains on modulating antiviral immunity is unclear. Our data revealed that the IgG isotype directly affects viral infection of HCs: (highest to lowest) 33.3A06 IgG3>IgG1>IgG4>> IgG2 (**Figure 5B**). This order is similar to the optimal Ab binding affinities of FcγRIIb, which is known to exert downstream inhibitory signals through its ITIM cytoplasmic domain (Smith and Clatworthy, 2010). This suggests that intrinsic ADE, in addition to extrinsic ADE, may be an important determinant in Ab-mediated augmentation of ZIKV infection in HCs.

Trafficking of IgG immune complexes coupled with high levels of cellular FcγR expression in HCs within the chorionic villi provides an ideal environment for virus immune complexes to evade the antiviral nature of the placental barrier and infect resident cells. Several congenital viruses, including hCMV and HIV-1, are known to utilize maternal antibodies to transcytose through the trophoblast layer and enter the fetal compartment through FcRn (Maidji et al., 2006; Toth et al., 1994). Similarly, we have demonstrated that DENV cross-reactive mAbs bound to ZIKV undergo FcRn-mediated transcytosis across the placenta to productively infect HCs within the villous stroma (**Figures 6-7**). These findings could have large implications concerning the role of serologic cross-reactivity on viral infections of the placenta. Past work has shown that related flaviviruses, including West Nile virus (WNV), Japanese encephalitis virus (JEV), and DENV, can be detected

within the placenta *in vivo* and have been associated with adverse outcomes such as spontaneous abortions, microcephaly, and post-natal growth defects (Centers for Disease and Prevention, 2002; Chaturvedi et al., 1980; O'Leary et al., 2006; Ribeiro et al., 2017). Our results presented here, along with previous studies concerning neurotropic flavivirus infection during pregnancy, underpin the importance of understanding of the effects of antibody-mediated viral transport in the placenta and the developing fetus.

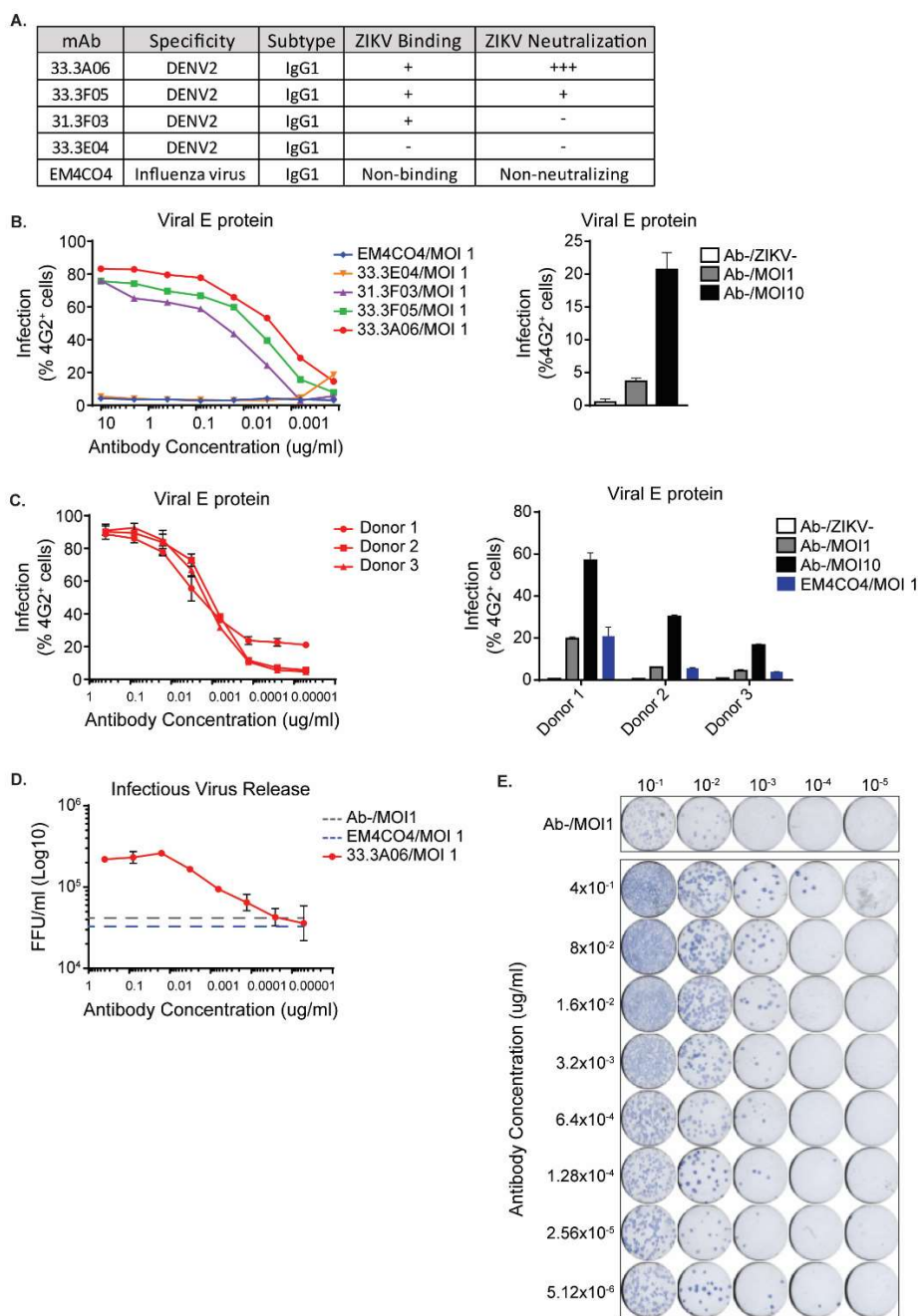


Figure 1: Cross-reactive DENV monoclonal antibodies (mAbs) enhance ZIKV infection of human placental macrophages (HCs). **A)** Binding and neutralization properties of mAbs. **B)** HC were infected with ZIKV (MOI 1) in the presence of DENV cross-reactive mAbs or EM4CO4 non-specific control (five-fold dilutions starting at 10 μ g/mL). Intracellular ZIKV E

protein was assessed by 4G2 staining at 24 hours post-infection (hpi). Antibody dilutions were performed in singlicate. Control conditions are shown as the average of biological triplicates \pm SD. Representative experiment from n=2 donors. Ab⁻, no mAb. ZIKV⁻, no ZIKV.

C) HCs were infected with ZIKV (MOI 1) in the presence of mAb 33.3A06 (five-fold dilutions starting at 0.4 ug/ml) or EM4CO4 (0.4 ug/ml). Intracellular ZIKV E protein was assessed by 4G2 staining at 24 hpi (biological triplicates \pm SD). Representative experiment from n=3 donors.

D) Infectious virus in the supernatant was assessed by focus-forming assay (FFA) at 24 hpi (biological triplicates \pm SD). Representative experiment from n=3 donors. FFU, focus-forming units.

E) Representative FFA.

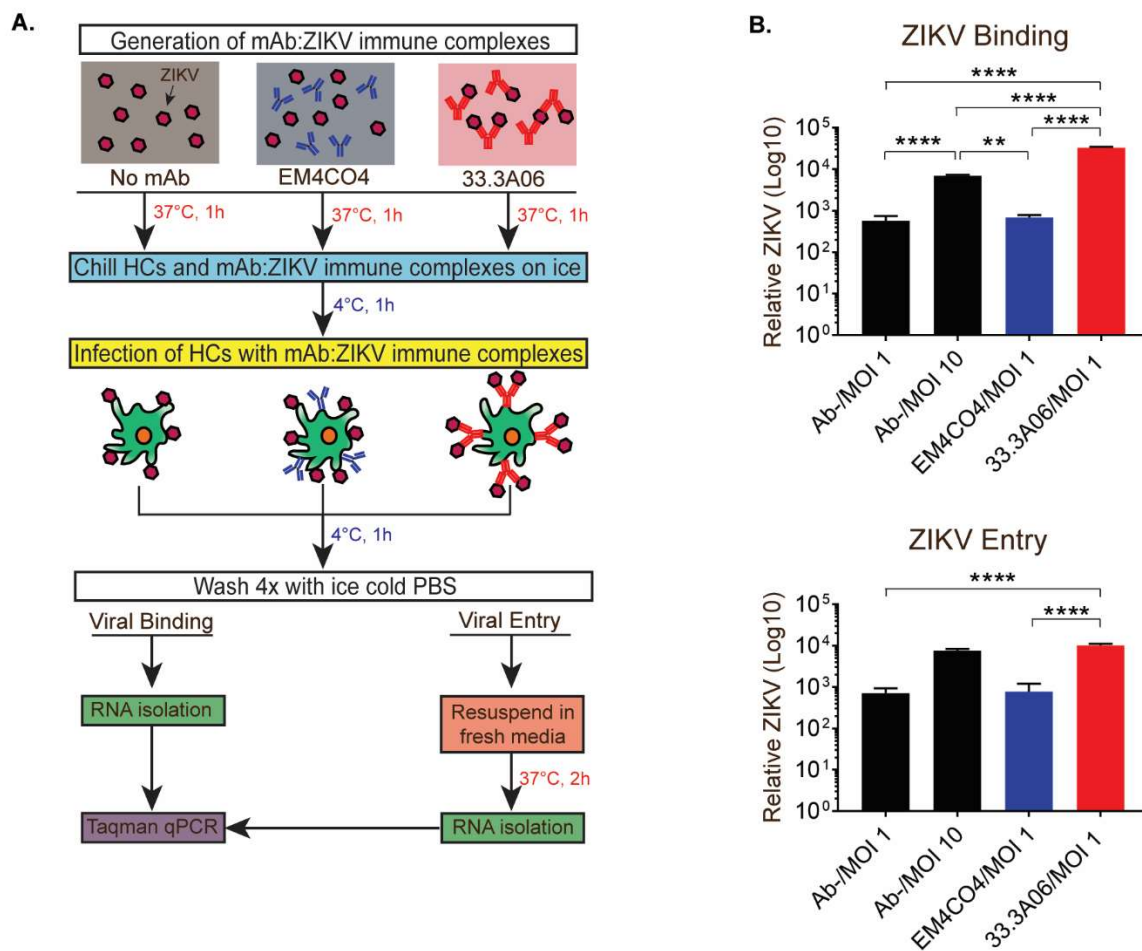


Figure 2: Infection with ZIKV in the presence of mAb 33.3A06 results in increased viral binding and entry of HCs. **A)** Binding/entry assay schematic. EM4CO4 and 33.3A06 mAbs were used at 0.4 $\mu\text{g}/\text{mL}$. **B)** ZIKV RNA from bound virus (top) or internalized virus (bottom) was measured by qRT-PCR. Representative experiment from $n=2$ donors (biological triplicates $\pm\text{SD}$). Data were analyzed by 1-way ANOVA and Tukey's multiple comparison test, $**p<0.01$, $***p<0.001$, $****p<0.0001$.

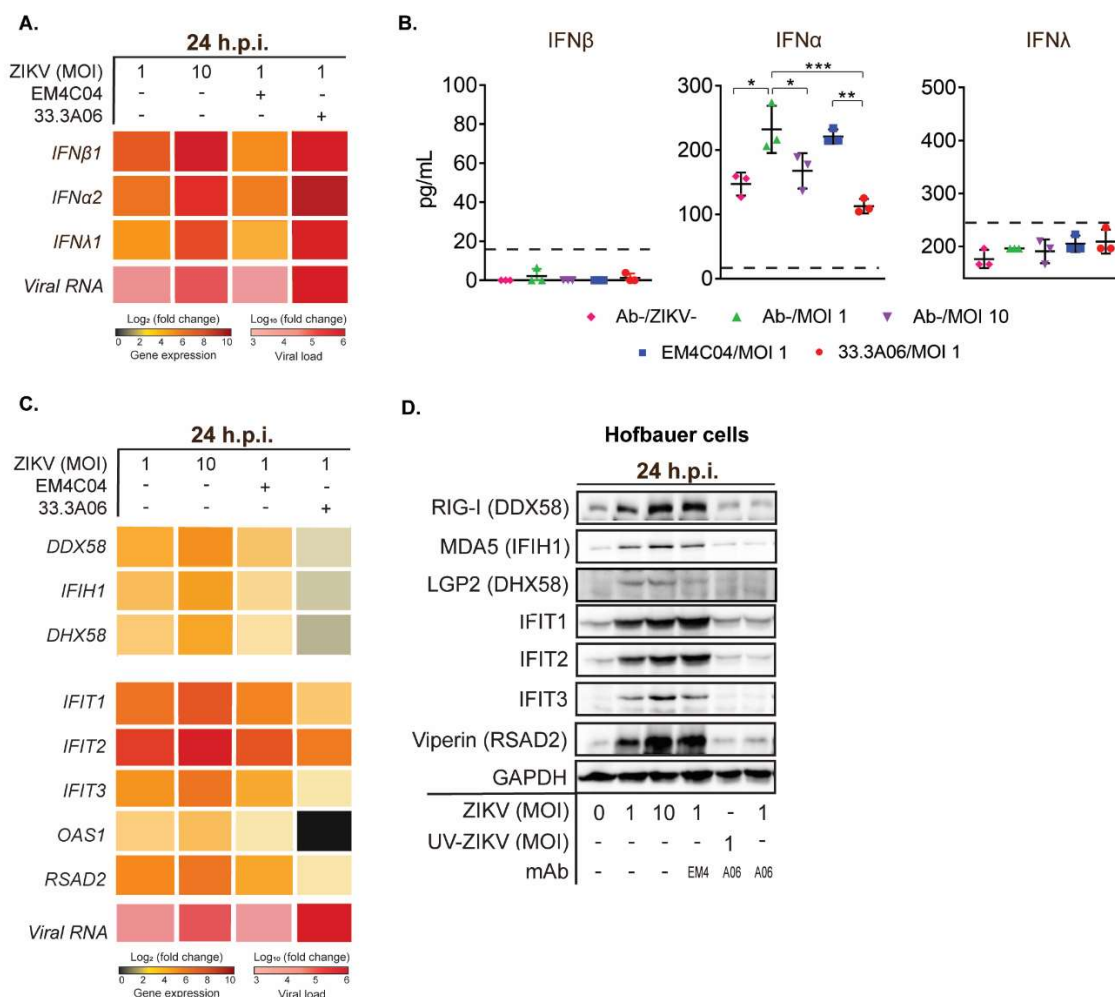


Figure 3: HCs infected with DENV mAb:ZIKV immune complexes result in blunted type I and type III IFN antiviral responses. **A)** Type I and type III IFN was measured by qRT-PCR at 24 hpi with ZIKV alone (MOI 1 and 10) or mAb:ZIKV (MOI 1) immune complexes. 33.3A06 and EM4C04 were used at 0.4 μ g/mL. Representative experiment from n=2 donors. **B)** Type I and type III IFN was measured in the supernatant at 24 hpi (biological triplicates \pm SD). Data were analyzed by 1-way ANOVA and Tukey's multiple comparison test, *p<0.05, **p<0.01, ***p<0.001. Representative experiment from n=3 donors. Dashed line indicates lower limit of detection. **C)** Antiviral effector gene

expression was measured by qRT-PCR at 24 hpi. Representative experiment from n=2 donors. **D)** Corresponding protein expression was measured at 24 hpi with the addition of mAb (0.4µg/mL): UV-inactivated ZIKV control (UV-ZIKV; MOI 1) immune complexes. Representative experiment from n=2 donors.

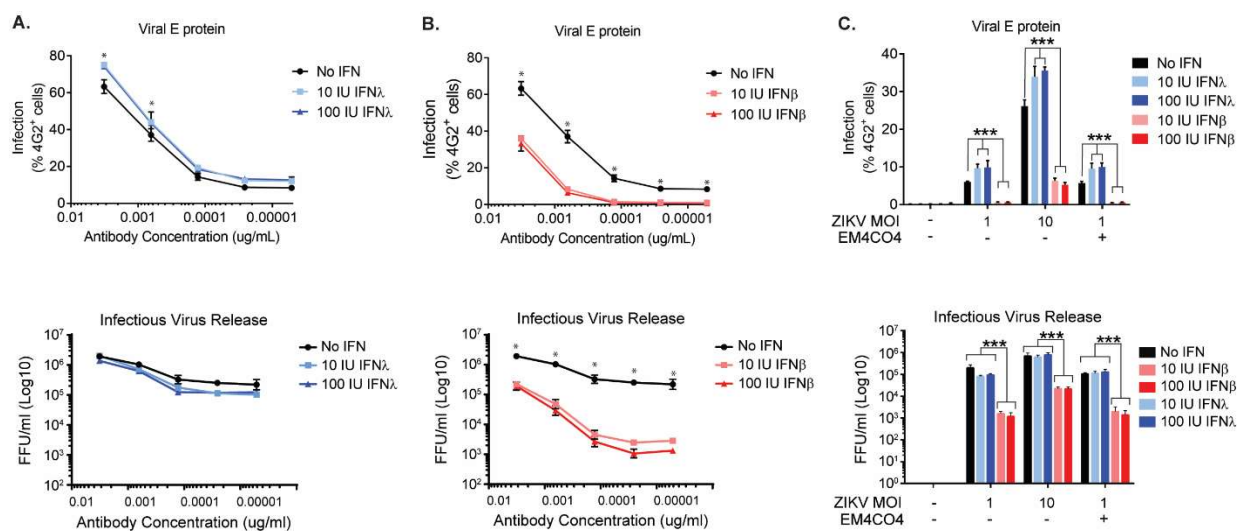


Figure 4: Type I IFN, but not type III IFN, restricts ZIKV infection of HCs. **A)** HCs were infected with ZIKV (MOI 1) in the presence of 33.3A06 mAb (five-fold dilutions starting at 3.2×10^{-3} $\mu\text{g}/\text{mL}$) and subsequently treated with 10 or 100 IU/ml of IFN- λ (blue) or left untreated (black). **B)** ZIKV-infected HCs were treated with 10 or 100 IU/ml of IFN- β (red) or left untreated (black). **C)** HCs were infected with ZIKV alone at MOI 1 or 10, or in the presence of EM4CO4 (3.2×10^{-3} $\mu\text{g}/\text{mL}$). Cells were subsequently treated with 10 or 100 IU/ml of IFN- λ (blue) or IFN- β (red) or left untreated (black). Upper panels: Intracellular ZIKV E protein was evaluated by 4G2 staining at 24 hpi. Lower panels: Supernatants from infected HCs were collected 24 hpi and assessed by FFA (biological triplicates \pm SD). Data were analyzed by 2-way ANOVA and Tukey's multiple comparison test. * $p < 0.05$, *** $p < 0.001$. Representative experiment from $n = 3-4$ donors.

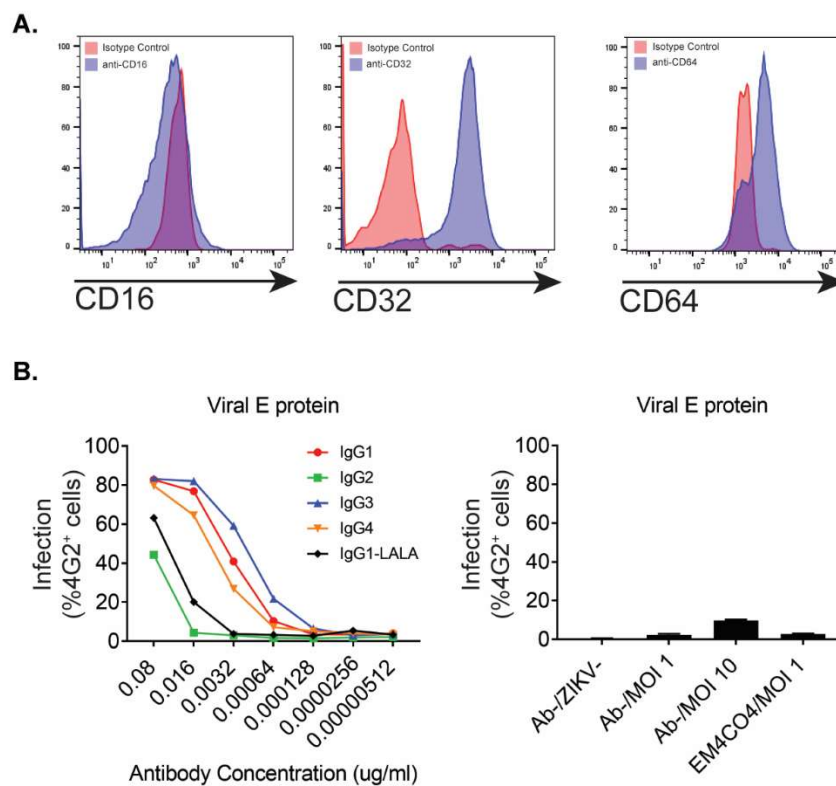


Figure 5: Enhanced ZIKV infection of HCs is modulated in an IgG subclass-dependent manner. **A)** Flow cytometry plots showing expression of FcγRIII (CD16), FcγRII (CD32), and FcγRI (CD64) of uninfected HCs. Representative experiment from n=2 donors. **B)** HCs were infected with ZIKV (MOI 1) in the presence of different 33.3A06 IgG subclasses (five-fold dilutions starting at 8×10^{-2} $\mu\text{g/mL}$). Intracellular ZIKV E protein was assessed by 4G2 staining at 24 hpi. mAb:ZIKV conditions were performed in singlicate (left) and controls (right) as the average of biological triplicates \pm SD. Representative experiment from n=3 donors.

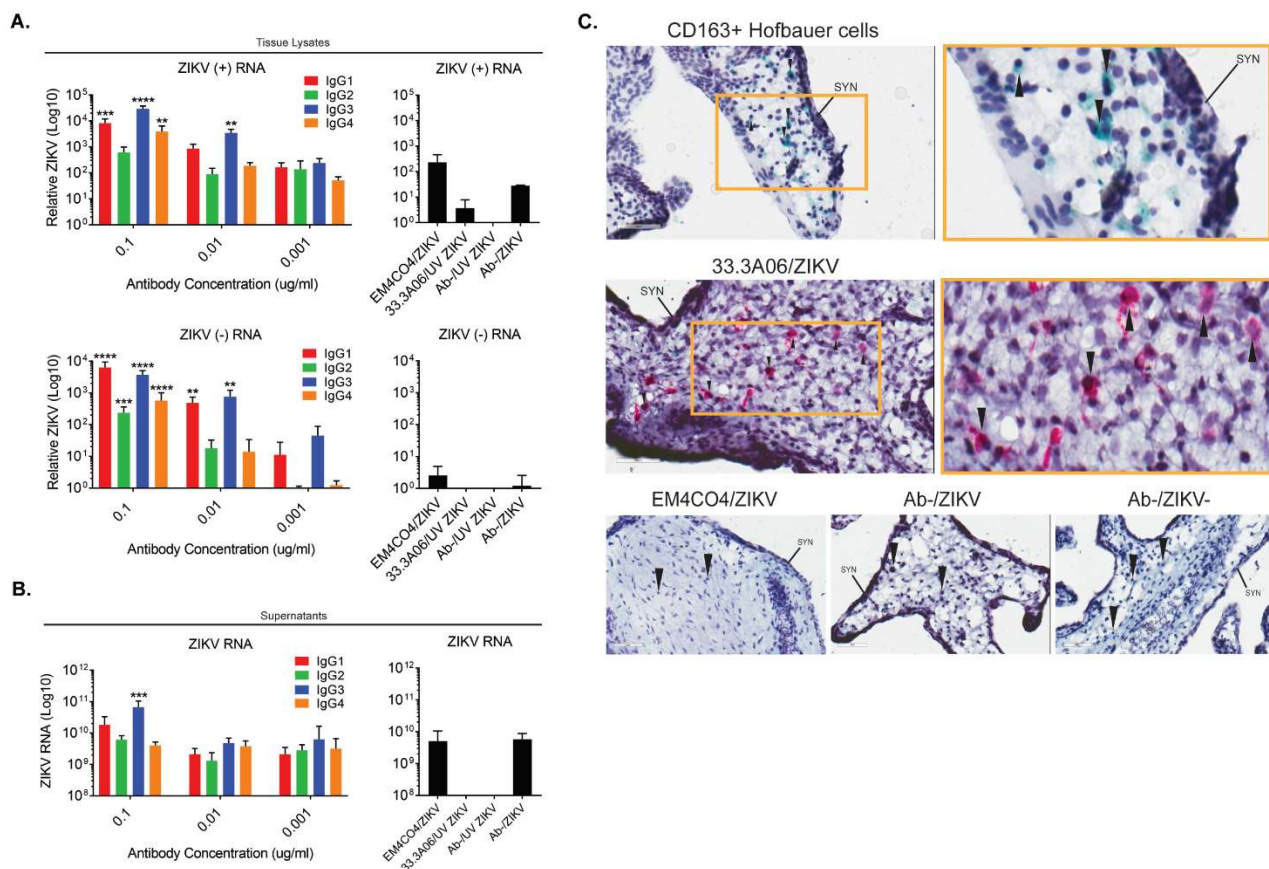


Figure 6: IgG1 and IgG3 subclasses preferentially enhance ZIKV infection of human placental explants. **A)** Human placental explants were infected with ZIKV (5×10^5 PFU/ml) in the presence of 33.3A06 mAb IgG subclasses (0.1, 0.01, 0.001 $\mu\text{g}/\text{mL}$). Viral replication within tissues was assessed by strand-specific qRT-PCR at 24 hpi (biological triplicates \pm SD). Control conditions used ZIKV alone and UV-ZIKV at 5×10^5 PFU/ml and mAbs at 0.1 $\mu\text{g}/\text{mL}$. Representative experiment from $n=3$ donors. **B)** Supernatants from human placental explants infected as in (A) were collected at 24 hpi and ZIKV RNA measured by qRT-PCR (biologic triplicates). $N=2$ donors. Data were analyzed by 1-way ANOVA and Dunnett's multiple comparison test comparing log-transformed ZIKV RNA with 33.3A06 IgG subclass ZIKV RNA levels to the log-transformed non-specific antibody control, * $p < 0.05$, ** $p < 0.01$, *** $p < 0.001$, **** $p < 0.0001$. **C)** Explants were infected with ZIKV (5×10^5 PFU/ml) in the presence of 33.3A06 (0.4 $\mu\text{g}/\text{mL}$) or EM4CO4 (0.4

ug/ml). HCs (top) and ZIKV E protein (middle and bottom) were visualized by chromogenic staining with anti-CD163 and anti-4G2 antibodies, respectively. Magnification is at 40x (left) and 80x (right, yellow box). Controls are shown across the bottom (40x magnification). SYN, syncytiotrophoblast layer. Arrows indicate HCs. N=2 donors.

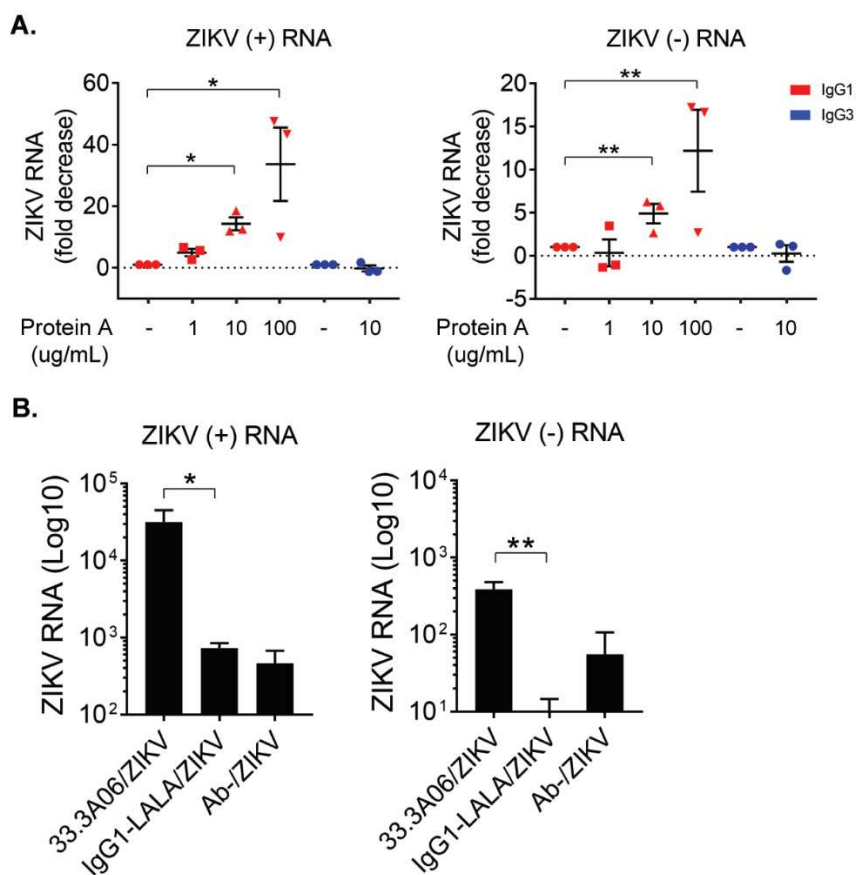
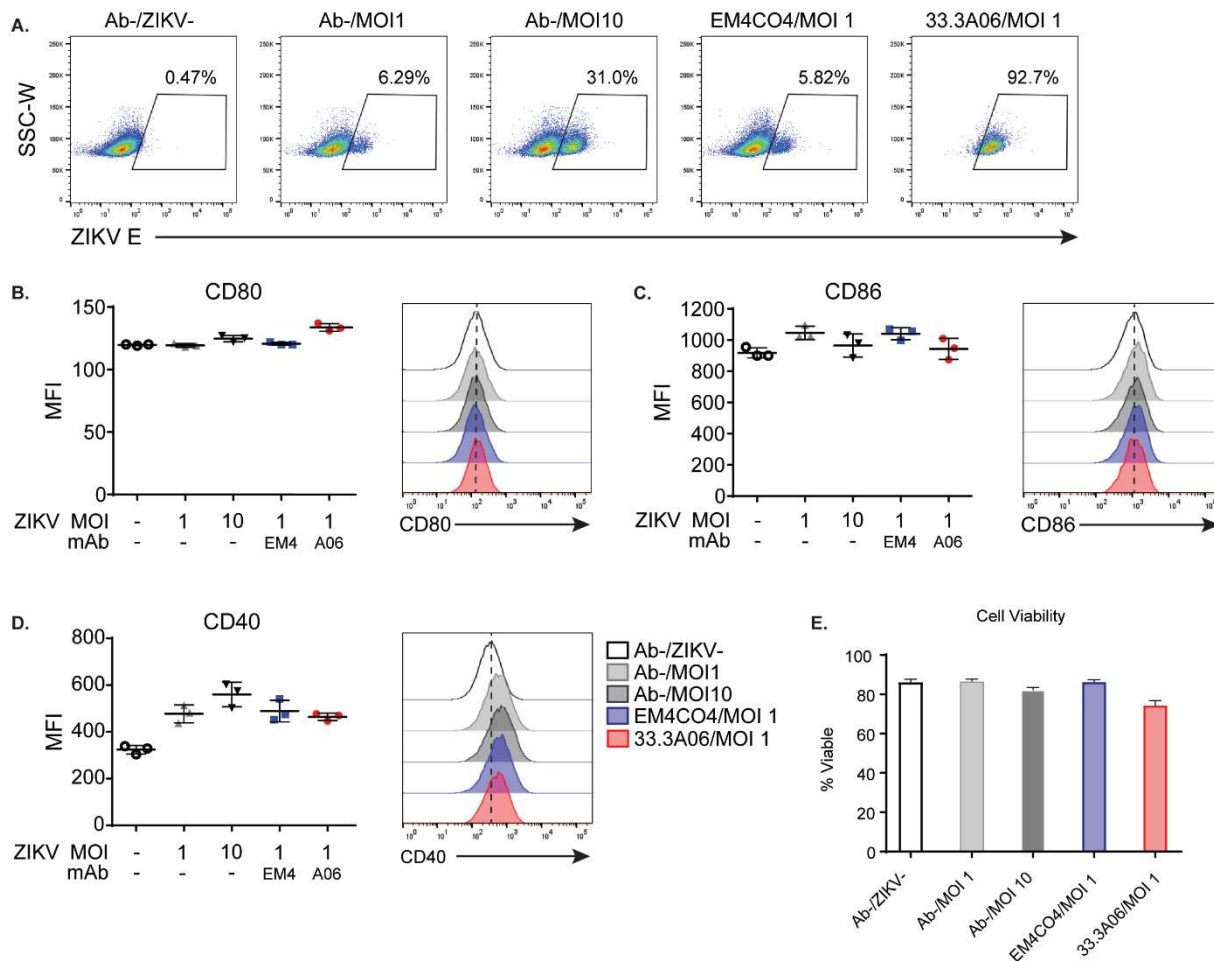
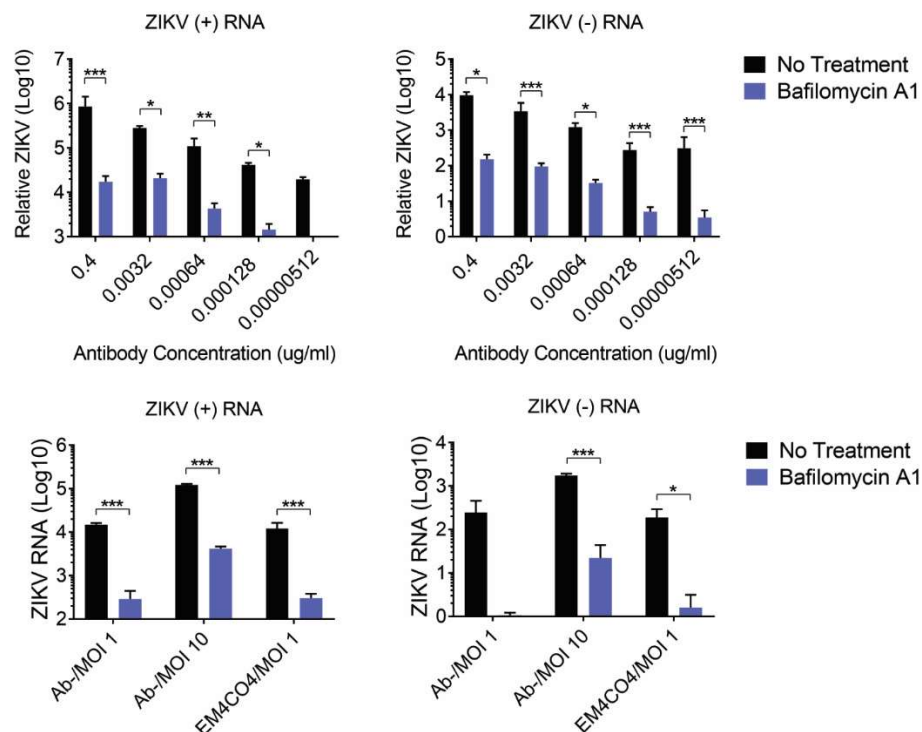


Figure 7: Targeting FcRn reduces ZIKV infection of human placental explants. **A)** Human placental explants were treated with 1, 10 or 100 ug/ml of Protein A and subsequently infected ZIKV (5×10^5 PFU/ml) in the presence of either 33.3A06 IgG1 or IgG3 mAb (0.4 ug/ml). Viral replication was assessed by strand-specific qRT-PCR at 24 hpi (biological triplicates \pm SEM). Data were analyzed by 1-way ANOVA and Dunnett's multiple comparison test, * $p < 0.05$, ** $p < 0.01$. Representative experiment from $n = 3$ donors. **B)** Human placental explants were infected with ZIKV (5×10^5 PFU/ml) in the presence of either 33.3A06 IgG1 or IgG1-LALA mutant mAbs. Viral replication was assessed by strand-specific qRT-PCR at 24 hpi (biologic triplicates \pm SD). Data were analyzed by Student's t-test, * $p < 0.05$, ** $p < 0.01$, Representative experiment from $n = 4$ donors.

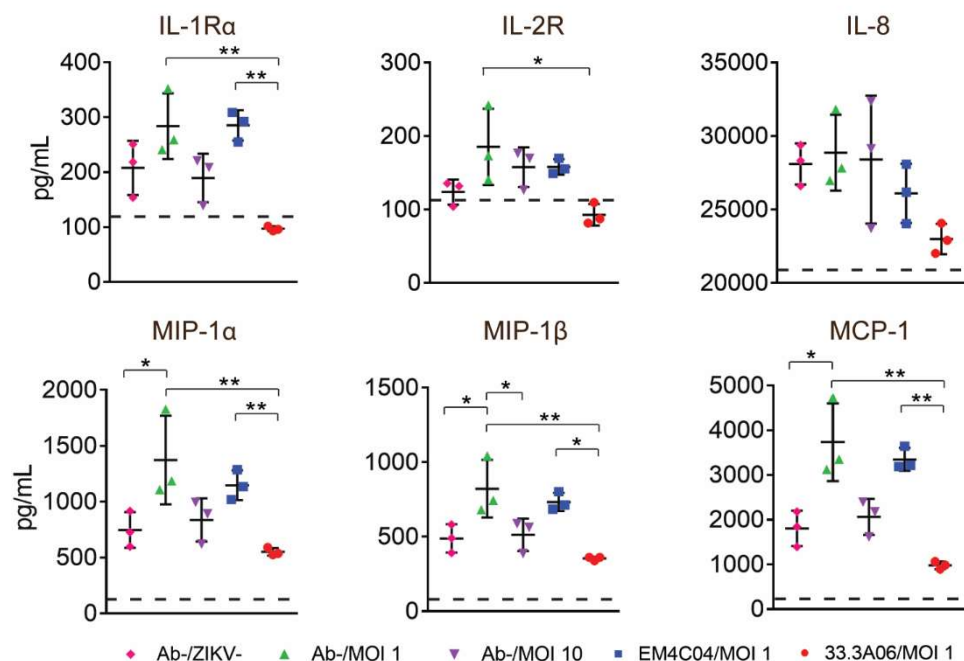


Supplementary Figure 1: HCs are modestly activated upon infection with DENV mAb:ZIKV immune complexes. **A)** Flow plots of percent infected HCs (4G2⁺) under control and ADE-ZIKV-infected conditions. 33.3A06 and EM4CO4 were used at 0.4µg/mL. Representative experiment from n=3-4 donors. Ab⁻, no mAb. ZIKV⁻, no ZIKV. **B)** Mean fluorescence intensity (MFI) of CD80 surface expression and representative histograms (right) of ADE-ZIKV-infected HCs and controls. EM4CO4 and 33.3A06 were used at 0.4µg/mL. All conditions are shown as the average of biological triplicates ±SD. Representative experiment from n=3 donors. **C)** MFI of CD86 surface expression and representative histograms (right). Conditions are identical to those in (B). Representative experiment from n=3

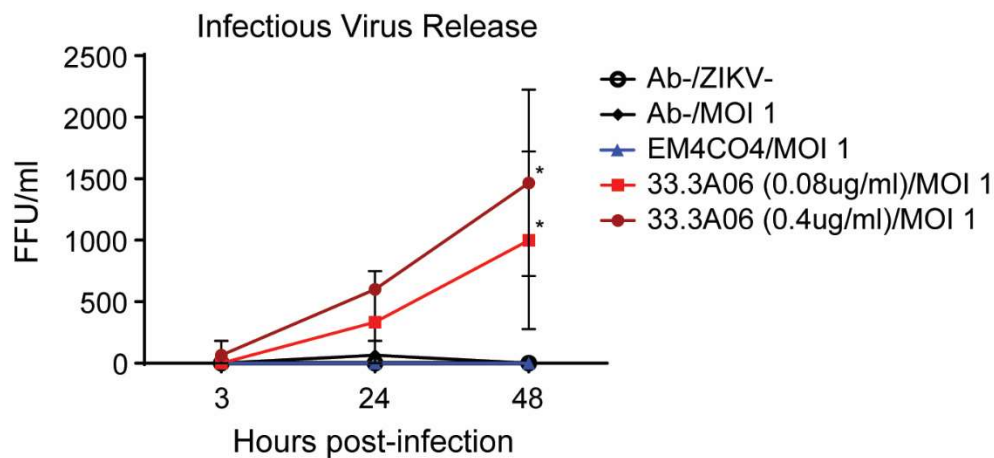
donors. **D)** MFI of CD40 surface expression and representative histograms (right). Conditions are identical to those in (B). Representative experiment from n=3 donors. **E)** Viability of HCs is not affected by ADE-ZIKV infection. Conditions are identical to those in (B). Percent viable cells was determined by Ghost dye staining and flow cytometry. Data are shown as the average of biological triplicates \pm SD. Representative experiments from n=3 donors.



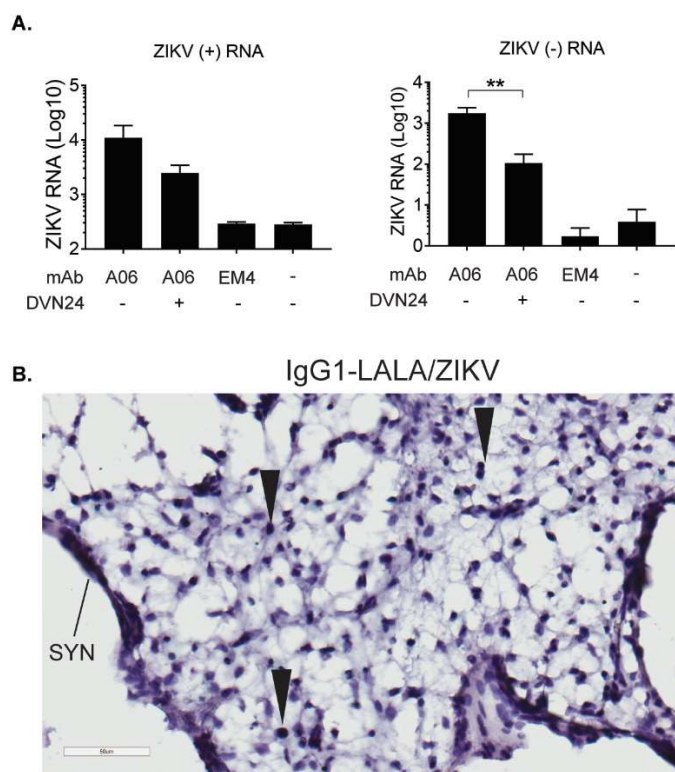
Supplementary Figure 2: DENV mAb:ZIKV immune complexes enter HCs through an endosomal pathway. HCs were treated with 100nM Bafilomycin A1 (blue) or left untreated (black) for 1 hour prior to infection with ZIKV (MOI 1) in the presence of 33.3A06 mAb (0.4, 0.0032, 0.00064, 0.000128, 0.00000512ug/ml; top) or EM4CO4 control (0.4ug/ml; bottom). Viral replication within tissues was assessed by strand-specific qRT-PCR at 24hpi. ZIKV RNA expression was normalized to *GAPDH* and is shown as the Log₁₀ fold change over time-matched Ab-/ZIKV- controls of biological triplicates \pm SD analyzed by Student's t-test for each antibody concentration, *p<0.05, **p<0.01, ***p<0.001. Representative experiment from n=2 donors.



Supplementary Figure 3: HCs infected with DENV mAb:ZIKV immune complexes fail to secrete pro-inflammatory cytokines. Cytokine concentrations in the supernatant of ADE-ZIKV-infected and control HCs were assessed by multiplex bead assay at 24hpi. 33.3A06 and EM4CO4 were used at 0.4μg/mL with ZIKV at MOI 1. Data are shown as the average of biological triplicates \pm SD analyzed by 1-way ANOVA and Tukey's multiple comparison test, * $p < 0.05$, ** $p < 0.01$. Dashed line represents lower limit of detection; IL-8: dashed line represents upper limit of detection. Representative experiments from $n=3$ donors. Ab⁻, no mAb. ZIKV⁻, no ZIKV.



Supplementary Figure 4: Cross-reactive DENV monoclonal antibodies enhance ZIKV infection of human placental explants. Explants were infected with ZIKV alone (5×10^5 pfu/ml) or in the presence of 33.3A06 mAb (0.4 and $0.08 \mu\text{g}/\text{mL}$) or EM4CO4 ($0.4 \mu\text{g}/\text{mL}$). Supernatants were collected at 3, 24, and 48 hpi and infectious virus release assessed by FFA. Data are shown as the average of biologic triplicates \pm SD analyzed by 2-way ANOVA and Tukey's multiple comparison test, $*p < 0.05$. N=2 donor. FFU, focus-forming units. Ab⁻, no mAb. ZIKV⁻, no ZIKV.



Supplementary Figure 5: FcRn facilitates enhanced infection of human placental explants. A) Human placental explants were treated with 1ug/ml of anti-FcRn blocking antibody (DVN24) and subsequently infected with ZIKV (5×10^5 pfu/ml) in the presence of 33.3A06 or EM4CO4 mAbs (0.4ug/ml). Viral replication within tissues was assessed by strand-specific qRT-PCR at 24hpi. ZIKV RNA expression was normalized to *GAPDH* and is shown as the Log_{10} fold change over time-matched Ab⁻/ZIKV⁻ controls of biological triplicates \pm SD analyzed by 1-way ANOVA and Tukey's multiple comparison test, ** $p < 0.01$. Representative experiment from $n=2$ donors. B) Human placental explants were infected with ZIKV (5×10^5 pfu/ml) in the presence of the 33.3A06 IgG1-LALA mutant mAb (0.4ug/ml). Chromogenic staining was performed for ZIKV E protein

and HCs using anti-4G2 and anti-CD163 antibodies, respectively. Magnification is at 40x. Arrows indicate HCs. SYN, syncytiotrophoblast layer.

Supplementary Table 1. Cytokine analysis of HCs infected with mAb:ZIKV immune complexes or ZIKV alone at 24 hpi

	33.3A06/MOI 1	EM4CO4/MOI 1	Ab-/ZIKV MOI 1	Ab-/ZIKV MOI 10	Ab-/ZIKV-
	Donor 27	Donor 27	Donor 27	Donor 27	Donor 27
IL-1 β	ND	ND	ND	ND	ND
IL-1Ra	ND	285.44	283.9666667	189.62	207.863333
IL-2	ND	ND	ND	ND	ND
IL-2R	ND	158.0466667	185.2766667	157.6433333	133.65
IL-4	ND	ND	ND	ND	ND
IL-5	ND	ND	ND	ND	ND
IL-6	ND	ND	ND	ND	ND
IL-7	ND	ND	ND	ND	ND
IL-8	ULD	ULD	ULD	ULD	ULD
IL-10	ND	ND	ND	ND	ND
IL-12	48.36	58.89666667	64.56333333	56.09	55.833333
IL-13	ND	ND	ND	ND	ND
IL-15	ND	ND	ND	ND	ND
IL-17	ND	ND	ND	ND	ND
TNF α	ND	ND	ND	ND	ND
IFN γ	ND	ND	ND	ND	ND
GM-CSF	ND	ND	ND	ND	ND
MIP-1 α	551.6733333	1147.326667	1373.306667	837.4533333	747.43
MIP-1 β	354.6733333	733.19	822.2266667	513.3666667	488.41333
IP-10	2.466666667	5.17	5.056666667	2.933333333	2.67
MIG	ND	ND	ND	ND	ND
Eotaxin	ND	ND	ND	ND	ND
RANTES	ND	ND	ND	ND	ND
MCP-1	981.27	3348.733333	3733.416667	2064.753333	1805.8933
IFN α	112.8566667	221.1566667	232.41	167.77	147.31
IFN β	ND	ND	ND	ND	ND

	33.3A06/MOI 1	EM4CO4/MOI 1	Ab-/ZIKV MOI 1	Ab-/ZIKV MOI 10	Ab-/ZIKV-
	Donor 29	Donor 29	Donor 29	Donor 29	Donor 29
IL-1 β	ND	ND	ND	ND	ND
IL-1Ra	ND	330.55	243.6033333	259.2066667	148.89
IL-2	ND	ND	ND	ND	ND
IL-2R	ND	ND	ND	ND	ND
IL-4	ND	ND	ND	ND	ND
IL-5	ND	ND	ND	ND	ND
IL-6	ND	ND	ND	ND	ND
IL-7	ND	ND	ND	ND	ND
IL-8	ULD	ULD	ULD	ULD	ULD
IL-10	ND	ND	ND	ND	ND
IL-12	38.01666667	50.45	47.78	46.97	40.2
IL-13	ND	ND	ND	ND	ND
IL-15	ND	ND	ND	ND	ND
IL-17	ND	ND	ND	ND	ND
TNF α	ND	ND	ND	ND	ND
IFN γ	ND	ND	ND	ND	ND
GM-CSF	ND	ND	ND	ND	ND
MIP-1 α	243	422.31	305.8833333	447.88	185.43333
MIP-1 β	204.4666667	413.4733333	318.6133333	387.05	220.67
IP-10	2.176666667	4.813333333	3.903333333	5.66	2.0333333
MIG	ND	ND	ND	ND	ND
Eotaxin	ND	ND	ND	ND	ND
RANTES	ND	ND	ND	ND	ND
MCP-1	469.39	1469.966667	1050.526667	1415.703333	431.74667
IFN α	70.10666667	131.74	111.6433333	128.2866667	76.333333
IFN β	ND	ND	ND	ND	ND

	33.3A06/MOI 1	EM4CO4/MOI 1	Ab-/ZIKV MOI 1	Ab-/ZIKV MOI 10	Ab-/ZIKV-
	Donor 30	Donor 30	Donor 30	Donor 30	Donor 30
IL-1 β	ND	ND	ND	ND	ND
IL-1Ra	212.0033333	452.52	378.9633333	484.6833333	303.32667
IL-2	ND	ND	ND	ND	ND
IL-2R	142.2366667	171.865	160.48	167.2666667	192.76
IL-4	ND	ND	ND	ND	ND
IL-5	ND	ND	ND	ND	ND
IL-6	21.16333333	19.245	17.81	20.40333333	113.85
IL-7	ND	ND	ND	ND	ND
IL-8	ULD	ULD	ULD	ULD	ULD
IL-10	ND	ND	ND	ND	ND
IL-12	53.08333333	62.90666667	60.19	57.77	55.753333
IL-13	ND	ND	ND	ND	ND
IL-15	ND	ND	ND	ND	ND
IL-17	ND	ND	ND	ND	ND
TNF α	ND	ND	ND	ND	ND
IFN γ	ND	ND	ND	ND	ND
GM-CSF	ND	ND	ND	ND	ND
MIP-1 α	712.32	858.9466667	891.68	1224.766667	893.62667
MIP-1 β	492.8533333	612.7033333	621.7533333	790.6733333	566.96333
IP-10	3.226666667	6.106666667	5.886666667	9.936666667	2.62
MIG	ND	ND	ND	ND	ND
Eotaxin	ND	ND	ND	ND	ND
RANTES	ND	ND	ND	ND	ND
MCP-1	1604.27	3424.093333	3491.36	3790.723333	2077.4933
IFN α	138.4833333	218.6166667	224.7	240.7933333	153.01667
IFN β	ND	ND	ND	ND	ND

Supplementary Table 1: Cytokine levels in the supernatants of non-ADE- and ADE-ZIKV-infected HCs at 24hpi as measured by multiplex bead array (n=3 donors). All values are represented as “pg/mL.” Cytokine levels that were above the limit of detection are indicated as “ULD” (upper limit of detection). Cytokine levels that are below the lower limit of detection are indicated as “ND” (not detected). N= 3 donors.

Supplementary Table 2. ZIKV-specific primer/probe sequences used for qRT-PCR

	Reaction	Name	Assay Target	Genome Position	Sequence (5' → 3')
ZIKV	qPCR primer 1	ZIKV_907	prM-E	907-929	TTGGTCATGATACTGCTGATTGC
	qPCR primer 2	ZIKV_983c	prM-E	983-962	CCTTCCACAAAGTCCCTATTGC
	Probe	ZIKV_932 FAM-NFQ	prM-E	932-958	CGGCATACAGCATCAGGTGCATAGGAG
ZIKV (+) strand	cDNA primer	T7_ZIKV_983c	prM-E (+)	983-962	<u>CGGTAATACGACTCACTATA</u> CCCTTCCACAAAGTCCCTATTGC
	qPCR primer 1	ZIKV_907	prM-E (+)	907-929	TTGGTCATGATACTGCTGATTGC
	qPCR primer 2	T7tag	prM-E (+)		CGGTAATACGACTCACTATA
	Probe	ZIKV_932 FAM-NFQ	prM-E (+)	932-958	CGGCATACAGCATCAGGTGCATAGGAG
ZIKV (-) strand	cDNA primer	GVA_ZIKV_907	prM-E (-)	907-929	<u>TTTGCTAGCTTTAGGACCTACTATATCTACCT</u> TTGGTCATGATACTGCTGATTGC
	qPCR primer 1	ZIKV_983c	prM-E (-)	983-962	CCTTCCACAAAGTCCCTATTGC
	qPCR primer 2	GVAtag	prM-E (-)		TTTGCTAGCTTTAGGACCTACTATATCTACCT
	Probe	ZIKV_932 FAM-NFQ	prM-E (-)	932-958	CGGCATACAGCATCAGGTGCATAGGAG

Supplementary Table 2: ZIKV-specific primer and probe sequences adapted from Lanciotti et al. (2008) and used for ZIKV RNA qRT-PCR and ZIKV strand-specific qRT-PCR. Genome position is in reference to Zika virus strain ZIKV/Homo Sapiens/PRI/PRVABC59/2015 (GenBank accession number: KX601168.1). Unique 5' tag sequences are underlined.

Materials and Methods

CONTACT FOR REAGENT AND RESOURCE SHARING

Further information and requests for resources and reagents should be directed to and will be fulfilled by the corresponding author Mehul Suthar (msuthar@emory.edu).

EXPERIMENTAL MODEL AND SUBJECT DETAILS

Ethics statement. Second trimester human placentae were obtained from consented donors who elected to terminate normal pregnancies between weeks 14-20 of gestation. Tissues were received from the University of Pittsburgh Health Sciences Tissue Bank via an honest broker system as approved by the University of Pittsburgh Institutional Review Board and in accordance with the University of Pittsburgh anatomical tissue procurement guidelines. Human term placentae (>37 weeks gestation) were collected from hepatitis B, HIV-1 seronegative women (>18 years of age) immediately after elective cesarean section without labor from Emory Midtown Hospital, Atlanta, GA. This study was approved by the Emory University Institutional Review Board (IRB 000217715). Written informed consent was acquired from all donors before cesarean section and sample collection. Samples were de-identified before being transferred to laboratory personnel for primary HC isolation.

Viruses and cells. Zika virus (ZIKV) strain PRVABC59 was used for all experiments. PRVABC59 was initially isolated in 2015 from a patient infected while in Puerto Rico. We obtained this strain from the Centers for Disease Control and Prevention in Fort Collins, CO. The virus used in these experiments has undergone a total of 5 passages in Vero cells. Viral titers were determined by plaque assay on Vero cells (ATCC® CCL81™). ZIKV was UV-inactivated (UV-ZIKV) by exposing virus to UV light in a Spectroline UV

Crosslinker for 1 hour. Vero cells were cultured in complete DMEM medium consisting of 1x DMEM (Corning Cellgro), 10% FBS, 25mM HEPES Buffer (Corning Cellgro), 2mM L-glutamine, 1mM sodium pyruvate, 1x Non-essential Amino Acids, and 1x antibiotics, and were maintained at 37°C and 5% CO₂.

Hofbauer cell model. HCs were isolated from membrane-free villous placenta as previously described (Johnson and Chakraborty, 2012). On average, the purity was >95%. After isolation, HCs were cultured in complete RPMI medium consisting of 1x RPMI (Corning Cellgro), 10% FBS (Optima, Atlanta Biologics), 2mM L-glutamine (Corning Cellgro), 1mM sodium pyruvate (Corning Cellgro), 1x Non-essential Amino Acids (Corning Cellgro), 1x antibiotics (penicillin, streptomycin, amphotericin B; Corning Cellgro) at 37°C and 5% CO₂. HCs were infected immediately following isolation. Monoclonal antibodies (mAb) were diluted in 1x PBS to the desired concentrations and mixed 1:1 with ZIKV at MOI of 1. No antibody (Ab-) conditions received 1x PBS; no virus (ZIKV-) conditions received RPMI. DENV mAb:ZIKV immune complexes were incubated at 37°C for 1 hour. HCs were then infected in 200ul mAb:ZIKV complexes, or with ZIKV alone at MOI of 1 or 10, as indicated, at 37°C for 1 hour. HCs were washed once with warm RPMI to remove residual immune complexes and re-suspended in complete RPMI medium. Infected cells were incubated at 37°C.

Human placental explant model. Chorionic villi were dissected from placental tissue and maintained in DMEM/F12 medium (ThermoFisher Scientific, Gibco) with 10% FBS and penicillin/streptomycin at 37°C and 5% CO₂. Villi were separated into individual wells of a 48-well plate each containing 800ul of DMEM/F12 medium for subsequent experiments. Following isolation of human placental explants, diluted mAbs were mixed 1:1 with 5x10⁵ PFU/ml ZIKV. After the 1 hour incubation, 200ul of explant medium was removed from

each well before addition of 200ul mAb:ZIKV complexes. Tissues were incubated at 37°C for 2 hours then washed 2x with warm complete DMEM/F12 medium to remove residual immune complexes and re-supplied with 800ul complete DMEM/F12 medium. Infected explant tissues were incubated at 37°C and 5% CO₂.

Antibodies. The human monoclonal antibodies (mAbs) used in these experiments were generated as previously described (Priyamvada et al., 2016b). Briefly, plasmablasts were isolated from DENV-infected patients and single cell sorted for use in expression cloning. Immunoglobulin (Ig) genes were amplified by RT-PCR and inserted into IgG1 expression vectors. IgG1 vectors were transiently expressed in expi293F cells and secreted IgG antibodies were purified from supernatants using protein A coupled sepharose beads (Pierce). Antibodies were stored in 1x PBS with 0.05% sodium azide. The pan-flavivirus anti-envelope protein 4G2 mAb (mouse IgG1) was isolated from the supernatant of mouse hybridoma D1-4G2-4-15 (ATCC; HB-112) using a protein G column (GE Life Sciences). IgG2, IgG3, and IgG4 variants of mAb 33.3A06 were generated by subcloning the heavy chain variable domain into the appropriate IgG subclass vector by restriction digest (AgeI and Sall) and ligation. IgG3 antibodies were purified using protein G coupled sepharose beads (Pierce). The IgG1-LALA variant of mAb 33.3A06 was generated by replacing the constant region of the wild-type IgG1 heavy chain expression vector with a gene synthesized construct (Integrated DNA Technologies), containing a leucine (L) to alanine (A) substitution at amino acid positions 234 and 235 of the IgG1 constant region by restriction digest (Sall and HindIII) and ligation.

Interferon treatment. IFN- β (PBL Assay Science) and IFN- λ (PBL Assay Science) were diluted in complete RPMI medium and added to HCs at 10 IU/ml or 100 IU/ml following the 1-hour infection incubation.

Flow cytometry. Most conditions were run with biological triplicate samples, and 2×10^5 HCs were used per sample. HCs were blocked for 10min on ice with 0.25ul/sample Human TruStain FcX (BioLegend) in FACS buffer (1x PBS, 0.1% BSA, 1mM EDTA) and stained for surface markers for 20min on ice using 0.25ul/sample of the following anti-human antibodies from BioLegend in FACS buffer: CD14 (M5E2), CD80 (2D10), CD86 (IT2.2), CD40 (5C3), and HLA-DR (G46-6; BD Biosciences); or CD16 (3G8), CD32 (FUN-2), CD64 (10.1), and Ms IgG Isotype Control (C1.18.4; TONBO Biosciences). Cells were also live/dead stained for 20min on ice with 0.1ul/sample either Ghost 780 or Ghost 510 viability dye (TONBO Biosciences) in 1x PBS. HCs were fixed with 1x Transcription Factor Fix/Perm (diluted in Transcription Factor Fix/Perm Diluent; TONBO Biosciences) for 20min on ice and permeabilized by washing twice with 1x Flow Cytometry Perm Buffer (diluted in ddiH₂O; TONBO Biosciences). HCs were re-blocked for 5min on ice with 0.25ul/sample Human TruStain FcX and 0.25ul/sample normal mouse serum (ThermoFisher Scientific) in Perm Buffer and stained for ZIKV E protein for 20min on ice using 0.5ul/sample of a 4G2-APC antibody in Perm Buffer. Unconjugated monoclonal 4G2 antibody was conjugated to APC using a Novus Lighting-Link kit per the manufacturer's instructions. Flow cytometry samples were re-suspended in 1x PBS and run on an LSR-II flow cytometry machine.

Focus-forming assay. Focus-forming assay (FFA) was performed on Vero cells with supernatants from ADE-ZIKV-infected HCs (2×10^5 cells per condition) or human placental explants and accompanying controls. Supernatants were initially diluted 1:10 in DMEM with 1% FBS followed by 10-fold serial dilution. Vero cells were plated in a 96-well plate and infected with 50ul diluted supernatant for 1 hour at 37°C. Cells and inoculum were then overlaid with methylcellulose (DMEM [Corning Cellgro], 1% antibiotic, 2% FBS, 2% methylcellulose [Sigma Aldrich]) and incubated at 37°C for 72 hours. Methylcellulose was

aspirated, and cells were washed 3x with 1x PBS and fixed/permeabilized with a 1:1 mixture of acetone and methanol. Cells were washed once with 1x PBS and blocked with 5% milk in 1x PBS for 20min at RT. Cells were incubated with primary mouse 4G2 antibody (1 μ g/mL) in 5% milk in 1x PBS for 2 hours at RT and washed 2x with 1x PBS. Goat anti-mouse HRP-conjugated secondary antibody was applied at 1:3000 dilution in 5% milk in 1x PBS for 1 hour at RT. Cells were washed 2x with 1x PBS and foci were developed with TrueBlue Peroxidase Substrate (KPL). Plates were read on a CTL50 ImmunoSpot S6 Micro Analyzer and spots were counted manually using ImageJ.

Binding and entry assay. DENV mAb:ZIKV immune complexes were prepared as described above and incubated for 1 hour at 37°C. mAb:ZIKV complexes and HCs were then chilled on ice for 1 hour prior to infection. HCs were infected with mAb:ZIKV complexes for 1 hour on ice and then washed 4x with ice cold 1x PBS. To assess virus binding to the cell surface, HCs were immediately lysed in RNA lysis buffer after washes as previously described (Boonnak et al., 2013). To assess viral entry into cells, HCs were re-suspended in pre-warmed complete RPMI medium and incubated at 37°C for 2 hours. HCs were then washed 4x with ice cold 1x PBS and lysed in RNA lysis buffer as previously described (Bowen et al., 2017a). ZIKV genomic RNA levels were assessed by qRT-PCR as described above.

Quantitative real time-PCR. HCs infected with DENV mAb:ZIKV immune complexes and control cells (1x10⁵ cells per condition) were lysed in RNA Lysis Buffer. Total RNA was isolated from cells using the Quick-RNA MiniPrep Kit (Zymo Research) per the manufacturer's instructions. For human placental explants, tissues infected with DENV mAb:ZIKV immune complexes and control conditions were suspended in TRI reagent and mechanically homogenized using ceramic bead tubes (Omni International) on a

Beadraptor Homogenizer. Total RNA was isolated from homogenized tissues using the Direct-zol RNA MiniPrep Plus Kit (Zymo Research) per the manufacturer's instructions. Purified RNA was reverse transcribed using random primers with the High-Capacity cDNA Reverse Transcription Kit (Applied Biosystems). HC gene expression and ZIKV viral RNA levels were quantified by qRT-PCR using PrimeTime Gene Expression Master Mix (Integrated DNA Technologies), ZIKV-specific primers and probe set (see **Table S2**) (Lanciotti et al., 2008) and TaqMan gene expression assays (ThermoFisher) for host genes (see **Table S3**): *Gapdh* (Hs02758991_g1), *Ifna2* (Hs00265051_s1), *Ifnb1* (Hs01077958_s1), *Ifnl1* (Hs00601677_g1), *Ifit1* (Hs03027069_s1), *Ifit2* (Hs01922738_s1), *Ifit3* (Hs01922752_s1), *Ddx58* (Hs01061436_m1), *Ifih1* (Hs00223420_m1), *Dhx58* (Hs01597843_m1), *Oas1* (Hs00973637_m1), and *Rsad2* (Hs00369813_m1). C_T values were normalized to the reference gene *Gapdh* and represented as fold change over values from time-matched mock samples using the formula $2^{-\Delta\Delta C_T}$. All primers and probes were purchased from Integrated DNA Technologies (IDT). qRT-PCR was performed in 384-well plates and run on an Applied Biosystems 7500 HT Real-Time PCR System.

ZIKV strand-specific qRT-PCR. Purified RNA was reverse transcribed using oligo(dT) and a ZIKV-specific cDNA primer. The two ZIKV-specific cDNA primers are complementary to either the positive-strand or negative-strand and include a unique 5' tag (see **Table S2**). Two cDNA and qRT-PCR reactions were run for each sample, one for positive-strand and one for negative-strand. For ZIKV strand-specific detection, a ZIKV-specific primer and tag-specific primer were used for targeted amplification of the tagged cDNA in addition to the ZIKV-specific probe. C_T values were normalized to the reference gene *Gapdh* and represented as fold change over values from time-matched mock samples using the formula $2^{-\Delta\Delta C_T}$.

qRT-PCR of viral RNA from supernatants. Total RNA was isolated from the supernatants of infected HCs and human placental explants using the QIAamp Viral RNA Mini Kit (QIAGEN) per the manufacturer's instructions. ZIKV RNA standard was generated by annealing two oligonucleotides spanning the target ZIKV prM-E gene region and performing *in vitro* transcription using the MEGAscript SP6 Transcription Kit (Ambion). For ZIKV RNA quantification in supernatants, a standard curve was generated using tenfold serial dilutions of ZIKV RNA standard, and qRT-PCR was performed using ZIKV-specific primers and probe (see **Table S2**) (Lanciotti et al., 2008). Viral RNA copies were interpolated from the standard curve using the sample C_T value and represented as copies per mL of supernatant.

Multiplex bead assay. Type I IFN and cytokine concentrations in the supernatants of ADE-ZIKV-infected HCs (2×10^5 cells per condition) and accompanying controls were assessed using a human cytokine 25-plex panel (Novex) and a ProcartaPlex human IFN-beta simplex kit (Invitrogen) per the manufacturers' instructions. Plates were read on a Luminex 100 Analyzer.

Western blot. ADE-ZIKV-infected HCs and control cells (1.2×10^6 cells per condition) were washed 2x with 1x PBS with 1mM EDTA and lysed with modified RIPA buffer (10mM Tris, 150mM NaCl, 1% NA-deoxycholate, 1% Triton X-100, 1x protease inhibitor cocktail [ThermoFisher Scientific], 1x phosphatase inhibitor cocktail [ThermoFisher Scientific]). Protein concentrations were determined by Bradford assay – 2ul cell lysate in 200ul 1x Bradford Reagent (BioRad) and read on a SynergyH1 Hybrid Reader (BioTek). Proteins were denatured with 1x loading buffer (0.25M Tris, 40% glycerol, 20% β -ME, 9.2% SDS, 0.04% Bromophenol Blue) and boiling for 15min. Lysates were then run on SDS-PAGE gel and transferred to nitrocellulose membrane for Western blotting. Blots were blocked in

5% milk in PBST (1xPBS, 0.1% Tween-20) and rinsed with ddiH₂O. Blots were incubated with the following primary antibodies in PBST with 10% FBS: Rb anti-IFIT1 (1:1000; Cell Signaling), Ms anti-IFIT2 (1:1000; Cell Signaling), Rb anti-IFIT3 (1:10,000; kindly provided by Dr. Ganes Sen), Rb anti-RIG-I (1:1000; Cell Signaling), Rb anti-MDA5 (1:1000; Cell Signaling), Rb anti-LGP2 (1:100; IBL), Rb anti-Viperin (1:1000; Cell Signaling), and Rb anti-GAPDH (1:2500; Cell Signaling). Blots were washed with PBST and incubated for 10min with anti-mouse or anti-rabbit HRP-conjugated secondary antibodies at 1:750 dilution in PBST with 1% FBS. Blots were washed again with PBST and developed with ThermoScientific SuperSignal West Femto Maximum Sensitivity Substrate. Blots were imaged on a BioRad ChemiDocXRS+.

Endosomal pathway inhibitor analysis. Human HCs were treated with 100nM Bafilomycin A1 (Cayman Chemical Company) 1 hour prior to infection with immune complexes. Infection was performed as described above and without the removal of Bafilomycin A1. RNA was extracted from tissues and analyzed by ZIKV strand-specific qRT-PCR as described above.

FcRn blocking analysis.

Protein A treatment. Human placental explants were treated with 1, 10 or 100 ug/ml of Protein A from *Staphylococcus aureus* (ThermoFisher Scientific) prior to infection with immune complexes. Infection was performed as described above and without the removal of Protein A. Upon removal of viral inoculum and re-suspension in complete DMEM/F12, 1, 10 or 100 ug/ml of Protein A was added back into cell supernatant. RNA was extracted from tissues and analyzed by ZIKV strand-specific qRT-PCR as described above.

FcRn blocking Ab. Human placental explants were treated with 1 ug/ml of an anti-FcRn blocking antibody (DVN24; Aldevron) prior to infection with immune complexes. Infection was performed as described above and without the removal of the blocking antibody. Upon removal of viral inoculum and re-suspension in complete DMEM/F12, 1 ug/ml anti-FcRn blocking antibody was added back into cell supernatant. RNA was extracted from tissues and analyzed by ZIKV strand-specific qRT-PCR as described above.

Chromogenic staining and imaging. Human placental explants were fixed in 4% PFA and incubated overnight in 30% sucrose solution. Tissues were then flash frozen in OCT media (Sakura) using 2-methylbutane (ACROS Organics) cooled on dry ice. 20 µm slices were made from tissue blocks and affixed to slides in chilled acetone. Tissues were washed once in 1x TBS Buffer (Abcam) for 5min and permeabilized with 0.3% Triton-X 100 (Fisher Scientific) in TBS for 20min at RT. After washing 3 times in 1x TBS, antigen retrieval was performed by submerging tissue slides in 1x DIVA Decloaker solution (Biocare Medical) and boiling in vegetable steamer for 30min. Tissues were washed 3 times in 1x TBS and incubated with primary antibodies (made up in TBS with 1% BSA and 0.05% Tween-20) overnight at 4°C – Ms anti-4G2 (3 ug/ml), Rb anti-CD163 (1:300; Abcam). Next, tissues were washed and incubated with either Mach 2 mouse AP polymer (Biocare Medical) or Mach 2 rabbit HRP polymer (Biocare Medical) for 30min at RT. Slides were washed and stained with Warp Red (for AP polymer; Biocare Medical) or Vina Green (for HRP polymer; Biocare Medical) for approximately 5min. Counterstain was performed with Hematoxylin (Vector Laboratories) for 30sec and washing in ddH₂O. Slides were dried for 3min at 60°C and mounted with Cytoseal (VWR). Slides were imaged using an Aperio Slide Scanner (Leica Biosystems) at 40x magnification.

QUANTIFICATION AND STATISTICAL ANALYSIS

Statistical analyses. Viral binding and entry assays were analyzed using 1-way ANOVA and Tukey's multiple comparison test, $p < 0.05$. Cytokine protein data (multiplex bead assay) and viral binding/entry data were analyzed by 1-way ANOVA followed by Tukey's test for multiple comparisons, $p < 0.05$. Interferon treatment data were analyzed by 2-way ANOVA followed by Tukey's test for multiple comparisons, $p < 0.05$. Viral RNA data for both the IgG subclass infections and Protein A treatments of mid-gestation placental explants were analyzed by 1-way ANOVA and Dunnett's multiple comparison test, $p < 0.05$. Viral RNA data from HCs treated with Bafilomycin A and explants infected with the 33.3A06 IgG1-LALA mutant mAb were analyzed by Student's t-test, $p < 0.05$. All statistical analysis was performed using GraphPad Prism software. In each of the main and supplemental figure legends, "N" represents the number of patient placental donors from which HCs or explants were derived. Further experimental statistical details can be found in the Figure legends.

Chapter 3: Anti-Zika virus IgM Inhibits Translocation and Enhancement of Zika virus Infection within the Human Placenta

Matthew G. Zimmerman^{1,2}, Matt Collins, Deepa Machiah^{2,4}, Robert C. Kauffman^{1,2}, Emery Register^{1,2}, Sarah Cordes^{3,6}, Valerie Jean, Lisa Haddad³, Jens Wrammert^{1,2}, Mehul S. Suthar^{1,2,*}

¹Department of Pediatrics, Division of Infectious Disease, Emory University School of Medicine, Atlanta, GA 30322, USA.

²Emory Vaccine Center, Yerkes National Primate Research Center, Atlanta, GA 30329, USA.

⁴Molecular Pathology Core Lab, Yerkes National Primate Research Center, Atlanta, GA 30329, USA.

⁶Department of Gynecology and Obstetrics, Emory University, School of Medicine, Atlanta, Georgia 30322, USA.

*Lead contact: msuthar@emory.edu (M.S.S)

Introduction

Zika virus (ZIKV) is a positive-sense RNA virus belonging to the *Flaviviridae* family alongside other pathogenic flaviviruses like dengue virus (DENV), Japanese encephalitis virus (JEV), West Nile virus (WNV), and yellow fever virus (YFV). Since its introduction to the Americas in 2015, ZIKV infection spread rapidly throughout regions co-endemic to DENV infection due to the shared *Aedes spp.* transmission vectors (Kraemer et al., 2019; Ribeiro et al., 2020). ZIKV transmission occurs primarily through the bite from an infected female *Aedes spp.* mosquito while secondary routes of transmission also include sexual contact and blood transfusion (Brasil et al., 2016b; de Araujo et al., 2016; de Oliveira et al., 2017; Martines et al., 2016; Paz-Bailey et al., 2019; van der Linden et al., 2016). A majority of ZIKV infections in adults are asymptomatic (~80%) and ~20% of patients will present with mild febrile illness characterized by headache, rash, fever and conjunctivitis, sometimes with severe neurological sequelae (Brasil et al., 2016a).

ZIKV exhibits a diverse tropism, infiltrating numerous immunologically privileged regions within the body, including the human placenta and fetal nervous system (Carroll et al., 2017; Figueiredo et al., 2019; Miner and Diamond, 2017; Oh et al., 2017; Retallack et al., 2016; Tabata et al., 2016). The most devastating complications of ZIKV occur vertical transmission to the developing fetus, leading to adverse pregnancy outcomes including spontaneous abortion, fetal brain abnormalities, and congenital malformations. Approximately 30% of congenitally-infected fetuses exhibit morphological abnormalities by ultrasound (e.g. microcephaly or brain calcifications) whereas the vast majority exhibit no overt clinical manifestations at birth (Brasil et al., 2016a; Musso et al., 2019). While microcephaly is associated with direct infection of radial glia, neural progenitor cells (Li et al., 2016; Miner and Diamond, 2016; Retallack et al., 2016; Tang et al., 2016), normocephalic neonates may exhibit neurodevelopmental abnormalities during the first

three years of life (Heald-Sargent and Muller, 2017; Kapogiannis et al., 2017; Mulkey et al., 2018; Nielsen-Saines et al., 2019). Indeed, recent reports of infants with congenital ZIKV infection revealed neurodevelopmental abnormalities in the absence of overt microcephaly, including vision loss, epilepsy and delays in age-appropriate developmental skills (Cardoso et al., 2019; Lopes Moreira et al., 2018; Nielsen-Saines et al., 2019; Rice et al., 2018; Wheeler et al., 2018). Currently, no antiviral therapy or vaccine exists for either DENV or ZIKV, and the immunologic correlates that dictate congenital infection of ZIKV are incompletely understood.

The placenta is the primary organ for nutrient, gas, and waste exchange between the mother and the developing fetus. In addition, the placenta is responsible for trafficking of maternal IgG across the STB layer starting at the second trimester (~12-13 weeks gestational age) (Ander et al., 2019). Anchoring and floating chorionic villi, fetal-derived tree-like projections are the functional unit of the placenta, affixing the placenta to the maternal decidua and housing the entrance to the fetal circulation. The chorionic villi are primarily hemomonochorial with an outermost syncytiotrophoblast (STB) layer and basolateral progenitor cytotrophoblast (CTB) layer which replenish the STB layer throughout pregnancy. Underneath the CTB layer lies the villous stroma or which contains placental fibroblasts, fetal endothelial cells comprising the fetal vasculature, and fetally-derived placental macrophages called Hofbauer cells (HCs).

The human placenta is a primary tropism of ZIKV and, once the placental barrier is breached, placental macrophages, Hofbauer cells (HCs), within the villous stroma are preferentially targeted and highly permissive to ZIKV infection (Bhatnagar et al., 2017; Martines et al., 2016; Quicke et al., 2016a; Reagan-Steiner et al., 2017; Rosenberg et al., 2017; Zimmerman et al., 2018). Due to the strong innate immune defenses of the STB layer (Bayer et al., 2016; Corry et al., 2017; McConkey et al., 2016; Robbins et al., 2010; Zeldovich et al., 2013), ZIKV has been hypothesized to seed the placenta through infection

of extravillous trophoblasts anchored to the decidua as well as a paraplacental route through the infection of the amniochorion adjacent to the maternal decidua. (Tabata et al., 2018; Tabata et al., 2016). We and others have also determined that cross-reactive DENV antibodies are capable of binding ZIKV, utilizing the FcRn-mediated transcytosis system to cross the highly antiviral STB layer, and targeting HCs within the villous core (Priyamvada et al., 2016b; Quicke et al., 2016a; Rathore et al., 2019; Zimmerman et al., 2018). Given the high level of ZIKV and CZS cases within DENV-endemic regions, the impact of prior flavivirus humoral immunity on secondary ZIKV pathogenesis in the placenta is still unclear.

Activation of B cells and potent humoral immune responses elicited by primary infection or vaccination are vital to protection against numerous pathogenic flaviviruses (Diamond et al., 2003a; Diamond et al., 2003b; Libraty et al., 2002; Plotkin, 2010). Recognition of viral antigen during primary flavivirus infection is initially characterized by a rapid increase in antigen-specific IgM antibodies in a T-cell independent manner approximately 4-11 days after infection (Bingham et al., 2016; Boes, 2000; Busch et al., 2008; Lanciotti et al., 2008). Following this robust, but relatively short-lived, IgM response (~7 days post-infection), proliferating B cells will traffic to germinal centers where they undergo T cell-mediated class-switch DNA recombination and somatic hypermutation to generate potent, high affinity IgG, IgA, and IgE responses (Xu et al., 2012). As IgG titers continue to increase and subsist past convalescence through establishment of long-lived memory B cells, anti-flavivirus IgM titers typically wane starting at 15 days and disappear by 6 months post symptom onset, but can last in the bloodstream up to 12-18 months post-infection (Griffin et al., 2019; Paz-Bailey et al., 2019; Prince and Matud, 2011; Roehrig et al., 2003). Secondary flavivirus infection elicits high levels of proliferating plasmablasts which produce both neutralizing type-specific and cross-reactive IgG at a swifter rate (<4-5 days post symptom onset) and larger magnitude compared to primary

infection (Beltramello et al., 2010; Priyamvada et al., 2016a; Sa-Ngasang et al., 2006; Wrammert et al., 2012). Notably, IgM titers tend to decrease in magnitude and exhibit high levels of type-specific neutralization activity with limited cross-reactivity during secondary infection with related flaviviruses (A et al., 2008; Chanama et al., 2004; Malafa et al., 2020).

While the impact of IgG is well-appreciated in restriction and clearance of viral infection, the role of IgM during flavivirus infection is not fully understood. IgM exists as pentamers and hexamers with 10 antigen-binding sites with low individual affinity but high overall valency and avidity. This valency and combined avidity allows these multimeric antibody complexes to recognize repeated protein and carbohydrate structures on the virion surface (Racine and Winslow, 2009). A majority of the circulating IgM in humans is considered natural IgM, IgM that is secreted constitutively by CD5+ B-1 cells located in the peritoneal and pleural spaces (Boes, 2000). B-1 cells are stimulated primarily, but not exclusively, by T-cell independent antigens, including polysaccharides and phospholipids (Racine and Winslow, 2009). Notably, antigen exposure during viral infection does not affect B-1 natural IgM secretion (Baumgarth et al., 1999). Natural IgM performs a variety of homeostatic functions such as C1q-mediated phagocytosis of apoptotic cells by macrophages and DCs as well as B-1 cell feedback loop signaling (Boes et al., 1998; Nguyen and Baumgarth, 2016). Induced immune IgM is rapidly secreted following recognition of viral antigens by B-2 conventional B cells located within the germinal centers of peripheral lymphoid organs like the spleen and lymph nodes (Baumgarth et al., 1999; Racine and Winslow, 2009). Unlike B-1 secreted natural IgM, immune IgM from B-2 cells exhibits greater specificity towards the invading pathogen; nevertheless, both natural and immune IgM play non-redundant roles essential for effective early antiviral responses and T-cell dependent induced antibody responses by conventional follicular B cells (Baumgarth et al., 2000). Both natural and induced IgM confer protection against

numerous viruses, including influenza, VSV, WNV, and JEV (Baumgarth et al., 1999; Baumgarth et al., 2000; Blandino and Baumgarth, 2019; Fehr et al., 1996; Libraty et al., 2002). $\text{IgM}^{-/-}$ mice exhibited greater mortality and decreased antigen-specific IgG production during WNV infection (Diamond et al., 2003b). In addition, increased levels of anti-JEV IgM correlated to improved outcomes and less neuroinvasive disease in humans (Libraty et al., 2002).

To elucidate the impact of induced anti-flavivirus antibodies on translocation and enhancement of ZIKV infection in placental tissues, we generated immune complexes by combining the 2015 Puerto Rican strain of ZIKV, ZIKV-PRVABC59 with early and late convalescent serum samples isolated from pediatric patients with confirmed primary DENV3, primary ZIKV, or secondary ZIKV infection. Infection of human second-trimester chorionic villous explants with these immune complexes demonstrated that diluted late convalescent serum from primary DENV3, primary ZIKV, and secondary ZIKV infection can enhance ZIKV infection. Notably, early convalescent serum from primary and secondary ZIKV-, but not DENV3-, infected patients restricted ZIKV replication, suggesting a role of type-specific ZIKV IgM responses in restricting infection. Depletion of IgM from primary and secondary ZIKV, but not DENV3, early convalescent serum increased ZIKV infection to levels similar to immune complexes generated from late convalescent ZIKV-immune sera. Our findings demonstrate that anti-flavivirus IgM can limit IgG-mediated trafficking of ZIKV across the placental barrier, restricting viral enhancement within the villous stroma.

Results

Primary and secondary DENV and ZIKV immune sera enhance ZIKV infection in placental tissue

To date, few studies have assessed the ability of anti-DENV monoclonal antibodies or dengue immune to enhance ZIKV infection in human *ex vivo* placental tissue (Brown et al., 2019; Hermanns et al., 2018; Zimmerman et al., 2018). However, our understanding of DENV or ZIKV immune sera augmenting ZIKV infection in human placental tissue remains limited. To test this, we generated immune complexes by combining ZIKV-PR with late convalescent primary DENV3, primary ZIKV, secondary ZIKV, and flavivirus-naive immune sera gathered from serology-confirmed DENV- and ZIKV-infected pediatric patients (Gordon et al., 2019; Katzelnick et al., 2017; Montoya et al., 2018) and infecting mid-gestation chorionic villous explants for 24h. After 24h, the samples were homogenized for RNA isolation and strand-specific qPCR was performed to determine both genomic, positive-sense and replicating, negative-sense ZIKV RNA in the chorionic villous tissue. We observed a 125-200-fold increase in positive-sense ZIKV RNA and a 1000-3000-fold increase in negative-sense replicating RNA in tissues infected in the presence of primary DENV3 immune sera (D1-D5) (**Figure 1A**). This indicates that primary DENV immune sera cross-reacts with ZIKV and enhances ZIKV infection within chorionic villous tissues. Primary (Z1-Z4) and secondary ZIKV immune sera (DZ1-DZ4) also demonstrated 13-40- and 32-63-fold increases in ZIKV (+) RNA, respectively, as well as a 200-315-fold increases in ZIKV (-) RNA in both serum sets (**Figure 1B**). Despite the robust type-specific antibody response elicited by ZIKV both with and without previous flavivirus infection (Andrade et al., 2019; Malafa et al., 2020; Stettler et al., 2016), these data suggest that sub-neutralizing levels of both cross-reactive and ZIKV-specific antibodies are capable of

binding ZIKV, translocating across the STB layer, and enhancing infection within the chorionic villous explants.

Early, not late, convalescent ZIKV-immune serum restricts ZIKV enhancement in chorionic villous explants

Early convalescent DENV sera (<6 months after infection) contain potent cross-reactive antibodies that can bind and neutralize ZIKV. However, studies using late convalescent DENV immune sera (>6 months after infection) have determined that the cross-reactive antibody response to ZIKV post-primary and secondary DENV infection have very little neutralizing activity against incoming ZIKV infection (Collins et al., 2017). Pooled DENV immune plasma has also been demonstrated to enhance ZIKV infection in first and second trimester chorionic villous explants (Brown et al., 2019). However, pooled DENV immune sera does not differentiate the enhancement effects due to the duration of convalescence. To understand the individual impacts of early and late convalescent sera on enhancement of ZIKV infection in chorionic villous explants, we generated ZIKV immune complexes using both early and late convalescent from primary DENV3, primary ZIKV, and secondary ZIKV immune sera and infected chorionic villous explants as described earlier. Chorionic villous explants infected with early convalescent primary and secondary ZIKV infection showed minor to moderate enhancement of ZIKV infection (primary ZIKV: (+) RNA 2.7-23 fold; (-) RNA 5-18 fold; secondary ZIKV: (+) RNA 3.3-6.7 fold; (-) RNA 30-120 fold). Explants infected with ZIKV in the presence of late convalescent primary and secondary ZIKV immune sera showed superior enhancement compared to the early convalescent samples (primary ZIKV: (+) RNA 22-44 fold; (-) RNA 209-324 fold; secondary ZIKV: (+) RNA 32-63 fold; (-) RNA 180-1300 fold) (**Figures 2A-B**). Surprisingly, minimal differences were seen in the ZIKV enhancement profiles in the

presence of both early and late convalescent primary DENV3 sera (early convalescent (+) RNA 7.58-80 fold; early convalescent (-) RNA 7-214 fold; late convalescent (+) RNA 8-98 fold; late convalescent (-) RNA 13-316 fold), indicating that a ZIKV-specific, not cross-reactive, antibody response must be responsible for the restriction of ZIKV enhancement in chorionic villous tissue (**Figure 2C**).

IgM depletion of early convalescent ZIKV-immune serum confers IgG-mediated enhancement of ZIKV infection

During flavivirus infection, levels of immune IgM rise sharply approximately 4-7 days post infection during the acute to early convalescence phase and typically wane to undetectable levels approximately 4-6 months later during late convalescence ((Bingham et al., 2016; Busch et al., 2008; Lanciotti et al., 2008)). Due to the differences in antibody composition between early and late convalescence, we hypothesized that ZIKV-specific IgM was responsible for the lack of ZIKV enhancement seen in explants infected in the presence of early convalescent ZIKV sera. To test this, we first depleted IgM from primary and secondary early convalescent ZIKV immune sera (**Figure 3A**). Next, we infected chorionic villous explants with immune complexes generated with non-depleted early convalescent, IgM-depleted early convalescent, and late convalescent primary and secondary ZIKV immune sera combined with ZIKV. We observed a modest effect of IgM depletion on ZIKV infection in explants treated with primary ZIKV. However, explants treated with early convalescent IgM-depleted sera showed increased enhancement to levels similar to late convalescent sera-treated explants (IgM-depleted early convalescent sera: (+) RNA 7-22 fold; (-) RNA 7-129 fold; late convalescent sera: (+) RNA 3-16 fold; (-) RNA 3-15 fold). (**Figure 3B**). Thus, these results indicate that ZIKV-specific IgM found

during the early convalescent phase of ZIKV infection is capable of inhibiting IgG-mediated transcytosis of ZIKV across the STB layer and viral seeding of the villous stroma.

Discussion

Previous work has established that natural and immune IgM play a significant role in control of early viral infection (Baumgarth et al., 1999; Baumgarth et al., 2000; Diamond et al., 2003a; Diamond et al., 2003b; Libraty et al., 2002). More recently, ZIKV-specific IgM has been found to account for 30-50% of neutralization activity in both acute primary ZIKV and vaccinated YF+, TBEV+ secondary ZIKV infections (Malafa et al., 2020). Malafa et al. also concluded that IgM-depletion significantly increased the levels of ZIKV ADE in FcγR-expressing K562 cells while IgG depletion diminished ZIKV ADE. However, the role of induced IgM on ZIKV infection and antibody-mediated translocation of ZIKV across the placental barrier has been underappreciated. In this study, we assessed whether early and late convalescent DENV and ZIKV immune sera can enhance ZIKV infection in second-trimester human chorionic villous explants. Infection of explants with ZIKV combined with late convalescent primary DENV3, primary ZIKV, and secondary ZIKV immune sera demonstrated that both sub-neutralizing cross-reactive and type-specific IgG can augment ZIKV infection. In contrast, type-specific, not cross-reactive, early convalescent primary and secondary ZIKV sera showed minimal ZIKV ADE compared to late convalescent sera. Finally, IgM depletion augmented the ZIKV ADE potential of early convalescent ZIKV immune sera, exhibiting similar levels of ZIKV enhancement in the chorionic explants.

Our study indicates that early convalescent ZIKV immune sera contains neutralizing, type-specific IgM that effectively reduces the ADE-capacity of cross-reactive or type-specific IgG present within the early convalescent phase post-flavivirus infection.

The reduction in ADE capacity of early convalescent serum might be attributed to the ability of IgM to outcompete IgG for binding sites on ZIKV. Due to its germline coding and lack of somatic hypermutation, IgM exists as a low affinity pentamer; however, because of its 10 potential binding sites, the IgM pentamer maintains high valency and avidity, making it particularly adept at binding repeated antigenic motifs found on viral particles (Blandino and Baumgarth, 2019). Thus, ZIKV-specific IgM may be occupying or sterically hindering access to available epitopes on the virion surface, effectively limiting IgG-mediated viral seeding and enhancement of ZIKV infection in *ex vivo* chorionic villous tissues seen in previous studies (Brown et al., 2019; Hermanns et al., 2018; Rathore et al., 2019; Zimmerman et al., 2018). Binding of IgM pentamers to ZIKV:IgG immune complexes may also hinder FcRn-mediated transcytosis across the placental barrier. Human FcRn (hFcRn) is known to traffic IgG away from lysosomal degradation and into the common recycling endosome to facilitate transcytosis or recycling of IgG between both the apical and basolateral surfaces of polarized epithelial cells (Pyzik et al., 2019; Tzaban et al., 2009). However, multivalent antigen-IgG immune complexes which cross-link FcRn are directed to late lysosomes for degradation, particularly for antigen presentation on myeloid cells (Guilliams et al., 2014; Weflen et al., 2013). However, the degree of FcRn cross-linking needed to direct immune complexes from the recycling endosome to late lysosomal compartments is not fully understood. Thus, it is plausible that bulky IgM:IgG:ZIKV immune complexes are causing high levels of FcRn cross-linking, and driving FcRn-containing recycling endosomal compartments for late endosomal degradation.

Of note, we observed that both diluted primary and secondary ZIKV late convalescent sera can enhance ZIKV infection in chorionic villous explants. Unlike DENV infection, which elicits type-specific and broadly cross-reactive humoral responses with

differing neutralization capacities to DENV1-4, ZIKV exists only as one serotype (Dowd et al., 2016). Thus, it is generally accepted that infection with ZIKV provides life-long humoral and cellular immunity to reinfection with ZIKV. Rhesus macaques re-challenged with ZIKV 22-28 months post primary ZIKV infection exhibited no detectable viremia within the serum, suggesting that ample humoral and cellular protection is sustained for at least 2-3 years (Moreno et al., 2020). On the other hand, *in vitro* infection of U937 cells with ZIKV incubated with rhesus macaque DENV immune sera demonstrated that ADE occurred at dilution of 1:10-1:100 during heterotypic infection and at 1:100-1:1000 with homotypic infection (Ito et al., 2010). Infection of pregnant *Ifnar^{-/-}* mice showed enhancement of ZIKV infection, increased mortality, and fetal resorption when sub-neutralizing levels of ZIKV immune serum were administered compared to mice receiving neutralizing or non-neutralizing levels of serum (Marques and Drexler, 2019; Shim et al., 2019). These studies, alongside our observation in human chorionic villous explants, suggest that that homotypic ZIKV antibodies at sub-neutralizing concentrations can potentially enhance ZIKV infection. This may have implications for ZIKV-experienced women of child-bearing age with sub-neutralizing levels of antibodies. With the development of numerous ZIKV vaccines, further longitudinal studies investigating the duration, breadth, and antibody titers needed to maintain neutralizing ZIKV humoral immunity is essential to develop vaccine strategies avoiding potential ADE.

One caveat of our work was the elimination of complement activity through heat-inactivation (HI) of our primary and secondary flavivirus-experienced sera prior to immune complex generation and infection of villous explants. The complement system is a vital arm of the innate immunologic response consisting of various soluble and membrane bound factors that can cause neutralization, opsonization, and/or lysis of invading pathogens and infected cells. Upon binding of a virion, IgM can recruit C1q, a large

multimeric protein involved in the classical complement pathway, and initiate an enzymatic cascade, leading to C3/C4-mediated opsonization, neutralization, or lysis of the virion through the C5-C9 membrane attack complex (MAC) (Stoermer and Morrison, 2011). IgM pentamers have 1,000-fold greater binding affinity to C1q compared to IgG, making them exceedingly efficient at initiating the complement cascade (Ehrenstein and Notley, 2010). Natural IgM was essential for C1q and C3-mediated agglutination and neutralization of influenza in mice (Jayasekera et al., 2007). Further studies in mice have also demonstrated that deletion of CR2 caused higher viral loads and susceptibility to influenza and West Nile virus infection (Fernandez Gonzalez et al., 2008; Mehlhop et al., 2009). Given the importance of IgM and complement to viral neutralization, addition of complement into our chorionic villous explant model system could have caused coating of ZIKV with IgM, C1q, and C3 complement factors, masking epitopes used by cross-reactive DENV or ZIKV-specific IgG. Thus, the inhibition of ZIKV enhancement seen in our HI early convalescent primary and secondary ZIKV immune sera may have been understated. However, other studies have also demonstrated that complement can alter viral ADE. Cardoso et al. have determined that C1q can enhance viral infection through phagocytosis of non-neutralizing IgM-bound virus recognized by CR3-expressing murine macrophages (Cardoso et al., 1986; Cardoso et al., 1983). C1q has also been shown to block ADE in an IgG-subclass dependent manner (Mehlhop et al., 2007). Altogether, the impact of complement on the complex interplay of neutralizing IgM and IgG-mediated transcytosis of ZIKV across the placental barrier warrants further investigation.

Despite the importance of IgM in controlling early viral infection (Baumgarth et al., 1999; Baumgarth et al., 2000; Diamond et al., 2003a; Diamond et al., 2003b; Libraty et al., 2002), current antiviral vaccine design relies heavily on induction of long-lasting memory IgG B cell responses while the impact of IgM responses is less appreciated. Our

finding that ZIKV-specific IgM, which cannot cross the placental barrier, inhibits the enhancing ability of IgG in chorionic villous explants suggests that induction of potent, durable IgM responses may control of early ZIKV infection and reduction of viral seeding in the placenta. Flavivirus specific IgM responses rise rapidly early in infection and normally wane within 4-6 months post-infection (Busch et al., 2008; Lanciotti et al., 2008; Prince and Matud, 2011). However, long-lasting IgM-producing plasma cells have been discovered in spleens of mice infected with mouse-adapted A/PR/8/34 influenza and LCMV for >1 year and >2 years, respectively (Bohannon et al., 2016). In the same study, germinal center and T-cell-depleted mice immunized against influenza developed durable IgM responses which were solely responsible for viral neutralization and survival post influenza challenge. Long-lasting IgM responses have also been detected in patients infected with WNV and ZIKV up to two years post-infection (Griffin et al., 2019; Roehrig et al., 2003), but, the neutralizing capacity of these flavivirus-specific IgM is currently unknown. IgM-bound antigen immune complexes also play an important role in proper IgG class switching and somatic hypermutation in germinal centers (Ilag, 2011). Malaria-specific IgM has been found to boost the murine IgG response if co-administered as an adjuvant with formalin-fixed malaria immunization (Harte et al., 1983). Lack of secreted IgM has been shown to globally inhibit germinal center-mediated IgG responses activated through recognition of T cell dependent-antigens (Boes et al., 1998). *sIgM^{-/-}* mice also have underdeveloped WNV-specific IgG responses and increased mortality (Diamond et al., 2003b), suggesting that IgM plays a significant role in proper B cell responses to viral infections. These effects of IgM immune complexes on T cell-dependent B cell reactions are hypothesized to occur through presentation of IgM:antigen complexes on follicular dendritic cells within germinal centers to activated B cells (Ehrenstein and Notley, 2010).

In conclusion, our study highlights that both cross-reactive and type-specific subneutralizing antibody responses can enhance ZIKV infection in human placenta tissue. In addition, our work demonstrates the impact of ZIKV-specific IgM in inhibiting IgG-mediated ZIKV ADE in primary human chorionic villous explants. Given the ability of IgM to efficiently neutralize virus and modulate potent antiviral B cell responses, further investigation into use of ZIKV-specific IgM as a prophylactic and ZIKV vaccine adjuvant is warranted to understand its influence on cross-reactive or type-specific IgG-mediated transcytosis of ZIKV and viral seeding of the placenta.

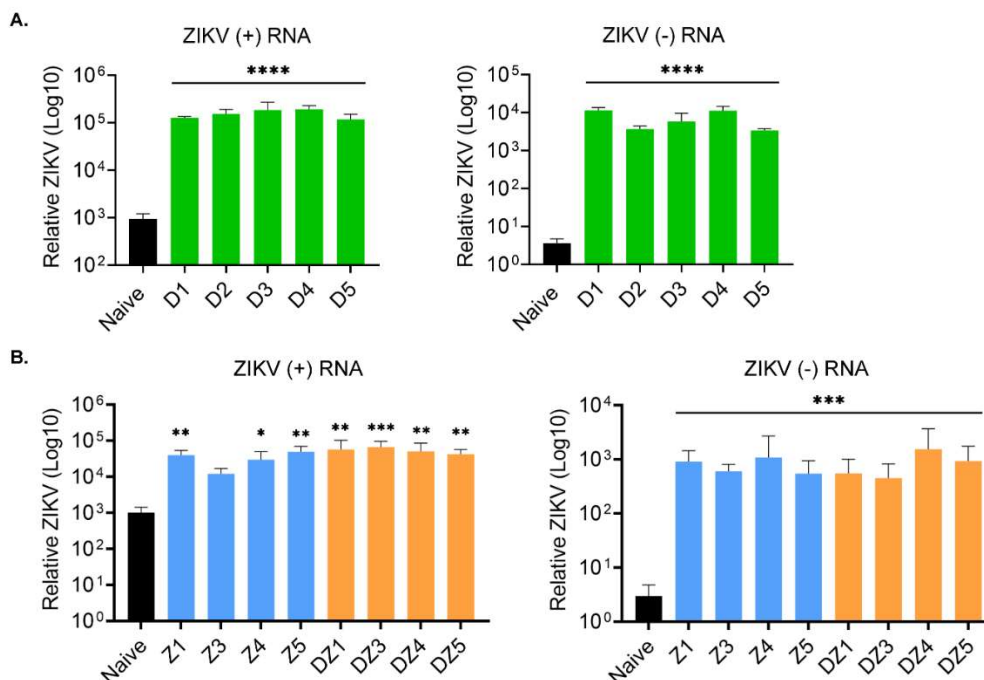


Figure 1: Primary DENV3, primary ZIKV, and secondary ZIKV immune sera

enhance ZIKV infection in human chorionic villous explants. A) Primary DENV (D1-

D5) and **B)** primary ZIKV (Z1, Z3-5) and secondary ZIKV with previous DENV infection

(DZ1, DZ3-DZ5) sera were diluted 1:100 in DPBS and coincubated with 5×10^5 PFU of

ZIKV for 1h to generate viral immune complexes. Flavivirus-naïve serum diluted to 1:100

was incubated with ZIKV as the naïve control. Following immune complex formation,

second-trimester chorionic villous explants were infected for 2h, washed, and incubated

for 24h. At 24 hours post-infection (hpi), tissues were collected and ZIKV (+) and (-)

sense RNA were measured using single-stranded ZIKV qPCR. Experimental and control

conditions were performed in triplicate and are shown as the average of biological

triplicates \pm SEM. Data were analyzed by 1-way ANOVA with Dunnett's multiple

comparisons test. * $p < 0.05$, ** $p < 0.01$, *** $p < 0.001$, **** $p < 0.0001$. Representative

experiments from $n=4$ donors with two independent experiments.

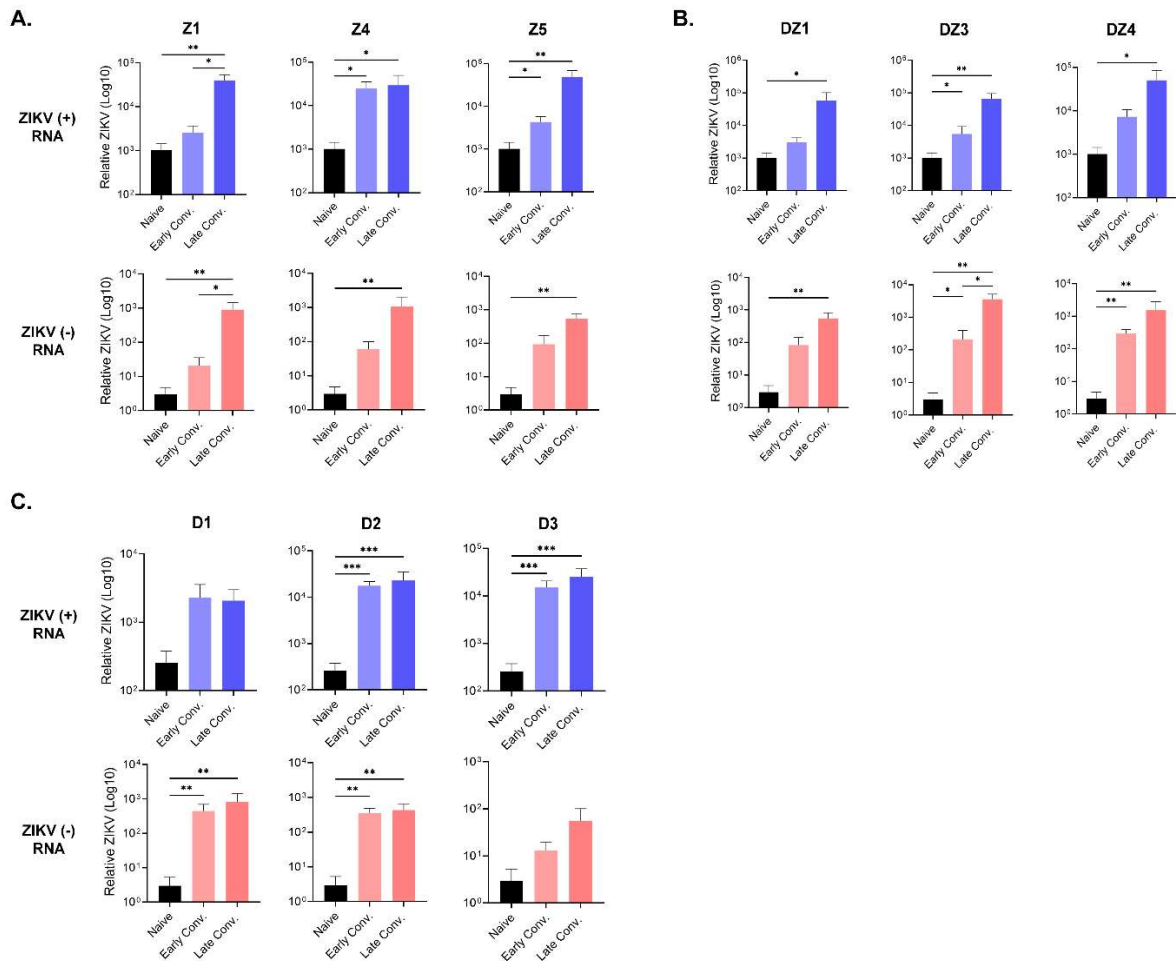


Figure 2: Early convalescent ZIKV sera, but not DENV3 sera, inhibit ADE of ZIKV infection in human chorionic villous explants Early (14 dpi) and late convalescent (6 months post-infection) **A**) primary ZIKV (Z1, Z4, Z5) and **B**) secondary ZIKV (DZ1, DZ3, DZ4) were diluted 1:100 in DPBS while **C**) primary DENV3 sera (D1-3) sera were diluted 1:10 in DPBS and cocubated with 5×10^5 PFU of ZIKV for 1h to generate viral immune complexes. Flavivirus-naïve serum diluted to 1:100 was incubated with ZIKV as the naïve control. Following immune complex formation, second-trimester chorionic villous explants were infected for 2h, washed, and incubated for 24h. Tissues were collected and ZIKV (+) and (-) sense RNA were measured using single-stranded ZIKV qPCR. Experimental and control conditions were performed in triplicate and are shown as the

average of biological triplicates \pm SEM. Data were analyzed by 1-way ANOVA with multiple comparisons test. * $p < 0.05$, ** $p < 0.01$, *** $p < 0.001$. Representative experiments from $n = 3$ donors with two independent experiments.

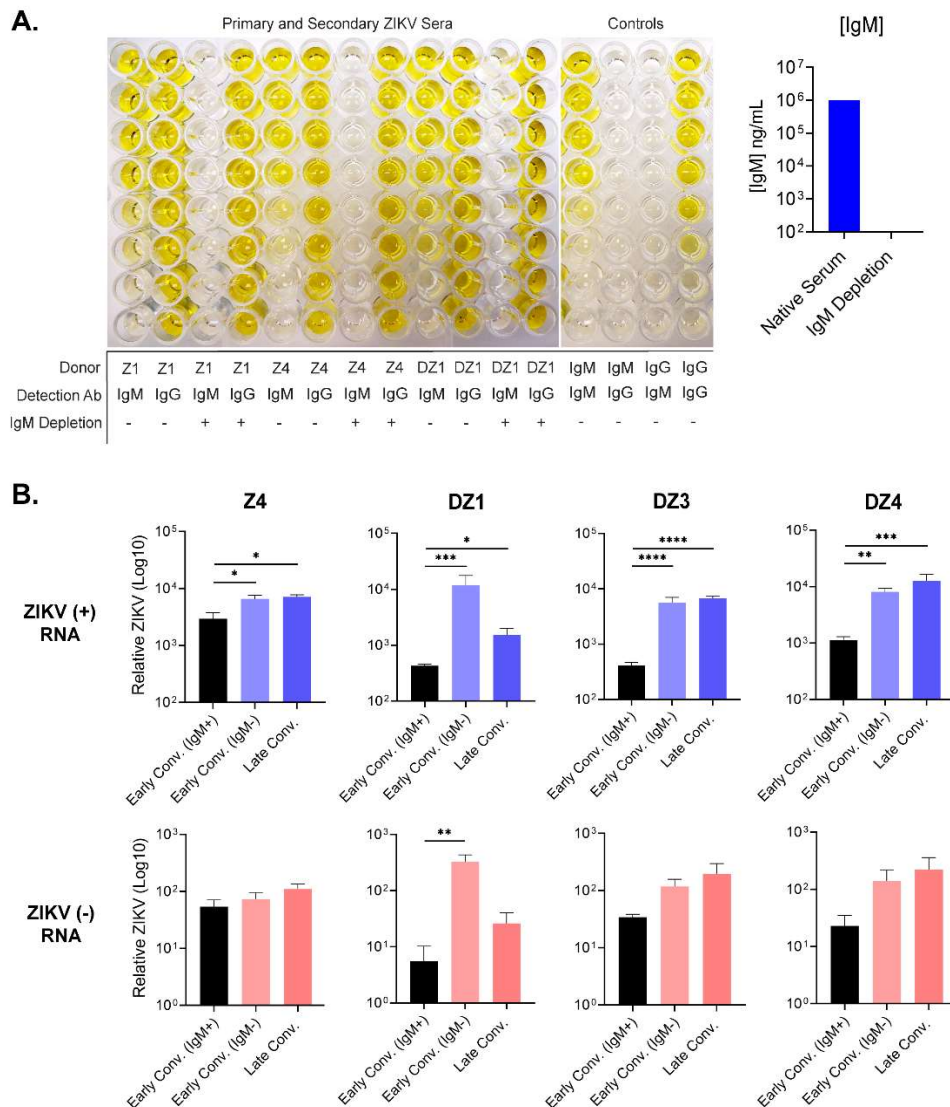


Figure 3: IgM-depleted early convalescent ZIKV sera enhances ZIKV infection in chorionic villous explants. Primary and secondary ZIKV immune sera were diluted 1:100 and incubated with Poros IgM Capture Select affinity chromatography beads at a 1:1 ratio for 2h at room temperature. Supernatants containing the IgM-depleted sera were isolated after centrifugation. **A)** Representative ELISA plate and bar graph demonstrating successful IgM depletion from primary (Z1, Z4) and secondary ZIKV (DZ1) sera. **B)** Chorionic villous explants were infected with ZIKV combined with wild-

type early-, IgM-depleted early-, and late-convalescent primary (Z4) and secondary (DZ1, DZ3, DZ4) for 2h, washed, and incubated for an additional 24h. Tissue was collected and ZIKV (+) and (-) sense RNA were measured using single-stranded ZIKV qPCR analysis. Experimental and control conditions were performed in triplicate and are shown as the average of biological triplicates \pm SEM. Data were analyzed by 1-way ANOVA with multiple comparisons test. * $p < 0.05$, ** $p < 0.01$, *** $p < 0.001$, **** $p < 0.0001$. Representative experiment from $n=2$ donors.

Materials and Methods

EXPERIMENTAL MODEL AND SUBJECT DETAILS

Ethics statement. Second trimester human placentae were obtained from consented donors who elected to terminate normal pregnancies between weeks 14-20 of gestation. This study was approved by the Emory University Institutional Review Board (IRB 000217715). Written informed consent was acquired from all donors before elective termination and collection of placentae. Samples were de-identified before being transferred to laboratory personnel for primary chorionic villous explant isolation.

Human sera collection. Samples were from 2 prospective studies of pediatric dengue and Zika in Managua, Nicaragua as described by Montoya et al. (Montoya et al., 2018).

Viruses and cells. Zika virus (ZIKV) strain PRVABC59 was used for all experiments. PRVABC59 was initially isolated in 2015 from a patient infected while in Puerto Rico. We obtained this strain from the Centers for Disease Control and Prevention in Fort Collins, CO. The virus used in these experiments has undergone a total of 6 passages in Vero cells. Viral titers were determined by plaque assay on Vero cells (ATCC® CCL81™). Vero cells were cultured in complete DMEM medium consisting of 1x DMEM (Corning Cellgro), 10% FBS, 25mM HEPES Buffer (Corning Cellgro), 2mM L-glutamine, 1mM sodium pyruvate, 1x Non-essential Amino Acids, and 1x antibiotics, and were maintained at 37°C and 5% CO₂.

Human placental explant model. Chorionic villi were dissected from placental tissue and maintained in DMEM/F12 medium (ThermoFisher Scientific, Gibco) with 10% FBS and

penicillin/streptomycin at 37°C and 5% CO₂. Villi were separated into individual wells of a 48-well plate each containing 600ul of DMEM/F12 medium for subsequent experiments. Following isolation of human placental explants, diluted sera were mixed 1:1 with 5x10⁵ PFU/ml ZIKV in non-supplemented 1x DMEM/F12. After the 1 hour incubation, the 200 µl of Ab:ZIKV immune complexes were added to the explants. Tissues were incubated at 37°C for 2 hours then washed 2x with warm complete DMEM/F12 medium to remove residual immune complexes and re-supplied with 800ul complete DMEM/F12 medium. Infected explant tissues were incubated at 37°C and 5% CO₂.

Quantitative real time-PCR. For human placental explants, tissues infected with DENV mAb:ZIKV immune complexes and control conditions were suspended in TRI reagent and mechanically homogenized using ceramic bead tubes (Omni International) on a Beadruptor Homogenizer. Total RNA was isolated from homogenized tissues using the Direct-zol RNA MiniPrep Plus Kit (Zymo Research) per the manufacturer's instructions. Purified RNA was reverse transcribed using random primers with the High-Capacity cDNA Reverse Transcription Kit (Applied Biosystems). HC gene expression and ZIKV viral RNA levels were quantified by qRT-PCR using PrimeTime Gene Expression Master Mix (Integrated DNA Technologies), ZIKV-specific primers and probe set as previously described (Zimmerman et al., 2018). C_T values were normalized to the reference gene *Gapdh* and represented as fold change over values from time-matched mock samples using the formula $2^{-\Delta\Delta C_T}$. All primers and probes were purchased from Integrated DNA Technologies (IDT). qRT-PCR was performed in 384-well plates and run on an Applied Biosystems 7500 HT Real-Time PCR System.

ZIKV strand-specific qRT-PCR. Purified RNA was reverse transcribed using oligo(dT) and a ZIKV-specific cDNA primer. The two ZIKV-specific cDNA primers are

complementary to either the positive-strand or negative-strand and include a unique 5' tag as previously described (Zimmerman et al., 2018). Two cDNA and qRT-PCR reactions were run for each sample, one for positive-strand and one for negative-strand. For ZIKV strand-specific detection, a ZIKV-specific primer and tag-specific primer were used for targeted amplification of the tagged cDNA in addition to the ZIKV-specific probe. C_T values were normalized to the reference gene *Gapdh* and represented as fold change over values from time-matched mock samples using the formula $2^{-\Delta\Delta CT}$.

ELISA for IgM and IgG Detection in Human Sera. Maxisorb ELISA plates (ThermoScientific #439454) were coated with 100 μ L of diluted anti-IgM, IgG, IgA Capture Reagent (diluted 1:1000 in DPBS) and incubated overnight at 4°C. Plates were washed 4x's with DPBS + 0.05% Tween-20 and blocked with DPBS + 1% BSA for 2 hours at 37°C. Serum samples were serially diluted in DPBS + 0.05% Tween-20 + 1% BSA starting at 1:1000 dilution with 7 subsequent 4-fold dilutions. Blocking buffer was removed and 100 μ L of sample were added to the ELISA plate and incubated at 37°C for 1.5 hours. ELISA plates were subsequently washed 4x's with DPBS + 0.05% Tween-20 and either HRP-F(ab') Goat Anti Human IgM (Jackson ImmunoResearch 109-036-129) or F(ab') Goat Anti Human IgG (Jackson ImmunoResearch 109-036-098) were added to detect bound IgM and IgG. Plates were incubated at room temperature for 1 hour and washed 4x's with DPBS + 0.05% Tween-20 and 3x's with DPBS to remove excess antibodies. OPD tablets (Sigma Aldrich) were added to citrate buffer (Sigma-Aldrich, P4809-100TAB), mixed, and 40 μ L of 3% H₂O₂ were added for every 10 mL of developing buffer. 100 μ L of developing buffer was added to each well and allowed to incubate for 5 minutes at room temperature. The reaction was halted by adding 100 μ L of 1 M HCl per well. The plate was read immediately at an OD490 on a Bio-Rad Synergy ELISA reader.

IgM Depletion from Human Sera. Human sera were diluted at 1:100 and mixed with POROS CaptureSelect IgM Affinity Matrix (ThermoFisher) at a 1:1 ratio. Samples were rotated at room temperature for 2 hours. Tubes were centrifuged at 10,000g and supernatants containing the IgM-depleted sera were collected. IgM-specific ELISA was performed to confirm IgM-depletion.

QUANTIFICATION AND STATISTICAL ANALYSIS

Statistical analyses. Viral RNA data from single-strange ZIKV qPCR analyses treatments of mid-gestation placental explants were analyzed by 1-way ANOVA and Dunnett's multiple comparisons test, $p < 0.05$. IgM depletion data were analyzed by Student's Test, $p < 0.05$. All statistical analysis was performed using GraphPad Prism software. In each of the main and supplemental figure legends, "N" represents the number of patient placental donors from which HCs or explants were derived. Further experimental statistical details can be found in the Figure legends.

Chapter 4: STAT5: A Target of Antagonism by Neurotropic Flaviviruses

Matthew G. Zimmerman^{1,2}, James R. Bowen^{1,2}, Circe E. McDonald^{1,2}, Ellen Young³,
Ralph S. Baric^{3,4}, Bali Pulendran^{2,5}, Mehul S. Suthar^{1,2,*}

¹Department of Pediatrics, Division of Infectious Diseases, Emory University School of Medicine, Atlanta, GA 30322, USA.

²Emory Vaccine Center, Yerkes National Primate Research Center, Atlanta, GA 30329, USA.

³Department of Epidemiology, Gillings School of Global Public Health, University of North Carolina, Chapel Hill, North Carolina, USA

⁴Department of Microbiology and Immunology, School of Medicine, University of North Carolina, Chapel Hill, North Carolina, USA

⁵*Department of Pathology and Laboratory Medicine, Emory University School of Medicine, Atlanta, GA 30329, USA*

*Correspondence: msuthar@emory.edu (M.S.S.)

Introduction

West Nile virus (WNV) is a neurotropic flavivirus and the leading cause of arboviral neuroinvasive disease since its introduction to the United States in 1999, accounting for >95% of reported cases (Burakoff et al., 2018). After inoculation by an infected mosquito, 20-25% of WNV-infected individuals develop symptoms ranging from mild flu-like symptoms to severe neurologic disease including meningitis, encephalitis, and acute flaccid paralysis (Chancey et al., 2015). Longer-lasting sequelae of WNV-induced fever and neuroinvasive disease include ocular abnormalities, arthralgias, psychological impairment, and permanent memory loss (Patel et al., 2015). Recently, WNV has also been shown in mice to translocate across the placenta and infect fetal neuronal tissue during pregnancy, prompting fetal demise (Platt et al., 2018). The lack of FDA-approved antiviral therapeutics or vaccines for human WNV infection reinforces the need to further understand innate immune signaling during WNV pathogenesis.

Dendritic cells (DCs) are vital components of both the innate and adaptive immune responses during flavivirus infection. DCs are professional antigen presenting cells that, upon infection, can process and present antigens on MHC molecules, express co-stimulatory markers, and produce cytokines necessary for activation of the adaptive immune response (Pulendran, 2015). Mouse models of WNV pathogenesis have demonstrated that DCs are initial targets of infection by WNV and that innate immune signaling in DCs is essential for clearance of neuroinvasive disease (Durrant et al., 2013; Pinto et al., 2014; Suthar et al., 2013; Suthar et al., 2010). In the absence of type I interferon (IFN) signaling in murine DCs, WNV shows increased replication in myeloid cells and enhanced tissue tropism, resulting in increased mortality in mice (Pinto et al., 2014). Adoptive transfer studies in mice have also demonstrated that immune competent DCs are essential for proper priming of WNV-specific T cell responses and viral

clearance from the central nervous system (Durrant et al., 2013). Recent studies have also established that WNV and a related neurotropic flavivirus, Zika virus (ZIKV), productively infect human monocyte-derived dendritic cells (moDCs) and suppress expression of co-stimulatory markers on infected DCs (Bowen et al., 2017b). WNV-infected DCs also display a reduced capacity to induce allogeneic CD4⁺ and CD8⁺ T cell proliferation (Zimmerman et al., 2019a). However, the exact mechanism of viral antagonism of human DC activation during WNV infection remains unknown.

During infection in DCs, intracellular WNV RNA is detected by the RIG-I like receptors (RLRs), RIG-I and MDA5, which interact with the adaptor protein MAVS to induce transcription of pro-inflammatory cytokines, antiviral effectors, and type I IFN (Errett et al., 2013; Loo and Gale, 2011). Upon release of type I IFN (IFN α/β), this signal is further potentiated through the type I IFN receptor (IFNAR), causing phosphorylation of bound Janus kinases (JAKs) and subsequent signal transducer and activator of transcription (STAT) proteins (Schneider et al., 2014). Once phosphorylated, STAT proteins will dimerize and translocate to the nucleus, bind to IFN-stimulated response elements (ISREs) on DNA, and initiate robust induction of interferon-stimulated genes (ISGs) to restrict viral replication. Canonically, IFNAR signals through STAT1 and STAT2 heterodimers, both of which are targets of flavivirus antagonism to inhibit antiviral responses (Best et al., 2005; Bowen et al., 2017b; Grant et al., 2016; Keller et al., 2006; Morrison et al., 2013).

In addition, IFNAR can signal through STAT5, a pleiotropic STAT protein activated downstream of numerous cytokines and growth factors. STAT5 exists as two homologs, STAT5a and STAT5b, which share 96% homology at the protein level, which homodimerize upon activation and bind gamma-activated sequences (GAS) elements on DNA (Hennighausen and Robinson, 2008). STAT5 signaling plays a variety of roles

involving DC development and activation. Generation of conventional DCs requires STAT5 signaling by inhibition of plasmacytoid DC development through induction of IRF8 (Esashi et al., 2008). Conditional knockout mouse studies have also established that STAT5 signaling is essential for thymic stromal lymphopoietin (TSLP)-induced activation of DCs and allergic Th2 responses in the lungs (Bell et al., 2013). Inhibition of STAT5 signaling in monocyte-derived dendritic cells (moDCs) also inhibits lipopolysaccharide-induced DC maturation, costimulatory marker expression, and stimulation of Th1 immune responses (Toniolo et al., 2015). Despite the role of STAT5 in DC development and maturation, the importance of STAT5 signaling in DCs during viral infection is currently unknown.

Here, we employed a co-expression network-based analysis combined with promoter scanning analysis, we identified STAT5, a critical transcription factor for regulating antiviral responses and activation within human DCs, downstream of RLR and type I IFN signaling. WNV and ZIKV infection induced minimal STAT5 signaling, corresponding with a failure to up-regulate innate immune mediators and molecules involved in DC activation. The minimal activation of WNV infected DCs reflected viral antagonism of STAT5, and to a lesser extent STAT1 and STAT2, phosphorylation. WNV and ZIKV antagonism of STAT5 in moDCs was also receptor-specific, inhibiting type I IFN, IL-4, but not GM-CSF, induced STAT5 phosphorylation downstream of JAK kinase signaling. Surprisingly, WNV and ZIKV, but neither DENV1-4 nor YFV-17D, blocked STAT5 signaling in Vero cells with differential upstream blockade of JAK kinase signaling, suggesting that targeting STAT5 may be a virus-specific strategy of WNV and ZIKV to subvert antiviral responses.

Results

STAT5 is a regulatory node of antiviral DC responses

Previous work from our lab utilized a systems biology approach to assess the global antiviral response during WNV infection within primary human monocyte-derived DCs. Using moDCs from 5 different donors, we performed messenger RNA sequencing following treatment with innate immune agonists targeting the RIG-I, MDA5, and IFNAR signaling pathways as well as infection with WNV at 12 and 24 hpi, signifying log phase viral growth (Zimmerman et al., 2019a). Using weighted gene co-expression network analysis (WGCNA) and Metacore pathway analysis, we determined that the innate immune agonist treatments and WNV infection at 24 hpi induced notable gene expression within the M5 module, a subset of differentially expressed genes (DEGs) highly enriched for pathways involved in type I IFN signaling, PRR signaling, and innate antiviral responses. WGCNA clusters together DEGs into modules based on co-expression, suggesting the presence of common transcriptional regulators driving gene expression within a module. To define the transcriptional regulatory network of the M5 antiviral module, we performed cis-regulatory sequence analysis to computationally predict regulatory nodes using iRegulon, which identifies enrichment of transcription factor binding motifs within the top highly connected genes comprising M5 (Janky et al., 2014). Consistent with pathway enrichment for antiviral pathways, our analysis identified the ISGF3 transcription complex, IRF1, and NF- κ B within the top predicted transcriptional regulators of M5 following RIG-I stimulation. Unexpectedly, we also found notable enrichment for STAT5, a transcriptional regulator with a previously described role in promoting DC activation (Bell et al., 2013; Toniolo et al., 2015) (**Fig. 1A**).

STAT5 regulates expression of genes associated with innate immunity and DC activation

Given that a role for STAT5 has not been previously implicated during flavivirus infection, we next evaluated the expression levels of predicted STAT5 target genes. Predicted STAT5 target genes included multiple genes associated with innate immunity (e.g. IRF1, TLR7, TRIM25) and DC activation (e.g. CD80, CXCL11, CCL2) (**Fig. 1B**). RIG-I agonist induced up-regulation of predicted STAT5 target genes. Transfected poly(I:C) and type I IFN, although to a lesser extent than RIG-I agonist treatment, also activated transcription of several STAT5 target genes. Given recent work implicating STAT5 signaling upstream of DC activation, in part through binding to the promoter regions of CD80 and CD83, we hypothesized that STAT5 might be an important regulator of DC activation downstream of RLR signaling (Bell et al., 2013; Toniolo et al., 2015). Indeed, multiple predicted STAT5 target genes were involved in processes related to DC activation, including molecules involved in T cell co-signaling (e.g. *CD80*, *IDO1*, *SLAMF1*) and cytokine signaling (e.g. *CCL2*, *CCL13*, *CXCL11*, *IL2RA*, *JAK2*, *SOCS*, *CISH*) (**Fig. 1C**). Treatment with RIG-I or MDA5 agonist induced significant up-regulation of STAT5 targets involved in DC activation, corresponding with dose-dependent phosphorylation of STAT5 at tyrosine residue 694, a critical event for STAT5 dimerization and DNA binding, following treatment with RIG-I or MDA5 agonist (Gouilleux et al., 1994). Notably, STAT5 phosphorylation coincided with the kinetics and magnitude of IRF3 phosphorylation (**Fig. 1D-E**). IFN β signaling also promoted STAT5 phosphorylation, confirming previous work describing the activation of STAT5 by type I IFN signaling in other cell types (**Fig. 1F**) (Fish et al., 1999; Meinke et al., 1996; Tanabe et al., 2005). Collectively, cis-regulatory analysis revealed STAT5 as a transcriptional

regulator of numerous antiviral genes within human moDCs and implicates STAT5 as a regulator of DC responses downstream of the RLR and type I IFN signaling axes.

WNV and ZIKV actively antagonize STAT5 activation

In contrast to RLR and type I IFN stimulation, STAT5 signaling was substantially less enriched during WNV infection, where almost 80% of predicted STAT5 target genes, including those involved in DC activation, were not significantly expressed over mock-infected cells (**Fig. 2A**). The minimal induction of STAT5 target genes corresponded to a lack of STAT5 phosphorylation following WNV infection during (24hpi; 53.3% E protein+ cells) and after (48hpi) log phase viral growth, despite increased amounts of STAT5 total protein by 48hpi (**Fig. 2B-D**). Given that WNV infection induces type I IFN secretion 48 hpi (Zimmerman et al. 2019) and the selective lack of STAT5 phosphorylation during WNV infection of moDCs, we hypothesized that WNV antagonizes type I IFN-mediated STAT5 signaling. Indeed, WNV infection potentially blocked STAT5 phosphorylation following both RIG-I stimulation and IFN β treatment at 24 and 48 hpi (**Fig. 2C-D**). Infection with UV-WNV failed to block RIG-I induced STAT5 phosphorylation, suggesting viral replication is required for inhibition of STAT5 signaling. In notable contrast to STAT5, both STAT1 and STAT2 were phosphorylated during WNV infection, suggesting that STAT5 may be differentially modulated by WNV. ZIKV, a closely related neurotropic flavivirus that productively infects human moDCs (Bowen et al., 2017b), also antagonized STAT5 phosphorylation downstream of RIG-I and type I IFN signaling despite relatively low levels of infection (14.7% E protein+ cells) (**Fig. 2B and 2E**). Combined, our data strongly suggest that STAT5 is a target of antagonism by both WNV and ZIKV in human moDCs.

WNV and ZIKV block STAT5 phosphorylation in a pathway specific manner

Next, we asked if WNV and ZIKV blocked STAT5 activation downstream of additional cytokine signaling pathways. Common gamma-chain family cytokines, such as IL-4, as well as multiple growth factors, including GM-CSF, signal through their respective receptors to promote STAT5 phosphorylation (Lutz et al., 2002; Watanabe et al., 1996) (**Fig. 3A**). Similar to our findings with type I IFN signaling, WNV infection dampened IL-4 induced STAT5 phosphorylation in moDCs (**Fig. 3B**). In contrast, WNV failed to antagonize GM-CSF signaling, where the increased STAT5 protein induced during infection led to increased STAT5 phosphorylation. ZIKV also potently inhibited IL-4, but not GM-CSF, mediated STAT5 phosphorylation in human DCs (**Fig. 3C**). Together, our findings suggest that WNV blocks STAT5 phosphorylation to antagonize STAT5-dependent gene induction in human moDCs in a pathway specific manner.

Blockade of STAT5 phosphorylation is flavivirus-specific

Secretion of type I IFN by infected moDCs may initiate negative regulators that downregulate type I IFN signaling independent of viral antagonism of STAT proteins. To remove confounding interpretations inherent with IFN-competent cells, we employed a Vero cell model of WNV infection, which allows for synchronous infection of cells that lack endogenous type I IFN signaling. Infection of Vero cells with WNV did not induce phosphorylation of STAT1, STAT2, or STAT5, consistent with the lack of an endogenous type I IFN response. Similar to our studies in human moDCs, pulse treatment of WNV infected Vero cells (MOI 0.01, 61.5% viral E protein+ cells) with IFN β revealed a substantial blockade of STAT5 phosphorylation (**Fig. 4A-B**). STAT1 and STAT2 phosphorylation were also blocked, but in contrast to STAT5, the blockade of STAT1 and STAT2 was less pronounced. Blockade of STAT5 phosphorylation paralleled

the large increase in WNV RNA and infectious virus release between 18 and 24 hpi seen during log phase viral growth (Zimmerman et al., 2019a). Together, this strongly suggests that antagonism of STAT5 is an active immune evasion mechanism in moDCs and not a bystander effect of endogenous type I IFN signaling during WNV infection. We next asked whether STAT5 antagonism was unique to neurotropic flaviviruses (WNV and ZIKV) or if this mechanism is conserved amongst other flaviviruses. We infected Vero cells with ZIKV PR-2015 at a MOI that achieved comparable levels of infection as our studies with WNV (**Fig. 4B**). ZIKV antagonized STAT5 phosphorylation in a dose-dependent manner at higher MOIs (MOI 1, 85% viral E protein+ cells) rather than at lower MOIs (MOI 0.25, 65% viral E protein+ cells) downstream of type I IFN signaling in Vero cells. ZIKV infection at the higher MOI of 1 showed similar levels of STAT5 antagonism as observed in human moDCs (**Fig. 4C-D**). Consistent with recent work on STAT antagonism by ZIKV, we also observed diminished STAT1 phosphorylation, as well as decreased STAT2 phosphorylation that corresponded with degradation of STAT2 total protein (Bowen et al., 2017b; Grant et al., 2016). In contrast to WNV at similar infection levels (DENV1: 53.9%; DENV2: 64%; DENV3: 60.5%; DENV4: 55.7%; YFV-17D 51.7% viral E protein+ cells), STAT5 phosphorylation was not blocked in Vero cells infected with DENV1-4 and YFV-17D following IFN β pulse treatment (**Fig. 5A-F**). Consistent with previous studies of DENV2 antagonism of type I IFN signaling (Morrison et al., 2013), we observed STAT2 degradation in Vero cells infected with DENV1, 2, and 4, while STAT1 phosphorylation was detected after IFN β pulse treatment. Markedly, DENV3 did not show degradation of STAT2 but showed a slight reduction in STAT2 phosphorylation, suggesting that antagonism of STAT2 by DENV may have a serotype-specific effect in Vero cells. Altogether, these findings demonstrate that antagonism of STAT5 is a virus-specific strategy used by WNV and ZIKV to potentially subvert the antiviral landscape in human DCs during infection.

ZIKV, but not WNV, blocks activation of Tyk2 and JAK1

The pathway specific inhibition of STAT5 through type I IFN, IL-4, but not GM-CSF, signaling within moDCs provides insight into the host target of viral antagonism. The type I IFN receptor and the type II IL-4 receptor, associate with JAK1 and TYK2 to mediate tyrosine phosphorylation of STAT1 and STAT2, while TYK2 constitutively associates with STAT5 and mediates its tyrosine phosphorylation (Fish et al., 1999; Lutz et al., 2002). GM-CSF signaling through the GM-CSF receptor predominately activates JAK2, but not JAK1 or TYK2, suggesting TYK2 and JAK1 may be targeted to block STAT5 phosphorylation (Al-Shami et al., 1998; Watanabe et al., 1996). To assess JAK inhibition, we infected Vero cells at MOI 0.1 with WNV for 12, 18, and 24 hours. Consistent with the lack of endogenous type I IFN production, WNV infection alone did not induce TYK2 phosphorylation. Although we did observe JAK1 phosphorylation, this is likely explained by the production of other cytokines that can activate JAK1 (Hammaren et al., 2019). In contrast to blockade of STAT protein phosphorylation, we observed no blockade of TYK2 and enhanced JAK1 phosphorylation following IFN β pulse treatment of infected cells (**Fig. 6A**). Despite its similarities to WNV in inhibiting STAT5 phosphorylation, ZIKV efficiently blocked phosphorylation of both JAK1 and Tyk2 downstream of type I IFN signaling (**Fig. 6B**). Previous work has shown that flaviviruses are capable of downregulating IFNAR1 from the cell surface (Evans et al., 2011; Lubick et al., 2015), so, we assessed whether ZIKV infection decreased expression of IFNAR1 or IFNAR2 from the Vero cell surface (**Fig. 6C**). At 24 hpi where we observed blockade of JAK1 and Tyk2 phosphorylation in ZIKV-infected Vero cells, we observed an increase in both IFNAR1 and IFNAR2 expression compared to mock infected cells. Combined, these findings suggest that WNV and ZIKV antagonize STAT5 signaling through two separate mechanisms: ZIKV at the level of JAK kinase phosphorylation and WNV

downstream of JAK kinases, potentially through more direct inhibition of STAT5 phosphorylation.

Discussion

In this study, we combined traditional virologic and immunologic measures with transcriptomic and computational approaches to define the global antiviral response during WNV infection in human primary cells. Using cis-regulatory sequence analysis, STAT5, a transcription factor previously described as a regulator of DC activation, was identified as an important regulatory node of antiviral DC responses downstream of innate immune signaling. In contrast, STAT5 signaling was minimally activated during WNV infection in human moDCs, corresponding with minimal expression of genes of inflammatory responses or molecules involved in T cell priming. Mechanistically, WNV and ZIKV blocked STAT5 phosphorylation downstream of RIG-I, IFN β , IL-4, but not GM-CSF signaling, suggesting pathway-specific antagonism of STAT5 activation in moDCs. Notably, neither the related flaviviruses DENV1-4 nor vaccine strain YFV-17D inhibited STAT5 phosphorylation. Mechanistically, WNV and ZIKV displayed differential inhibition of JAK1 and TYK2 phosphorylation, indicating two distinct mechanisms to antagonize STAT5 signaling. Combined, our study identifies antagonism of STAT5 phosphorylation as a conserved immune countermeasure used by certain pathogenic flaviviruses.

Cis-regulatory sequence analysis revealed STAT5 as a regulatory node of multiple components of DC activation downstream of RLR and type I IFN signaling. Indeed, we observed significant enrichment for multiple STAT5 target genes involved in DC activation, which corresponded with increased gene expression and secretion of pro-inflammatory cytokines and up-regulation of proteins involved in T cell activation (Zimmerman et al., 2019a). While this confirms previous studies that have implicated STAT5 upstream of DC activation, our work reveals a new facet of STAT5 activation during flavivirus infection through engagement of innate immune signaling (Bell et al., 2013; Toniolo et al., 2015). The rapid kinetics of STAT5 phosphorylation following RIG-I

or MDA5 stimulation suggest that RLR signaling may directly induce phosphorylation of STAT5 through activation of a tyrosine kinase, such as Src or Lyn, both of which are induced by RLR signaling (Chin et al., 1998; Johnsen et al., 2009; Lim et al., 2015; Okutani et al., 2001; Xiao et al., 2010). Alternatively, rapid production of type I IFN, which also promotes STAT5 activation, may mediate STAT5 phosphorylation following RLR signaling. Combined, our data suggests that STAT5 is an important regulatory node downstream of the RLR and type I IFN signaling axis.

In contrast to RLR and IFN β signaling, WNV infection did not up-regulate most predicted STAT5 target genes, and STAT5 was not phosphorylated during infection despite secretion of IFN β and IFN α . Corresponding with minimal STAT5 enrichment, WNV infection failed to promote up-regulation of inflammatory mediators and molecules involved in antigen presentation and T cell co-signaling. These findings are similar to previous work, where WNV infection also failed to induce inflammatory cytokine secretion (Silva et al., 2007). Infection of moDCs with a non-pathogenic WNV isolate, WNV Kunjin, also induced minimal production of IL-12, despite notable up-regulation of both CD86 and CD40 (Kovats et al., 2016). This suggests that an inability to induce inflammatory cytokine responses may be shared among WNV strains, while pathogenic strains have evolved unique mechanisms to subvert antigen presentation and T cell activation. The lack of activation of WNV-infected human moDCs is also similar to our recent work with ZIKV (Bowen et al., 2017b). In contrast to WNV and ZIKV, infection of moDCs with the YFV vaccine strain (YFV-17D) up-regulates multiple inflammatory mediators and surface expression of CD80 and CD86 (Querec et al., 2006). The ability of YFV-17D to induce strong DC activation may reflect the loss of a viral antagonist during the attenuation process, similar to the ability of WNV Kunjin to induce up-regulation of CD86 and CD40 (Kovats et al., 2016). Alternatively, the ability of YFV-17D

to induce DC activation may be an inherent property of certain flaviviruses. Indeed, DENV has also been found to activate inflammatory responses and up-regulate co-stimulatory molecules following infection despite its ability to degrade STAT2 in infected cells (Morrison et al., 2013; Olganier et al., 2014; Rodriguez-Madoz et al., 2010). We demonstrate here that, unlike WNV and ZIKV, YFV-17D and DENV1-4 do not inhibit STAT5 phosphorylation in Vero cells. This raises the possibility that the inability to block STAT5 may explain the activation induced during YFV-17D and DENV infection. Altogether, we demonstrate that WNV, similar to ZIKV, induces minimal DC activation during productive infection, contrasting with both DENV and YFV-17D.

Blockade of STAT5 signaling by WNV was found to be multi-frontal, as multiple STAT5 signaling cytokines induced downstream of RIG-I signaling (GM-CSF, IL-4, IL-15) are not produced during infection with WNV (Zimmerman et al., 2019a). The lack of GM-CSF secretion may also overcome the need for WNV to block GM-CSF-induced STAT5 phosphorylation. Similar to WNV, ZIKV has also been found to induce minimal secretion of cytokines, including IL-4, GM-CSF, IL-12, IL-15, and RANTES, during infection of human moDCs (Bowen et al., 2017b). In contrast, DENV and YFV-17D infection in human moDCs has been reported to induce proinflammatory cytokine expression and secretion, including IL-12 and RANTES (Costa et al., 2017; Gandini et al., 2011; Ho et al., 2001; Lim et al., 2014). This robust cytokine response could potentially reflect the inability of DENV and YFV-17D to inhibit STAT5 signaling cytokines. Combined, this suggests that the ability to antagonize STAT5 signaling may be an important feature of WNV and ZIKV pathogenesis.

Surprisingly, viral blockade of STAT5 phosphorylation during WNV, but not ZIKV infection, did not correspond with impaired activation of TYK2 and JAK1, members of the Janus associated kinase (JAK) family that phosphorylate STAT5 downstream of type I

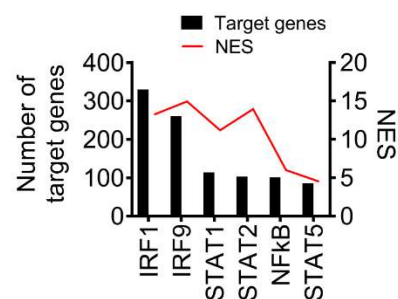
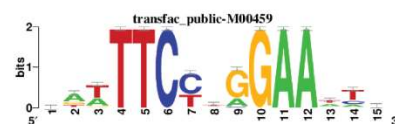
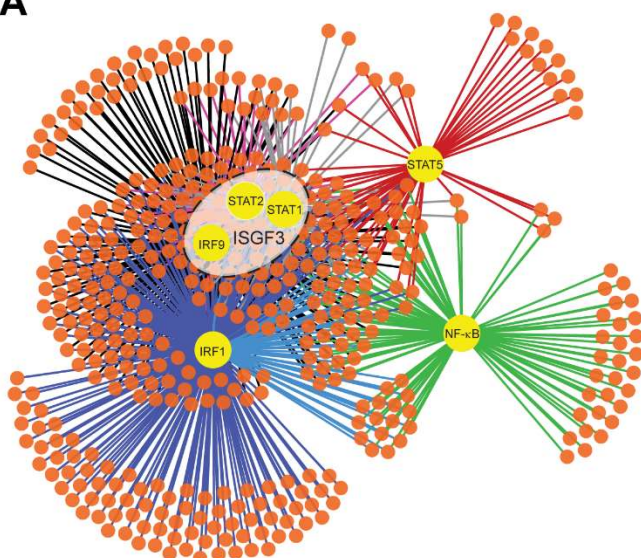
IFN, IL-4, but not GM-CSF signaling. Numerous flaviviruses, including the closely related Japanese encephalitis virus (JEV) and Langkat virus, have been shown to inhibit TYK2 activation through the NS5 protein to subvert JAK/STAT signaling (Best et al., 2005; Lin et al., 2006). Nevertheless, our work suggests that inhibition of TYK2 or JAK1 activation is likely not the mechanism used by WNV to block STAT5 phosphorylation. Indeed, STAT1 and STAT2, which are also phosphorylated by TYK2 and JAK1, were not blocked as strongly as STAT5, suggesting viral inhibition may be occurring at a step unique to STAT5 signaling. STAT5 itself is likely not targeted directly, given that GM-CSF induced STAT5 signaling remains intact during WNV infection. One possibility is that WNV may specifically disrupt the interaction between STAT5 and TYK2 or JAK1. WNV infection may also directly induce negative regulators of STAT5 signaling, such as facilitating interactions between STAT5 and the protein tyrosine phosphatase, SHP-2, a well-known regulator of cytosolic STAT5 signaling (Yu et al., 2000). Another possibility includes induction of the suppressor of cytokine signaling family, which broadly regulate JAK/STAT signaling and can be modulated during flavivirus infection (Sharma et al., 2016). Importantly, UV-inactivated virus, which undergoes cellular binding and entry but is replication incompetent, was unable to inhibit STAT5. This suggests that viral replication is required for STAT5 antagonism, potentially through a secreted viral protein that would affect both infected and uninfected cells. The observation that DENV1-4 and YFV-17D do not block STAT5 phosphorylation provides a valuable tool to further define the viral and host factors within subsets of flaviviruses that mediate STAT5 blockade.

In summary, our systems biology approach identified STAT5 as a regulator of DC activation that is blocked by WNV as a mechanism to subvert DC activation and T cell priming. ZIKV, but not YFV-17D or DENV1-4, also blocked STAT5 signaling, suggesting that viral antagonism of STAT5 may be a common strategy of particular subsets of

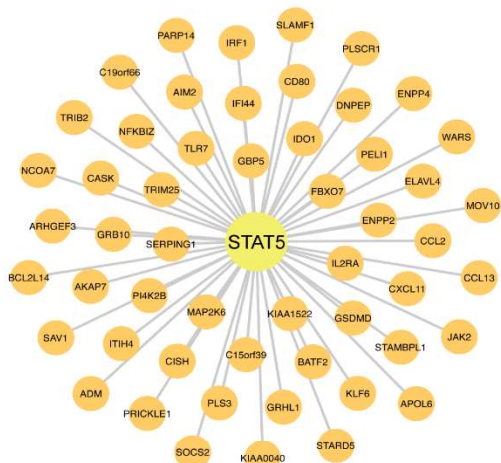
pathogenic flaviviruses to evade the pressures of host immunity. Our study advances our understanding of how pathogenic flaviviruses subvert antiviral immunity during human infection.

Figure 1

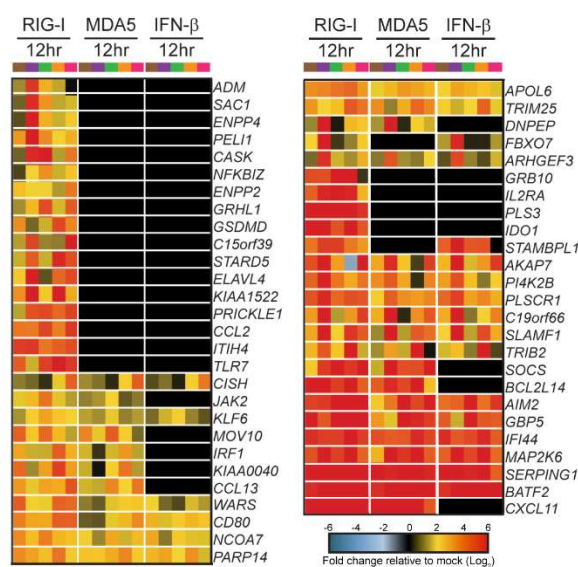
A



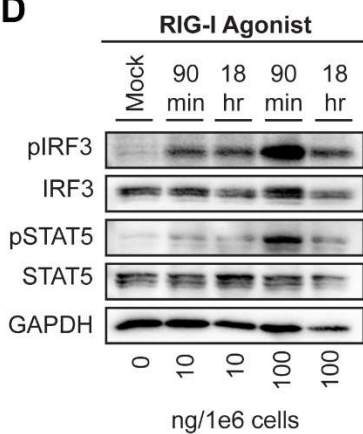
B



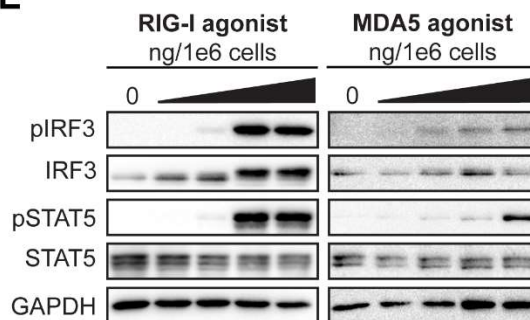
C



D



E



F

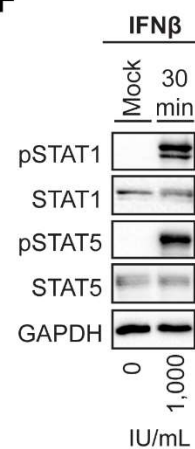


Fig 1. Systems biology reveals STAT5 as a regulatory node of antiviral DC responses. **(A)** Transcription factor regulatory network of module 5 gene expression as predicted by iRegulon (left panel). The top predicted transcriptional regulators (large, yellow nodes) are shown with a connecting line to predicted target genes (small, orange nodes). The consensus sequence for promoter regions targeted by STAT5 as generated by iRegulon and annotated as transfac_public-M00459 (top right panel). The number of predicted target genes and the normalized enrichment score (NES) for a given regulator is shown below (bottom right panel). **(B)** STAT5 regulatory node (large, central node) is shown with the predicted target genes indicated (small nodes), as determined by iRegulon. **(C)** Heatmap of predicted STAT5 target genes after stimulation with innate immune agonists with the \log_2 normalized fold change relative to uninfected, untreated cells is shown (>2-fold change, significance of $p < 0.01$). Genes that did not reach the significance threshold are depicted in black color. Each column within a treatment condition is marked by a unique color and represents a different donor ($n = 5$ donors). **(D)** moDCs were treated with RIG-I agonist (10 or 100ng/1e6 cells) for 90 mins or 18 hrs. **(E)** moDCs were treated with RIG-I or MDA5 agonist for 90 min (10, 100, 1,000, and 10,000ng/1e6 cells). **(F)** moDCs were treated with IFN β (1000 IU/mL) for 30 mins. For D-F, Western blot analysis was performed for the indicated proteins. Western blots are representative of data obtained from 3-8 donors.

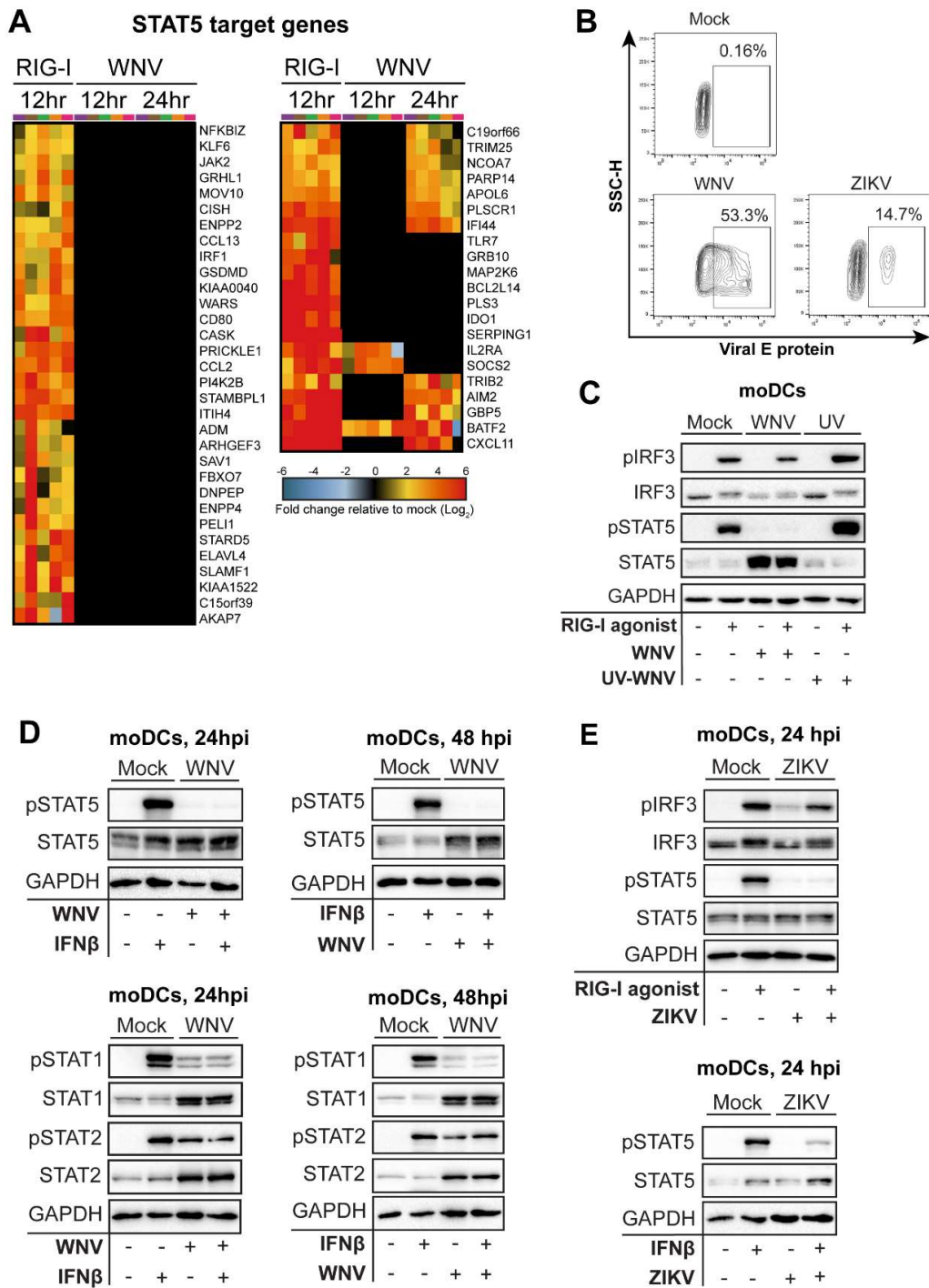


Fig 2. WNV actively blocks STAT5 phosphorylation and expression of STAT5 target genes. (A) Heatmap of predicted STAT5 target genes after stimulation with RIG-I agonist or infection with WNV (12, 24 hpi) with the log₂ normalized fold change relative to

uninfected, untreated cells is shown (>2-fold change, significance of $p < 0.01$; right panel). Genes that did not reach the significance threshold are depicted in black color. Each column within a treatment condition is marked by a unique color and represents a different donor (n= 5 donors). **(B)** Representative flow cytometry plot of viral E protein+ cells after infection in moDCs after WNV or ZIKV infection (24 or 48 hrs, MOI 10 based on Vero titer). **(C)** moDCs were treated with RIG-I agonist treatment (100ng/1e6 cells) for 90 min following no infection (“Mock”), infection with UV-inactivated WNV (MOI 10, “UV-WNV”), or infection with replication competent WNV (MOI 10, “WNV”). **(D, E)** Human moDCs were left uninfected (“Mock”) or infected with WNV or ZIKV (24 or 48 hrs, MOI 10 based on Vero titer). Cells were left untreated or pulse-treated with IFN β (1,000 IU/mL) for 30 min. Data in B is representative of results obtained from two independent experiments. Data from C and D representative of results obtained from 3-8 donors.

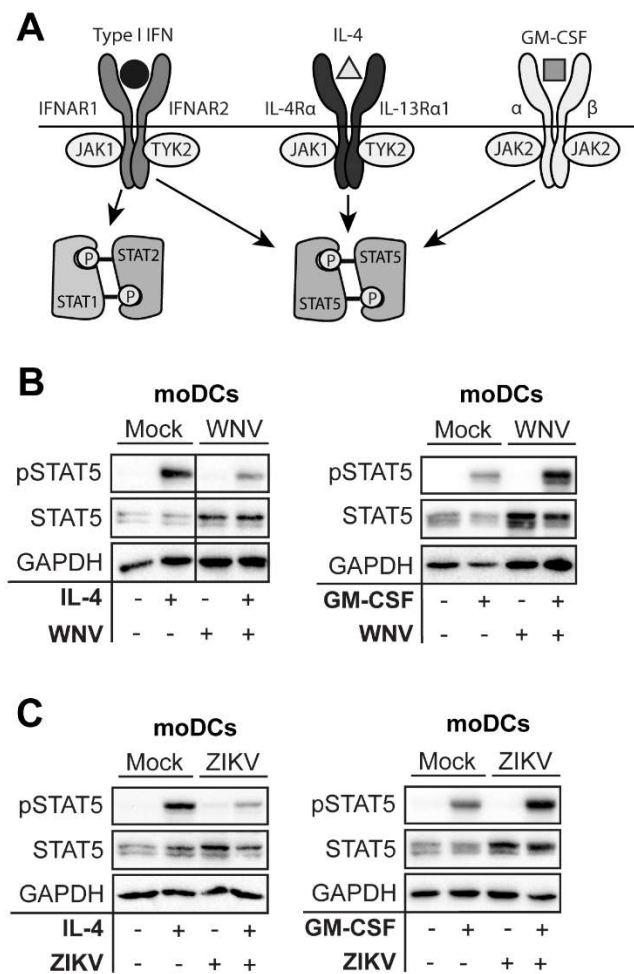


Fig 3. WNV and ZIKV inhibit STAT5 phosphorylation in a pathway-dependent manner (A) Schematic of STAT signaling downstream of type I IFN, IL-4, and GM-CSF signaling. **(B, C)** moDCs were infected with WNV or ZIKV (MOI 10 based on Vero cell titer) for 48 hrs and treated with IL-4 (10 ng/mL) for 30 min or GM-CSF (10 ng/mL) for 30min. For B and C, Western blot analysis was performed for the indicated proteins. Data is representative of results obtained from 3-8 donors

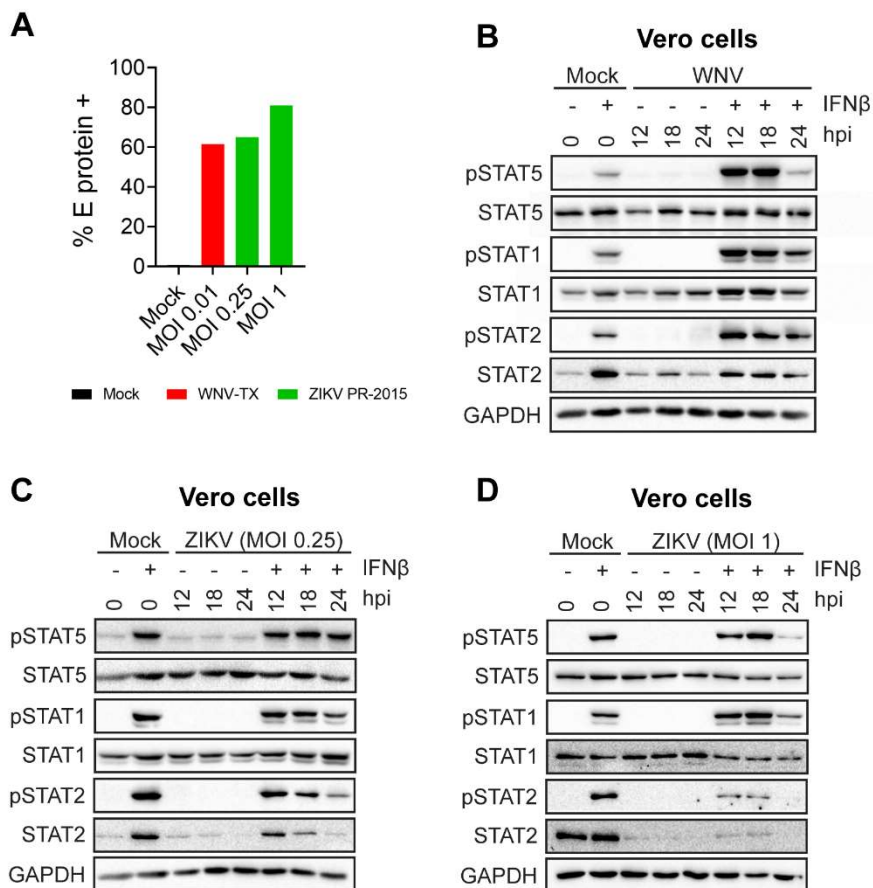


Fig 4. WNV and ZIKV antagonize STAT5 phosphorylation in the absence of IFN signaling. (A) Vero cells were infected with WNV-TX (MOI 0.01 based on Vero titer) or ZIKV-PRVABC59 (MOI 0.25, 1 based on Vero titer) and percent E protein+ cells were determined by flow cytometry at 24 hpi (B) Vero cells were left uninfected (“Mock”) or infected with WNV-TX (MOI 0.01 based on Vero titer) at 24 hpi. (C-D) Vero cells were left uninfected (“Mock”) or infected with ZIKV (MOI 1 based on Vero titer) at 24 hpi. Data is representative of results obtained from three independent experiments.

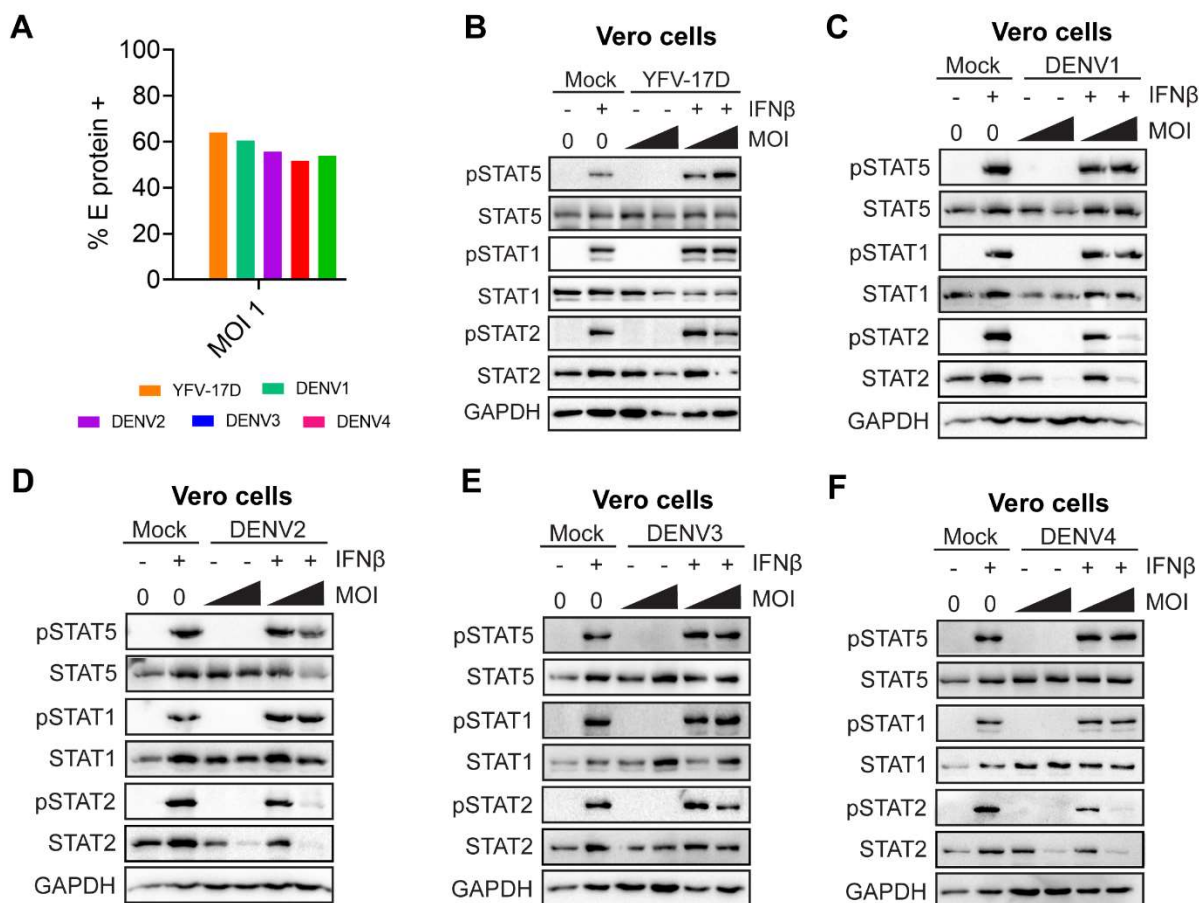


Fig 5. DENV1-4 and YFV-17D do not antagonize STAT5 phosphorylation at similar infection levels as WNV. (A) Vero cells were infected with DENV1-4 or YFV-17D (MOI 1 based on Vero titer) and percent E protein+ cells were determined by flow cytometry at 24 hpi. Vero cells were left uninfected ("Mock") or infected (B), YFV-17D (MOI 0.1, 1 based on Vero titer) (C-F) or DENV1-4 (MOI 0.1, 1 based on Vero titer) for 24 hrs. Cells were then left untreated, or pulse treated with IFN β (1,000 IU/mL) for 30 min. For B-F, Western blot analysis was performed for the indicated proteins. Data in C-H is representative of results obtained from two independent experiments.

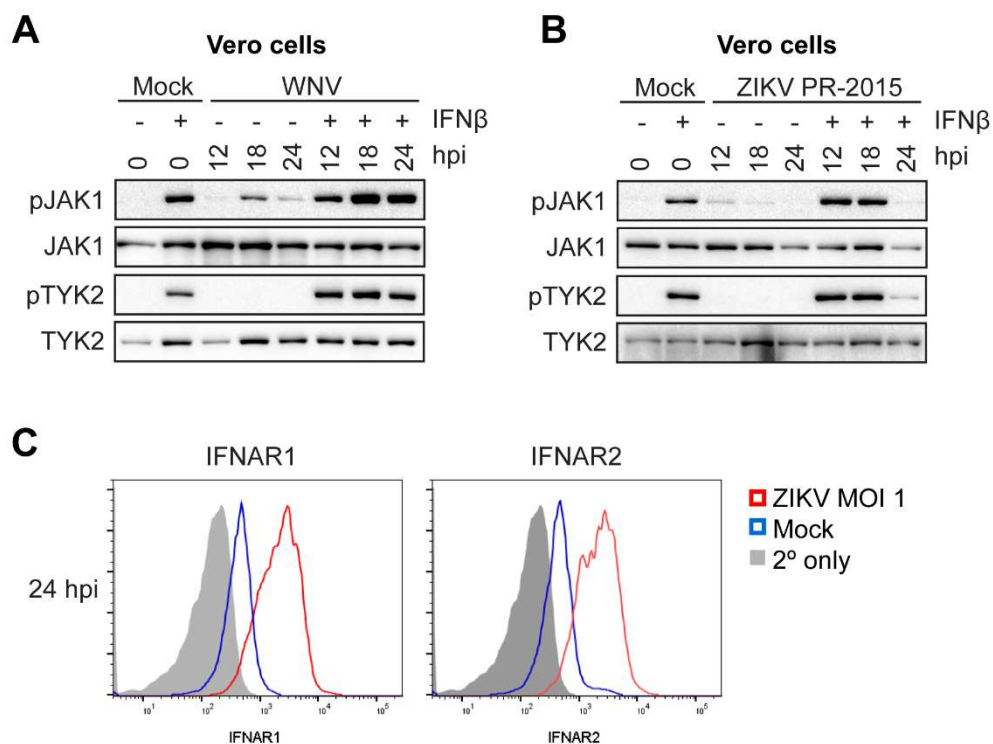


Fig 6. ZIKV, but not WNV, blocks TYK2 or JAK1 activation to compromise STAT5 phosphorylation. (A, B) Vero cells were left uninfected (“Mock”) or infected with WNV (MOI 0.1 based on Vero titer) or ZIKV-PRVABC59 (MOI 1 based on Vero titer) for 24 hrs. Cells were then left untreated, or pulse treated with IFN β (1,000 IU/mL) for 30 min. **(C)** Vero cells were left uninfected (“Mock”) or infected with WNV (MOI 1 based on Vero titer) for 24hrs and levels of surface IFNAR1 and IFNAR2 expression were measured by flow cytometry. For A-B, Western blot analysis was performed for the indicated proteins. Data in A and B is representative of results obtained from two independent experiments.

Materials and Methods

Ethics statement. Human peripheral blood mononuclear cells (PBMCs) were obtained from de-identified healthy adult blood donors and processed immediately. All individuals who participated in this study provided informed consent in writing in accordance to the protocol approved by the Institutional Review Board of Emory University, IRB#00045821, entitled “Phlebotomy of healthy adults for the purpose of evaluation and validation of immune response assays”.

Cell lines. Vero cells (WHO Reference Cell Banks) were maintained in complete DMEM. Complete DMEM was prepared as follows: DMEM medium (Corning) supplemented with 10% fetal bovine serum (Optima, Atlanta Biologics), 2mM L-Glutamine (Corning), 1mM HEPES (Corning), 1mM sodium pyruvate (Corning), 1x MEM Non-essential Amino Acids (Corning), and 1x Antibiotics/Antimycotics (Corning). Complete RPMI was prepared as follows: cRPMI; RPMI 1640 medium (Corning) supplemented with 10% fetal bovine serum (Optima, Atlanta Biologics), 2mM L-Glutamine (Corning), 1mM Sodium Pyruvate (Corning), 1x MEM Non-essential Amino Acids (Corning), and 1x Antibiotics/Antimycotics (Corning).

Generation of monocyte derived dendritic cells. To generate human moDCs, CD14+ monocytes were differentiated in cRPMI supplemented with 100ng/mL of GM-CSF and IL-4 for 5-6 days, as previously described (Bowen et al., 2017b). In brief, freshly isolated PBMCs obtained from healthy donor peripheral blood (lymphocyte separation media; StemCell Technologies) were subjected to CD14+ magnetic bead positive selection using the MojoSort Human CD14 Selection Kit (BioLegend). Purified CD14+ monocytes were cultured in complete RPMI supplemented with 100ng/mL each of recombinant

human IL-4 and GM-CSF (PeproTech) at a cell density of 2×10^6 cells/mL. After 24hr of culture, media and non-adherent cells were removed and replaced with fresh media and cytokines. Suspension cells ("moDCs") were harvested after 5-6 days of culture and were consistently CD14⁻, CD11c⁺, HLA-DR⁺, DC-SIGN⁺, and CD1a⁺ by flow cytometry. For experimentation, moDCs were maintained in complete RPMI without GM-CSF or IL-4. For experiments measuring STAT5 phosphorylation, moDCs were rested in cRPMI without GM-CSF or IL-4 for 24hrs prior to experimentation.

Viruses. WNV stocks were generated from an infectious clone, WNV isolate TX 2002-HC, and passaged once in Vero cells, as previously described (Suthar et al., 2012a). ZIKV strain PRVABC59 was obtained from the Centers for Disease Control and Prevention as previously described (Quicke et al., 2016a). YFV -17D was subpassaged from YF-VAX (Aventis Pasteur) in SW-480 cells followed by passaging in Vero cells as previously described (Querec et al., 2006). The DENV1, DENV3, and DENV4 strains were derived from low passage clinical isolates and generated from infectious clones (ic) as previously described (Gallichotte et al., 2015; Messer et al., 2012; Widman et al., 2017). The DENV2 ic was generated in the Baric laboratory in a similar manner to the DENV1, DENV3 and DENV4 ic. The generation and characterization of the DENV2 S16803 ic will be described in a future publication. WNV and ZIKV were titrated by plaque assay on Vero cells with a 1% agarose overlay and crystal violet counterstain, as previously described (Suthar et al., 2012a). DENV was titrated by focus forming assay as previously described (Widman et al., 2017). moDCs were infected with WNV or ZIKV at MOI 10 for 1 hr at 37°C in cRPMI (without GM-CSF or IL-4). After 1 hr, virus was washed off and cells were resuspended in fresh cRPMI and incubated at 37°C for 3-72 hr.

Quantitation of infectious virus. Infectious virus was quantitated using a plaque assay on Vero cells with a 1% agarose overlay and crystal violet counterstain, as previously described (Suthar et al., 2012a).

Innate immune agonists. To stimulate RIG-I signaling, 100ng of RIG-I agonist derived from the 3'-UTR of hepatitis C virus (Saito et al., 2008) was transfected per 1e6 cells using TransIT-mRNA transfection kit (Mirus). For stimulation of MDA5 signaling, 100ng of high molecular weight poly-(I:C) was transfected per 1e6 cells using LyoVec transfection reagent (Invivogen). To stimulate type I IFN signaling, cells were incubated with 100 IU/mL of human recombinant IFN β . In select experiments, different doses of agonists were used and this is indicated within the respective Figure legend.

RNA sequencing and bioinformatics. moDCs were generated from 5 donors and either treated with innate immune agonists for 12hr (RIG-I, MDA5, or IFN β) or infected with WNV (12hpi and 24hpi). Total RNA was purified (Quick-RNA MiniPrep Kit; Zymo Research) and mRNA sequencing libraries were prepared for RNA sequencing (Illumina TruSeq chemistry). RNA sequencing was performed on an Illumina HiSeq 2500 System (100bp single end reads). Sequencing reads were mapped to the human reference genome 38. Weighted gene co-expression module analysis was performed on DESeq2 normalized mapped reads (TIBCO Spotfire with Integromics Version 7.0) from RIG-I agonist, MDA5 agonist, IFN β , and mock treated samples. First, the datasets were reduced to focus the network analysis on the 5446 most variable genes (as determined by variation value greater than 1) using the Variance function in R. We constructed a signed weighted correlation network by generating a matrix pairwise correlation between all annotated gene pairs. The resulting biweight mid-correlation matrix was transformed

into an adjacency matrix using the soft thresholding power (β_1) of 12. The adjacency matrix was used to define the topological overlap matrix (TOM) based on a dissimilarity measurement of $1 - TO$. Genes were hierarchically clustered using average linkage and modules were assigned using the dynamic tree-cutting algorithm (module eigengenes were merged if the pairwise calculation was larger than 0.75). This resulted in the construction of six modules. Transcriptional regulators within the M5 module were computationally predicted with iRegulon (Janky et al., 2014), using the top most connected M5 genes using an eigengene-based connectivity cutoff of 0.4. Differentially expressed genes within the M5 module were identified as having a >2-fold change (significance of $p < 0.01$) relative to uninfected and untreated cells. Pathway analysis was performed on M5 genes using MetaCore pathway map analysis (version 6.29, Thomson Reuters). The raw data of all RNA sequencing will be deposited into the Gene Expression Omnibus (GEO) repository and the accession number will be available following acceptance of this manuscript.

Flow cytometry. Cells were prepared for analysis as previously described (Bowen et al., 2017b). For intracellular staining of WNV E protein, human moDCs and Vero cells were fixed and permeabilized (Transcription Factor Staining Buffer Kit, Tonbo Biosciences). The cells were re-blocked for 5min on ice with 0.25ul/sample Human TruStain FcX and 0.25ul/sample normal mouse serum (ThermoFisher Scientific) in Perm Buffer and E protein for 20 min on ice using 0.5ul/sample of an E16-APC (WNV) (Oliphant et al., 2005) or the pan-flavivirus 4G2-APC antibody (ZIKV, DENV1-4, and YFV-17D) in Perm Buffer. Unconjugated monoclonal 4G2 antibody was conjugated to APC using a Novus Lighting-Link kit per the manufacturer's instructions. Flow cytometry

data was analyzed using FlowJo version 10 software. Primary antibodies are listed in **Table 1**.

Western blot. Whole-cell lysates were collected in modified radioimmunoprecipitation assay buffer (10 mM Tris [pH 7.5], 150 mM NaCl, 1% sodium deoxycholate, and 1% Triton X-100 supplemented with Halt Protease Inhibitor Cocktail [ThermoFisher] and Halt Phosphatase Inhibitor Cocktail [ThermoFisher]). Protein lysates were separated by SDS-PAGE and western blot analysis was performed using the ChemiDoc XRS+ imaging system (BioRad). Western blots were analyzed using Image Lab version 5.2.1 software (BioRad) and prepared for publication using Adobe Illustrator. Primary antibodies are listed in **Table 1**.

Statistics. All statistical analysis was performed using GraphPad Prism version 8 software. The number of donors varied by experiment and is indicated within the Figure legends. Statistical significance was determined as $P < 0.05$ using a Kruskal-Wallis test (when comparing more than two groups lacking paired measurements), a Wilcoxon test (when comparing two groups with paired measurements). All comparisons were made between treatment or infection conditions with a time point matched, uninfected and untreated control.

Chapter 5: Discussion

Written by Matthew G. Zimmerman

Summary of WNV and ZIKV antagonism of STAT5 findings

Using a systems biology-based approach, we identified STAT5 as a primary transcriptional regulator downstream of type I IFN, RIG-I, and MDA5 signaling in human monocyte-derived dendritic cells (moDCs). Flaviviruses, like WNV and ZIKV, are known to inhibit numerous arms of the RIG-I and type I IFN signaling pathways (Bowen et al., 2017b; Grant et al., 2016; Keller et al., 2006; Morrison et al., 2013). We demonstrated that WNV and ZIKV infection, despite less than 100% infection (as determined by flow cytometry staining the envelope protein), potently blocked IFN β and RIG-I agonist-driven STAT5 phosphorylation, a necessary step in STAT5 dimerization and activation, as well as STAT5 target gene expression in moDCs. In addition, WNV and ZIKV inhibited STAT5 downstream of IL-4, but not, GM-CSF signaling, suggesting that viral antagonism of STAT5 is pathway-dependent. To account for potential negative regulation of IFNAR signaling seen in infected IFN-competent moDCs, we infected Vero cells with WNV and ZIKV at similar MOIs. We found that pSTAT5 activation downstream of IFN β signaling was greatly diminished between 18-24 hpi at low MOIs with WNV infection (MOI 0.01) and greater MOIs with ZIKV infection (MOI 1). The diminished STAT5 signaling by 24 hpi suggest that viral non-structural proteins, which normally rise dramatically between 18-24 hours (Keller et al., 2006; Suthar et al., 2012b), are responsible for STAT5 antagonism. Unlike WNV and ZIKV, infection of Vero cells with DENV1-4 and YFV-17D did not inhibit STAT5 phosphorylation downstream of type I IFN stimulation. However, we did observe that STAT2, a known target of antagonism by DENV (Morrison et al., 2013), was degraded in Vero cells infected with DENV1, DENV2, and DENV4 at higher MOIs. Finally, ZIKV, but not WNV, infection showed inhibition of JAK1 and TYK2 phosphorylation between 18-24 hpi. Altogether, these results indicate that WNV and ZIKV utilize different mechanisms of

inhibiting STAT5 activation with ZIKV antagonizing STAT5 phosphorylation through blockade of upstream JAK kinase activation.

Viral factors affecting STAT5 activation

We observed that inhibition of STAT5 phosphorylation occurred between 18-24 hpi in moDCs in close relation with exponential viral growth. This growth is accompanied by dramatic increases in flavivirus non-structural (NS) proteins (Bowen et al., 2017a; Keller et al., 2006; Suthar et al., 2012b), indicating NS proteins are actively targeting and blocking STAT5 activation. WNV and ZIKV NS proteins have evolved to antagonize and evade numerous arms of the innate immune response, including type I IFN signaling. (Quicke and Suthar, 2013; Serman and Gack, 2019). We observed near complete loss of RIG-I-agonist and IFN β -induced STAT5 phosphorylation despite <100% infection of moDCs (**Chapter 3, Figure 2B-E**). One possibility is that viral soluble factors, like secreted NS1, may impact STAT5 phosphorylation in both infected and bystander cells. NS1 exists as a monomer within infected cells and is important in replication of the viral genome whereas secreted NS1 exists in a hexameric form and has been implicated in innate immune evasion (Rastogi et al., 2016). Recent reports have demonstrated that DENV NS1 binds to glyocalyx components on endothelial cells and disrupts the endothelial cell barrier through a non-inflammatory mechanism, leading to vascular permeability (Beatty et al., 2015; Glasner et al., 2017; Modhiran et al., 2015; Puerta-Guardo et al., 2016). NS1 has also been implicated in WNV pathogenesis through inhibition of TLR3 signaling (Wilson et al., 2008); however, the effects of NS1 on TLR3 are still controversial. To further address whether STAT5 phosphorylation is inhibited in bystander cells, WNV and ZIKV E protein⁺ and phosphorylated STAT5⁺ co-expressing moDCs could be identified by flow cytometry and would allow us a single-cell analysis to determine the effects of infected

cells on bystander cells. We observed that STAT5 was not inhibited by YFV-17D nor DENV1-4 (**Chapter 4, Figure 5**). Thus, chimeric viruses could be generated by replacing individual WNV or ZIKV NS proteins and infecting moDCs. These chimeric viruses could also be used in animal studies to assess the overall role of STAT5 inhibition in the host, although this may be affected other innate immune antagonistic roles of those individual NS proteins.

Potential STAT5 antagonism in other target tissues

Although our study demonstrated that STAT5 phosphorylation is inhibited by WNV and ZIKV in moDCs, the biological relevance of this finding is not completely understood. Pharmacologic inhibition of STAT5 using the bromodomain inhibitor JQ1 has been shown to inhibit LPS-induced activation of human moDCs and subsequent stimulation of CD8+ T cells (Toniolo et al., 2015). Earlier work in our lab has also demonstrated that WNV-infected moDCs are less capable of stimulating CD4+ and CD8+ T cell proliferation and activation (Zimmerman et al., 2019a). This finding corroborates well with the lack of CD80 gene expression in WNV-infected moDCs (**Chapter 3, Figure 2A**). Our work focused primarily on *in vitro* differentiated inflammatory moDCs; however, whether WNV can infect DC precursors is not well characterized. STAT5 signaling is critical in proper conventional and tissue-resident DC development from pre-DC precursors (Eddy et al., 2017; Esashi et al., 2008; Li et al., 2012). Although we did not observe inhibition of GM-CSF activated STAT5 phosphorylation in WNV-infected moDCs, the ability of WNV to infect and impact GM-CSF signaling in DC precursor populations warrants further investigation.

Outside of its role in immune cell activation, STAT5 signaling is downstream of numerous growth and neurotropic factors, including erythropoietin (EPO) and growth

hormone (GH) (Able et al., 2017). Recent work has demonstrated that brain-specific *Stat5*^{-/-} mice exhibit limited learning capacity and memory formation with no effect on hippocampal neurogenesis (Furigo et al., 2018). STAT5 has also been implicated in EPO and GH-mediated protection from glutamate neurotoxicity (Byts et al., 2008), a condition also seen in WNV and Sindbis virus-infected patients suffering from acute flaccid paralysis (Blakely et al., 2009; Darman et al., 2004). Neurologic sequelae of WNV neuroinvasive disease include memory deficits, word-finding difficulty, and impaired cognition (Carson et al., 2006; Davis et al., 2006). Given this, inhibition of STAT5 in WNV-infected neurons and glia may contribute to neuronal death. Infection of primary mouse and human neurons and glia with WNV and treatment with STAT5-activating growth factors and cytokines are needed to assess STAT5 antagonism in neuronal tissue. In addition, increases in brain parenchymal or spinal cord neuronal excitotoxicity and death in WNV-infected brain-specific *Stat5*^{-/-} knockout mice may elucidate this potential role of STAT5 during neurotropic viral infection.

Blockade of STAT5 may also be involved in the neuropathogenesis of during prenatal ZIKV infection. Seeding of ZIKV into the fetal compartment and infection of the fetus can cause devastating neurologic sequelae in both microcephalic and normocephalic children (Nielsen-Saines et al., 2019; Teixeira et al., 2020). Once in the fetal CNS, ZIKV primarily infects precursor neural radial glia, astrocytes, and microglia with less infection found within maturing neurons in the cortical plate (Onorati et al., 2016; Retallack et al., 2016). STAT5 has been implicated in post-mitotic neuronal differentiation in the pre-cortical plate as well as axonal migration from the telencephalon of mice (Markham et al., 2007). Although STAT5 deletion did not contribute to neuronal apoptosis in this study, inhibition of STAT5 signaling by ZIKV could contribute to abnormal neuronal development in infected fetuses.

Summary of Placental ZIKV Infection Findings

In Chapter 2, we assess the ability of cross-reactive DENV antibodies to enhance ZIKV infection in human placental tissues. Due to the high sequence homology (~54%) between the DENV and ZIKV E proteins (Priyamvada et al., 2016b), we hypothesized that cross-reactive antibodies elicited by DENV infection can bind ZIKV and cause antibody-dependent enhancement of ZIKV infection in placental macrophages (Hofbauer cells (HCs)), the primary tropism for ZIKV in the human placenta (Bhatnagar et al., 2017; Martines et al., 2016; Quicke et al., 2016a). Infection of HCs with immune complexes generated with ZIKV and cross-reactive DENV antibodies show high levels of ZIKV enhancement (>80%) that titrate with increasing antibody dilutions. Our results suggest that this enhancement results from increased binding and entry of ZIKV into HCs as well as dampening of innate immune responses. We also observed ZIKV enhancement in both HCs and second trimester human chorionic villous explants in an IgG-subclass specific manner. We found that the ZIKV immune complexes take advantage of the physiologic IgG transport across the placental barrier utilizing FcRn on the apical side of the STB layer. Imaging of infected explants also confirmed that these viral immune complexes preferentially target HCs within the villous stroma, not the STB and CTB layers.

In Chapter 3, we found that diluted late convalescent primary DENV3, primary ZIKV, and secondary ZIKV immune sera can enhance ZIKV infection in our human placental explant model. This indicates that sub-neutralizing levels of type-specific, as well as cross-reactive, flavivirus antibodies are capable of ZIKV ADE in placental tissues. Notably, early convalescent primary and secondary ZIKV sera, but not DENV3 sera, can limit the ZIKV enhancement seen in explants infected in the presence of late convalescent sera. IgM depletion from the early convalescent ZIKV sera increased ZIKV

ADE to levels similar to late convalescent sera. Altogether, Chapters 2 and 3 demonstrate the collective ability of both type specific ZIKV and cross-reactive DENV antibodies to traffic ZIKV across the placental barrier and establish high levels of infection within the villous stroma.

New Paradigm: Viral transcytosis using the placental FcRn pathway?

With the growing number of new flavivirus infections emerging in non-endemic regions, the impact of cross-reactive antibodies on the clinical severity of secondary infection with structurally similar flaviviruses remains controversial. More recently, understanding how cross-reactive antibodies facilitate viral transport across immunologically privileged barriers, particularly the placenta, has become an emerging field of interest. After the transfer of maternal IgG across the placenta through FcRn, HCs reside in the villous stroma and express high levels of FcγRs, allowing them to bind and phagocytose IgG immune complexes with high affinity. HCs are highly permissive to ZIKV infection and are the primary target of infection in ZIKV-infected pregnant mothers within the placenta (Bhatnagar et al., 2017; Quicke et al., 2016b ; Zimmerman et al., 2018). Several congenital viruses, including hCMV and HIV-1, have been implicated in utilization of maternal antibodies to transcytose through the trophoblast layer and enter the fetal compartment (Maidji et al., 2006; Toth et al., 1994). Using mid-gestation explants, immune complexes generated from DENV cross-reactive antibodies bound to ZIKV were found to cross the human placental barrier in an FcRn-dependent manner (Zimmerman et al., 2018). Human mid-gestation placental explants are a powerful system for studying viral infections within the normal architecture of the placenta; however, they have limited lifespans (<10 days), lack normal blood perfusion, and can be problematic to procure. Given the limitations of the human *ex vivo* explant system, pregnant animal model systems

have been utilized to try and recapitulate the human placenta to study the influence of DENV immunity on viral seeding of the placenta during secondary ZIKV infection.

Recently, Brown et al. evaluated the effects of DENV cross-reactive antibodies on ZIKV infection in both a pregnant mouse model system and in human *ex vivo* placental explants. In their study, pregnant mice were infected with ZIKV in the presence of purified DENV immune plasma. They observed that increased fetal resorption, increased infection of the placenta, and placental damage in ZIKV-infected pregnant mice inoculated with DENV immune plasma at embryonic age day 5.5 (E5.5). This effect was diminished if the pregnant mice were infected at an advanced gestational age, E10.5 (Brown et al., 2019). In another study, Rathore and colleagues demonstrated that previous DENV immunity or administration of the pan-flavivirus binding antibody, 4G2, in pregnant mice caused enhanced infection in the fetus, causing fetal resorption and limited cortical growth. They also determined that increased fetal ZIKV infection was facilitated by translocation of viral immune complexes across the placenta by murine FcRn (Rathore et al., 2019). Sub-neutralizing levels of homotypic ZIKV-experienced sera have also been shown to mediate enhancement of ZIKV infection and fetal resorption in pregnant infected *Ifnar*^{-/-} mice (Shim et al., 2019). One limitation of these studies is the embryonic age, E6.5-E7, at which the pregnant DENV- or 4G2-experienced mice were inoculated with ZIKV. Infection of pregnant mice at E6.5-7, when the development of the vitelline yolk sac placenta is variable and the chorioallantoic placenta has not yet formed. In contrast to the singular monochorial placenta of humans, fetal mice obtain nutrients from two separate placenta, the vitelline yolk sac (VYS) and labyrinthine placenta, at different times during gestation. The VYS arises at embryonic age E7-E9 and is comprised of a single-cell layer of endodermal epithelium with underlying mesodermal vitelline vasculature bathed in uterine secretions containing maternal IgG (Cross et al., 1994; Kim et al., 2009). Unlike humans, approximately 20% of IgG transfer is facilitated across the yolk sac through murine FcRn

while a majority of IgG transfer is absorbed in the mouse gut postnatally through breastmilk (Ander et al., 2019) (**Figure 2C, see Introduction Figure 2**). Around E12 of pregnancy, the trichorioallantoic labyrinthine placenta is fully functional with two outer layers of CTBs and one inner layer of STBs, neither of which express FcRn (Kim et al., 2009; Latvala et al., 2017). (**Figure 2D, see Introduction Figure 2**). To more accurately model human FcRn (hFcRn) expression and trafficking of flavivirus immune complexes within the murine placenta, future animal studies could utilize the transgenic humanized mouse strains Tg32 and Tg276, which express copious amounts of human FcRn within different layers of the labyrinthine placenta (Latvala et al., 2017). Additionally, the innate immune functionality of the murine STB layer, which has been shown to halt bacterial and viral infections through the impermeability of the STB syncytium as well as type III IFN signaling, is not present at these early gestational ages (Bayer et al., 2016; Chen et al., 2017; Jagger et al., 2017; Robbins et al., 2010; Zeldovich et al., 2013). This suggests that the trophoblasts layers found in the murine chorioallantoic, but not VYS, placenta should be considered in future studies for accurately recapitulating mechanisms of placental translocation by invading pathogens observed in humans.

Because of their high level of homology to humans, non-human primates, particularly rhesus macaques, have been used extensively to understand transplacental ZIKV infection and subsequent neurological birth defects within the developing fetus. NHPs utilize a bidiscoidal, hemomonochorial placenta that expresses FcRn on the STB surface, allowing for >80% efficiency of maternofetal IgG transfer during pregnancy (Latvala et al., 2017; Pentsuk and van der Laan, 2009). Recent work has shown that early ZIKV infection (<7 wks) of pregnant rhesus macaques initiates infection of the placenta and causes widespread neuropathology in infected fetuses (Martinot et al., 2018). In contrast, macaques infected later in pregnancy (>12 weeks) showed minimal placental

ZIKV infection despite detectable ZIKV RNA within the fetal meninges. Concurrent findings also showed that ZIKV infection in pregnant macaques altered the hemodynamics of maternofetal blood flow downstream of decidual spiral artery fibrin deposition as well as villous damage, including numerous infarctions and calcifications (Hirsch et al., 2018). Rhesus macaques previously exposed to DENV-1 or DENV-2 over 2.8 years ago, despite causing serologic enhancement of ZIKV infection *in vitro*, also did not show enhanced viremia nor clinical severity upon challenge with ZIKV (Pantoja et al., 2017). Previous DENV infection also did not contribute to increased ZIKV viremia or disease severity regardless of DENV serotype (Breitbach et al., 2019). In contrast to *ex vivo* human and *in vivo* mouse model systems, this robust body of work would suggest that previous DENV immunity has very little effect on ZIKV clinical severity in the original host. However, these NHP studies still do not assess the impact of previous flavivirus immunity on ZIKV infection in pregnant animals. Thus, it remains unclear whether previous dengue humoral immunity can enhance *in vivo* viral seeding of the fetal compartment during subsequent ZIKV infection in NHPs. Given the growing literature suggesting that cross-reactive DENV mAbs as well as type-specific ZIKV antibodies may augment ZIKV transcytosis and infection in both *in vivo* mouse and human explant model systems (Bardina et al., 2017; Brown et al., 2019; Castanha et al., 2020; Hermanns et al., 2018; Rathore et al., 2019; Shim et al., 2019; Zimmerman et al., 2018), the effects of previous dengue immunity on ZIKV infection in pregnant rhesus macaques warrants further investigation.

The Reciprocity of Immune Enhancement between ZIKV and DENV

Given the high seroprevalence of DENV1-4 when ZIKV was introduced to the Americas in 2015, major efforts have been undertaken to understand the impact of cross-reactive DENV antibodies on ZIKV pathogenesis. Seroprevalence surveys in Fiji and

French Polynesia have demonstrated that seroprevalence and neutralizing antibody titers to ZIKV wane at a higher rate than DENV titers (Henderson et al., 2020). Given that ZIKV antibodies can cross react with DENV (Fowler et al., 2018; Stettler et al., 2016), sub-neutralizing levels of cross-reactive ZIKV antibodies may result in reciprocal enhancement of DENV infection. In a human skin model of flavivirus infection, Langerhans cells and dermal DCs exhibited increased ZIKV and DENV3 infectivity when co-inoculated with DENV3 and ZIKV sera, respectively (Castanha et al., 2020). Pre-administration of cross-reactive ZIKV mAbs to DENV-2 infected immunodeficient AG129 mice, a ZIKV permissive mouse model lacking alpha/beta IFN and gamma IFN receptors, also led to severe symptoms and increased lethality by day 5 compared to non-antibody treated controls (Stettler et al., 2016). Using mice with type I IFN signaling specifically ablated in macrophages, ZIKV-experienced dams displayed increased viral burden and higher mortality attributed to increased production of the proinflammatory cytokine TNF- α when challenged with DENV (Fowler et al., 2018). In another study, rhesus macaques were infected with ZIKV subcutaneously and subsequently infected with DENV-2 and monitored for an enhanced infection phenotype. The ZIKV-immune macaques showed higher levels of DENV-2 viremia, larger pro-inflammatory cytokine responses, and notably, a strong anamnestic cross-reactive B cell response (George et al., 2017). This finding was corroborated by Breitbach and colleagues who also observed increased DENV2 viremia in macaques pre-inoculated with ZIKV immune sera (Breitbach et al., 2019). However, prior ZIKV immunity, particularly during late convalescence, displayed increased cross-reactive antibody and T cell responses with no observable effect on DENV viremia (Perez-Guzman et al., 2019). The antibody response to DENV infection secondary to ZIKV infection is not well characterized due to the already high seroprevalence of DENV during the 2015 ZIKV outbreak. The durability of DENV cross-reactive neutralizing antibodies to ZIKV are maintained for approximately 6 months post-infection (Collins et al., 2017). Thus,

it is plausible that the ZIKV cross-reactive immune responses to secondary DENV infections equally temporary. Longitudinal surveillance of patients with primary ZIKV infection are needed to fully understand the effects of ZIKV infection on DENV pathogenesis.

Vertical Transmission of other Flaviviruses

ZIKV is the first flavivirus classified as a TORCH pathogen alongside other pathogenic viruses, including enteroviruses, parvoviruses, HIV, VZV, rubella virus, CMV, and HSV-1/2 (Coyne and Lazear, 2016). The overt neurologic malformations, like microcephaly, brain calcifications, and developmental disorders, that characterize CZS have not been as widely observed in pregnant women infected with related flaviviruses. Thus, it has been generally accepted that ZIKV is the first teratogenic flavivirus; however, due to the rare occurrence of fetal malformation and high number of asymptomatic cases, the congenital effects caused by other flaviviruses may be underreported (Charlier et al., 2017).

At the height of WNV infection in New York City in 2002, the CDC confirmed the first case of intrauterine WNV infection from a woman presenting with flu-like symptoms at 27 weeks of pregnancy. The child was born at 38 weeks and had tested positive for anti-WNV IgM within the serum and CSF. Ophthalmologic and neurologic testing showed bilateral chorioretinitis and white matter loss in the temporal and occipital lobes, suggesting transplacental WNV infection and productive infection in the developing fetus (Centers for Disease and Prevention, 2002). Since this initial observation, several clinical studies have assessed whether WNV breach the placental barrier and establish infection in the fetal compartment (O'Leary et al., 2006; Pridjian et al., 2016; Sirois et al., 2014). Between 2003-2004, O'Leary et al. clinically also followed 77 women who were reported

to have PCR-verified WNV infection during pregnancy. 6 of the 72 live infants developed severe abnormalities of which two presented with microcephaly and one with lissencephaly correlating with maternal WNV infection (O'Leary et al., 2006). Only 1/50 placenta tested were positive for WNV RNA with no detection in the maternal decidual tissue. In addition, anti-WNV IgM and WNV RNA were not detected systemically nor within the CNS of these children. Two more recent studies found no abnormal birth outcomes nor postpartum developmental delays in children up to three years of age in their prospective cohort of 36 WNV-infected pregnant women (Pridjian et al., 2016; Sirois et al., 2014). The rarity of vertical transmission of WNV compared to ZIKV might suggest that the innate immune defenses of the placenta are capable of restricting WNV seeding of the placenta. Type III IFN, which is produced constitutively by the human STB layer (Bayer et al., 2016; Corry et al., 2017) has been shown to have a moderate effect on WNV infection in cell lines (Ma et al., 2009) as well as restricting access to CNS through tightening of the blood-brain barrier (Lazear et al., 2015a). This may imply that the STB layer provides ample protection against WNV infection. The inability of WNV to infect the decidua may indicate that, unlike ZIKV (Tabata et al., 2018; Tabata et al., 2016), WNV may not enter the placenta through anchoring villi EVT's or the chorioamnion. More recently, Platt et al. determined that pregnant mice inoculated with WNV and Powassan virus (POWV), another related neurotropic flavivirus, showed establishment of infection in the placenta and fetal demise. They also observed productive infection in human second-trimester chorionic villous explants (Platt et al., 2018). Although the human clinical cohorts and animal studies provide contrasting results, once past the placental barrier, WNV enter the evolutionarily immune-suppressed placental core and infect highly susceptible HCs, establishing productive infection in the placenta.

Although DENV is not considered a teratogenic virus, several clinical studies have documented prenatal transmission of DENV from pregnant mothers to their children. In one study, placenta and ovular remnants were isolated from 28 women with confirmed dengue fever or dengue hemorrhagic fever/shock syndrome (DHF/DSS) in Rio de Janeiro, Brazil. Presence of anti-DENV IgM was found in 7 cases and 5 cases had observable DENV viral proteins in the decidua and chorionic villi by immunohistochemistry, suggesting perinatal transmission of DENV during the third trimester (Ribeiro et al., 2013). The median time to infection was 3 days, and 6 of the 7 children presented with thrombocytopenia, lymphocytosis, and leukocytosis indicative of DHF/DSS, suggesting swift establishment of infection within the fetus following maternal infection. Ribeiro et al. also observed positive immunostaining in 92% (22 of 24) for DENV in the placenta of infected pregnant mothers, resulting in miscarriages (5 of 24), fetal death (2 of 24), and prematurity (3 of 24) (Ribeiro et al., 2017). Abnormal birth outcomes were associated with DENV infection of the fetus during the first and second trimester; however, a majority of fetal DENV infections occurred during the third trimester. Postmortem histological analysis of a 27-week-old fetus from a pregnant woman with severe DENV4 disease also showed productive infection with the brain, liver, lung and placenta, particularly in HCs and CTBs (Nunes et al., 2019).

The prevalence of vertical transmission of DENV during the third trimester indicates that DENV takes advantage of this stage of pregnancy to enter the fetal compartment. As the surface area of the STB layer becomes larger with increasing gestational age, the abundance of progenitor cytotrophoblasts decreases (Coyne and Lazear, 2016), thinning the barrier between the maternal blood and the villous stroma. In addition, severe DENV infection has been associated with inflammatory cytokine storms characterized by high levels of IL-1 β , IL-2, IL-6, IL-8, IL-18, IFN γ , and TNF α (Martina et

al., 2009). Administration of IL-1 β and TNF α to pregnant rats results in trophoblastic necrosis, hemochorial breakdown, and destruction of fetal tissue (Silen et al., 1989). Treatment of pregnant mice with IL-1R antagonist also limits LPS-induced placental and neurodevelopmental defects (Girard et al., 2010). Indeed, histopathologic findings during DENV infection of pregnant women include placental hemorrhage, stromal edema, syncytial knots, and villitis (Nunes et al., 2019; Nunes et al., 2016; Ribeiro et al., 2013; Ribeiro et al., 2017). Thus, DENV may take advantage of placental trophoblastic breakdown as a result of inflammatory cytokine production in the maternal bloodstream to enter the placenta. ZIKV can hijack the FcRn-mediated IgG transfer mechanism to cross the placenta without causing a widespread placental inflammatory response (Rosenberg et al., 2017; Zimmerman et al., 2018). The presence of cross-reactive DENV antibodies during secondary infection with a heterotypic serotype of DENV may also cause antibody-dependent transcytosis of DENV into the villous stroma. However, this is less likely given the lack of abnormal pregnancy outcomes and fetal DENV infection without the presence of DHF/DSS and inflammatory cytokine production.

The Many Flavors of ZIKV Vaccines

Due to a lack of approved flavivirus-specific antiviral therapeutics, numerous groups have studied various ZIKV vaccine platforms to confer immunologic protection in both mice and NHPs. Lipid nanoparticle (LNP) mRNA vaccines have been widely tested during the ZIKV epidemic due to its non-infectivity and capacity to express high levels of viral protein. ZIKV prM-E mRNA LNP vaccines have been shown induce high levels of neutralizing ZIKV-specific IgG production as well as antiviral CD4⁺ T cell responses in both immunocompetent and immunocompromised mice. Mutation in the fusion loop epitope in the ZIKV mRNA LNP vaccine alleviated potential DENV enhancement effects

without compromising protection from ZIKV challenge (Richner et al., 2017). Low dose administration of ZIKV prM-E mRNA LNP vaccine to rhesus macaques also exhibited sterilizing immunity and complete protection from subcutaneous challenge with ZIKV (Pardi et al., 2017). Recent work has also shown that vaccines with ZIKV prM/M-E engineered into low-circulation AdC7 and RhAd52 adenovirus constructs can provide single-dose protection in *IFNAR*^{-/-} mice lacking the type I IFN receptor and rhesus macaques, respectively (Abbink et al., 2017; Xu et al., 2018). High levels of humoral protection against ZIKV infection were also observed in both pregnant *Ifnar*^{-/-} mice and their pups after inoculation of dams with the adenovirus-based ZIKV vaccines, RhAd52.M-Env and Ad26.M-Env (Larocca et al., 2019). Live attenuated vaccines (LAVs) induce robust and durable adaptive immune responses but carry risk of viral reversion and pathogenesis, especially in immunocompromised and pregnant patients. To ameliorate this concern, one group developed a live-attenuated ZIKV vaccine with trans-complemented wild-type capsid protein while encoding a mutant capsid protein, allowing for only one round of replication (Xie et al., 2018). Upon ZIKV challenge 28 days post-immunization, viremia was not detectable in either the mother or fetus in pregnant A129 mice. Because of the presence of ZIKV non-structural proteins within the LAV construct, the viral protection in these pregnant mice were attributed to the high neutralizing antibody titers and robust CD4⁺ and CD8⁺ T cell responses.

Dussupt et al. recently demonstrated that vaccination of flavivirus-experienced individuals with an inactivated purified ZIKV exhibited substantial neutralization activity to both ZIKV and DENV (Dussupt et al., 2020). These results are promising given the high prevalence of DENV-experienced individuals in ZIKV-endemic countries. However, the latest timepoint for cross-protective neutralization activity was measured at 8 weeks. The durability of cross-reactive DENV antibody responses to ZIKV has been shown to only last

approximately 6 months post infection (Collins et al., 2017). Andrade and colleagues have also determined that previous DENV infection, regardless of the number of previous infections, only modestly affects the ZIKV type-specific and cross-reactive responses. Notably, the cross-reactive DENV MBCs stimulated by ZIKV infection only expanded and produced cross-reactive antibodies until late convalescence (~ 6 months) (Andrade et al., 2019). Thus, the strong DENV neutralizing activity observed by Dussupt et al. may wane to sub-neutralizing levels within 6 months post-vaccination. More longitudinal data is needed to assess the robustness of the cross-reactive ZIKV responses to DENV in vaccine recipients.

In the wake of the Dengvaxia, a looming concern remains: Could a ZIKV vaccine cause antibody-mediated enhancement of DENV in flavivirus-naïve individuals? *In vivo* animal models and *ex vivo* human explants models have observed DENV ADE when virus was coincubated with ZIKV serum (Castanha et al., 2020; Fowler et al., 2018; Stettler et al., 2016). We and others have also observed ZIKV enhancement with increasing dilution of primary human ZIKV immune sera in placental model systems (Shim et al., 2019) (**Chapter 3, Figures 1 and 2**). The possibility of sub-neutralizing antibodies, whether type-specific or cross-reactive, causing systemic enhancement in the host or facilitating enhanced placental infection warrants the creation of a DENV/ZIKV co-vaccination and booster platform to elicit strong type-specific responses to both DENV and ZIKV.

Monoclonal Antibodies as Therapeutics and Vaccine Adjuvants

With the concern of potential ADE effects caused by vaccine-elicited antibody responses, passive administration of monoclonal Abs (mAbs) has been studied as a potential prophylactic measure against ZIKV infection. Infusion of rhesus macaques with a cocktail of three engineered ZIKV neutralizing mAbs with LALA mutations, all of which

target domains II and III of the E protein (EDII and EDIII) but cannot bind to FcγRs, conferred sterilizing immunity upon ZIKV challenge. Moreover, these ZIKV mAbs maintained high neutralizing concentrations up to 42 days post-infusion (Magnani et al., 2017). Keeffe and colleagues also showed that administration of two potently neutralizing DENV cross-reactive ZIKV mAbs, including their non-FcγR binding variants, bind the lateral ridge of EDIII and provide moderate protection while eliminating escape mutant variants in NHPs (Keeffe et al., 2018). Despite providing immunity in non-pregnant NHPs, administration of Fc-engineered anti-EDIII antibody cocktails to pregnant rhesus macaques previous to ZIKV challenge lowered maternal viral loads and alleviated ZIKV-mediated damage to the fetus, but did not prevent vertical transmission (Magnani et al., 2018; Van Rompay et al., 2020). Despite the lack of FcγR binding with monoclonal antibodies generated by Magnani et al. and Van Rompay et al., immune complexes generated in the maternal serum could still cross the placental barrier via FcRn. We found that blockade of FcRn using Protein A significantly reduced the ZIKV enhancement seen in the presence of cross reactive DENV-antibodies (**Chapter 2, Figure 7A**). The FcRn and FcγR binding regions are distinct and do not interact with each other (Martin et al., 2001); thus, alanine substitutions at His310 and His435. Future *in vivo* therapeutic monoclonal antibody studies should test the efficacy of dual-engineered type-specific antibodies to eliminate the effects of ADE as well as transplacental transcytosis of viral immune complexes.

Several groups have focused on the role of engineered anti-ZIKV IgG antibodies to prevent fetal complications from ZIKV infection; however, comparatively few studies have focused on the use of IgM as a therapeutic during flavivirus infection. Recent work from Malafa et al. identified that ZIKV-specific IgM accounts for approximately 44-51% of neutralizing activity in primary and secondary ZIKV sera (Malafa et al., 2020). Shim et al.

also determined that early convalescent ZIKV serum containing high levels of IgM were incapable of causing ZIKV ADE in an *Ifnar*^{-/-} mouse model system (Shim et al., 2019). These results corroborate with our findings that type-specific IgM in early convalescent ZIKV immune sera, but not cross-reactive IgM in primary DENV immune sera, is capable of restricting IgG-mediated ZIKV enhancement in human second-trimester chorionic villous explants (**Chapter 3, Figure 3**). Unlike IgG, IgM is pentavalent, with five times as many binding sites, and its unique Fc-region cannot bind FcRn, which inhibits their ability to cross the placental barrier. In addition, robust IgM responses are necessary for effective IgG generation within the germinal center against viral infections (Boes et al., 1998; Diamond et al., 2003b; Harte et al., 1983). Pathogen-specific IgM has also been used as a vaccine adjuvant due to its ability to enhance IgG responses to the invading pathogen (Harte et al., 1983; Ilag, 2011). IgM-generated immune complexes have been reported to enhance WNV and Ebola virus *in vitro* through interaction with complement factors C3 and C1q, respectively (Cardosa et al., 1986; Cardosa et al., 1983; Takada et al., 2003); however, the reports on IgM-mediated ADE are quite limited and require further investigation. Vaccination of high-risk patients with a ZIKV vaccine in combination with ZIKV-specific IgM would potentially provide not only immediate IgM-mediated early fetal protection but also boosted long-term memory against ZIKV infection.

The Spread of ZIKV and Potential for Reemergence

As of 2019, autochthonous ZIKV infection has been established in 87 countries, including all of the Americas except Canada, Chile, and Uruguay (World Health Organization, 2019). In October 2019, the first three cases of *Aedes albopictus*-acquired, locally transmitted ZIKV infection were reported in southern France (Brady and Hay, 2019). The first documented emergence of CZS with microcephaly from acquired Asian

lineage strain of ZIKV has also recently arisen in Angola (Hill et al., 2019; Sasseti et al., 2018). Since then, 16 cases of CZS with microcephaly cases have also been observed in Guinea-Bissau and seven confirmed cases of ZIKV infection in Ethiopia (World Health Organization, 2019). The spread of Asian lineage ZIKV throughout southern Europe and Africa has been attributed to the expanding *Aedes aegypti* and *Aedes albopictus* populations into naïve populations. Human mobility models have estimated that long-distance importation will allow *Aedes aegypti* to enlarge its urban ecological niche throughout tropical Africa and northern regions of the US and China, including Chicago and Shanghai (Kraemer et al., 2019). *Aedes albopictus* populations showed spread through short-distance importation and is expected to expand throughout France, Germany, the northern US, the cooler highlands of South America, and East Africa over the next 30 years. The spatial dispersal models only account for anthropogenic ecological niches and were generated independently of increasing global climate change, suggesting that these niches can enlarge once ecological capacity has been attained for each *Aedes* species (Kraemer et al., 2019). Using these computational models to understand arbovirus spread into flavivirus-naïve regions in conjunction with extensive serologic testing will also illuminate the potential roles of previous flavivirus immunity on flavivirus pathogenesis in pregnant and non-pregnant individuals.

The increasing spread of arboviral vectors into naïve urban populations heralds new pockets of ZIKV infection; however, a lingering question remains: Will ZIKV re-emerge in endemic regions? DENV undergoes cyclical epidemics where, after infection with the prevalent serotype, herd immunity against homotypic serotypes is lifelong and heterotypic serotypes lasts 3-5 years. Serologic surveillance in Brazil and the Americas from 1980 to 2019 have demonstrated that introduction of a new DENV serotype is accompanied by an initial rise in new infections followed by a subsequent decline in cases

due to strong homotypic and temporary heterotypic humoral immunity. As heterotypic immunity decreases, a new serotype emerges and spreads throughout the population, potentiating the DENV serotype cycle (Ribeiro et al., 2020). The cycling levels of DENV antibody response may provide transient, cross-reactive protection against ZIKV. Indeed, human epidemiologic studies that found that multiple DENV infections protect against symptomatic ZIKV, but not susceptibility to ZIKV infection (Gordon et al., 2019). Other work has claimed that prior DENV immunity also protects against CZS (Halai et al., 2017b); however, DENV-experienced pregnant mothers were not stratified based on DENV cross-reactive antibody titers nor time since previous DENV infection. In contrast, the durability of DENV cross-reactive antibodies capable of neutralizing ZIKV are quite low, lasting approximately 6 months after the most recent DENV infection (Collins et al., 2017). These results agreed with Brazilian epidemiologic studies that found the highest levels of ZIKV infection less than two years after circulation of DENV4. This population had also experienced DENV1, DENV2, and DENV3 infections, indicating that secondary and tertiary responses to DENV do not ultimately provide long-lasting cross-reactive protection to ZIKV (Ribeiro et al., 2020). Thus, the extent that DENV cross-reactive antibodies truly protect against ZIKV infection, seeding of the fetal compartment, and potential CZS is still uncertain.

Unlike DENV1-4, ZIKV, despite the existence of different African and Asian lineage strains, exists as a single serotype (Dowd et al., 2016). Thus, the homotypic antibody response may be enough to inhibit further infection with ZIKV, but the duration of neutralizing levels of ZIKV antibodies after homotypic infection is currently unknown. The current dogma states that type-specific flavivirus antibodies provide lifelong immunity to homotypic flaviviruses or serotypes. However, we observed enhancement of ZIKV infection in human chorionic villous explants in the presence of diluted IgM-depleted early

convalescent and late convalescent ZIKV immune sera (**Chapter 3, Figures 2 and 3**). Subneutralizing levels of homotypic ZIKV antibodies are also capable of mediating ZIKV ADE *in vivo*, placental damage, and fetal resorption in ZIKV-infected pregnant mice (Shim et al., 2019). Population turnover and introduction of naïve individuals into ZIKV-endemic areas may cause pockets of ZIKV outbreaks due to waning herd immunity. If ZIKV can truly re-establish infection in ZIKV-experienced patients, individuals with sub-neutralizing antibody responses, especially pregnant women, may be at risk for ZIKV ADE, enhanced seeding of the placenta, or CZS. Careful monitoring of ZIKV-specific antibody responses in convalescent ZIKV patients should be established to affirm whether lifelong humoral immunity to ZIKV endures.

Concluding Thoughts and Questions

Considering the co-circulation of both DENV and ZIKV within endemic regions, identifying innate immune targets of viral antagonism in cocirculating viruses will help us predict how re-emerging and newly emerging flaviviruses evade the immune system and establish productive infection. The increasing co-endemicity and shared vectors utilized by flaviviruses also underpins the importance of elucidating how pre-existing flavivirus immunity affects the pathogenesis of secondary flavivirus infection. While serious complications from primary DENV infections can occur, increasing epidemiologic and experimental evidence continues to solidify the role of pre-existing DENV antibodies in mediating severe dengue disease. Due to the recent emergence of ZIKV in 2015 and limited epidemiologic studies, whether cross-reactive antibodies elicited from a primary DENV or ZIKV infection ameliorate or exacerbate subsequent flavivirus infection is a multifactorial issue that remains unresolved. While the epidemiological evidence does not yet support the concept that pre-existing dengue immunity worsens the clinical severity of

ZIKV infection in the mother or fetus, our group and others have evaluated the ability of ZIKV to utilize the FcRn-mediated transcytosis pathway to gain access and seed the placenta (Brown et al., 2019; Hermanns et al., 2018; Rathore et al., 2019; Shim et al., 2019; Zimmerman et al., 2018). We have also validated the importance of ZIKV-specific IgM in inhibition of IgG-mediated placental transcytosis and ZIKV ADE, a finding substantiated by other recent studies (Malafa et al., 2020; Shim et al., 2019). While the *ex vivo* and *in vivo* model systems used in these studies have their respective limitations, the information gleaned from these works has furthered our insight and sparked many questions regarding the impact of cross-reactive and type-specific flavivirus antibodies on ZIKV pathogenesis in the placenta. How does ZIKV survive the low pH environment during transcytosis? Do cross-reactive antibodies bind to specific ZIKV epitopes, stabilizing ZIKV as it crosses the STB layer? What are innate immune targets of viral antagonism within placental cells? What impact will the widespread use of multivalent DENV and ZIKV vaccines have on the cross-reactive antibody repertoire and potential transcytosis across the placenta in pregnant women? Can flavivirus-specific IgM be used prophylactically in at-risk populations? Hopefully, the growing interest in antibody-mediated vertical transmission of ZIKV will stimulate further *in vivo* studies in pregnant NHPs or women to dissect the immunological and molecular mechanisms of ZIKV transcytosis across the placenta.

Works Cited

- A, A.N., Panthuyosri, N., Anantapreecha, S., Chanama, S., Sa-Ngasang, A., Sawanpanyalert, P., and Kurane, I. (2008). Cross-reactive IgM responses in patients with dengue or Japanese encephalitis. *J Clin Virol* 42, 75-77.
- Abbink, P., Larocca, R.A., Visitsunthorn, K., Boyd, M., De La Barrera, R.A., Gromowski, G.D., Kirilova, M., Peterson, R., Li, Z., Nanayakkara, O., *et al.* (2017). Durability and correlates of vaccine protection against Zika virus in rhesus monkeys. *Sci Transl Med* 9.
- Abdiche, Y.N., Yeung, Y.A., Chaparro-Riggers, J., Barman, I., Strop, P., Chin, S.M., Pham, A., Bolton, G., McDonough, D., Lindquist, K., *et al.* (2015). The neonatal Fc receptor (FcRn) binds independently to both sites of the IgG homodimer with identical affinity. *MAbs* 7, 331-343.
- Able, A.A., Burrell, J.A., and Stephens, J.M. (2017). STAT5-Interacting Proteins: A Synopsis of Proteins that Regulate STAT5 Activity. *Biology (Basel)* 6.
- Al-Shami, A., Mahanna, W., and Naccache, P.H. (1998). Granulocyte-macrophage colony-stimulating factor-activated signaling pathways in human neutrophils. Selective activation of Jak2, Stat3, and Stat5b. *J Biol Chem* 273, 1058-1063.
- Ander, S.E., Diamond, M.S., and Coyne, C.B. (2019). Immune responses at the maternal-fetal interface. *Sci Immunol* 4.
- Ander, S.E., Rudzki, E.N., Arora, N., Sadovsky, Y., Coyne, C.B., and Boyle, J.P. (2018). Human Placental Syncytiotrophoblasts Restrict *Toxoplasma gondii* Attachment and Replication and Respond to Infection by Producing Immunomodulatory Chemokines. *mBio* 9.
- Andrade, P., Gimblet-Ochieng, C., Modirian, F., Collins, M., Cardenas, M., Katzelnick, L.C., Montoya, M., Michlmayr, D., Kuan, G., Balmaseda, A., *et al.* (2019). Impact of pre-existing dengue immunity on human antibody and memory B cell responses to Zika. *Nat Commun* 10, 938.
- Anteby, E.Y., Natanson-Yaron, S., Greenfield, C., Goldman-Wohl, D., Haimov-Kochman, R., Holzer, H., and Yagel, S. (2005). Human placental Hofbauer cells express sprouty proteins: a possible modulating mechanism of villous branching. *Placenta* 26, 476-483.
- Arora, N., Sadovsky, Y., Dermody, T.S., and Coyne, C.B. (2017). Microbial Vertical Transmission during Human Pregnancy. *Cell Host Microbe* 21, 561-567.
- Bardina, S.V., Bunduc, P., Tripathi, S., Duehr, J., Frere, J.J., Brown, J.A., Nachbagauer, R., Foster, G.A., Krysztof, D., Tortorella, D., *et al.* (2017). Enhancement of Zika virus pathogenesis by preexisting antinflavivirus immunity. *Science* 356, 175-180.
- Baumgarth, N., Herman, O.C., Jager, G.C., Brown, L., Herzenberg, L.A., and Herzenberg, L.A. (1999). Innate and acquired humoral immunities to influenza virus are mediated by distinct arms of the immune system. *Proc Natl Acad Sci U S A* 96, 2250-2255.
- Baumgarth, N., Herman, O.C., Jager, G.C., Brown, L.E., Herzenberg, L.A., and Chen, J. (2000). B-1 and B-2 cell-derived immunoglobulin M antibodies are nonredundant components of the protective response to influenza virus infection. *J Exp Med* 192, 271-280.
- Bayer, A., Delorme-Axford, E., Sleighter, C., Frey, T.K., Trobaugh, D.W., Klimstra, W.B., Emert-Sedlak, L.A., Smithgall, T.E., Kinchington, P.R., Vadia, S., *et al.* (2015). Human trophoblasts confer resistance to viruses implicated in perinatal infection. *Am J Obstet Gynecol* 212, 71 e71-71 e78.
- Bayer, A., Lennemann, N.J., Ouyang, Y., Bramley, J.C., Morosky, S., Marques, E.T., Jr., Cherry, S., Sadovsky, Y., and Coyne, C.B. (2016). Type III Interferons Produced by Human Placental Trophoblasts Confer Protection against Zika Virus Infection. *Cell Host Microbe* 19, 705-712.
- Beatty, P.R., Puerta-Guardo, H., Killingbeck, S.S., Glasner, D.R., Hopkins, K., and Harris, E. (2015). Dengue virus NS1 triggers endothelial permeability and vascular leak that is prevented by NS1 vaccination. *Sci Transl Med* 7, 304ra141.

- Bell, B.D., Kitajima, M., Larson, R.P., Stoklasek, T.A., Dang, K., Sakamoto, K., Wagner, K.U., Kaplan, D.H., Reizis, B., Hennighausen, L., *et al.* (2013). The transcription factor STAT5 is critical in dendritic cells for the development of TH2 but not TH1 responses. *Nat Immunol* 14, 364-371.
- Beltramello, M., Williams, K.L., Simmons, C.P., Macagno, A., Simonelli, L., Quyen, N.T., Sukupolvi-Petty, S., Navarro-Sanchez, E., Young, P.R., de Silva, A.M., *et al.* (2010). The human immune response to Dengue virus is dominated by highly cross-reactive antibodies endowed with neutralizing and enhancing activity. *Cell Host Microbe* 8, 271-283.
- Best, S.M., Morris, K.L., Shannon, J.G., Robertson, S.J., Mitzel, D.N., Park, G.S., Boer, E., Wolfenbarger, J.B., and Bloom, M.E. (2005). Inhibition of interferon-stimulated JAK-STAT signaling by a tick-borne flavivirus and identification of NS5 as an interferon antagonist. *J Virol* 79, 12828-12839.
- Bhatnagar, J., Rabeneck, D.B., Martines, R.B., Reagan-Steiner, S., Ermias, Y., Estetter, L.B., Suzuki, T., Ritter, J., Keating, M.K., Hale, G., *et al.* (2017). Zika Virus RNA Replication and Persistence in Brain and Placental Tissue. *Emerg Infect Dis* 23, 405-414.
- Bhatt, S., Gething, P.W., Brady, O.J., Messina, J.P., Farlow, A.W., Moyes, C.L., Drake, J.M., Brownstein, J.S., Hoen, A.G., Sankoh, O., *et al.* (2013). The global distribution and burden of dengue. *Nature* 496, 504-507.
- Bhattacharyya, S., Zagorska, A., Lew, E.D., Shrestha, B., Rothlin, C.V., Naughton, J., Diamond, M.S., Lemke, G., and Young, J.A. (2013). Enveloped viruses disable innate immune responses in dendritic cells by direct activation of TAM receptors. *Cell Host Microbe* 14, 136-147.
- Bingham, A.M., Cone, M., Mock, V., Heberlein-Larson, L., Stanek, D., Blackmore, C., and Likos, A. (2016). Comparison of Test Results for Zika Virus RNA in Urine, Serum, and Saliva Specimens from Persons with Travel-Associated Zika Virus Disease - Florida, 2016. *MMWR Morb Mortal Wkly Rep* 65, 475-478.
- Blakely, P.K., Kleinschmidt-DeMasters, B.K., Tyler, K.L., and Irani, D.N. (2009). Disrupted glutamate transporter expression in the spinal cord with acute flaccid paralysis caused by West Nile virus infection. *J Neuropathol Exp Neurol* 68, 1061-1072.
- Blandino, R., and Baumgarth, N. (2019). Secreted IgM: New tricks for an old molecule. *J Leukoc Biol* 106, 1021-1034.
- Boes, M. (2000). Role of natural and immune IgM antibodies in immune responses. *Mol Immunol* 37, 1141-1149.
- Boes, M., Esau, C., Fischer, M.B., Schmidt, T., Carroll, M., and Chen, J. (1998). Enhanced B-1 cell development, but impaired IgG antibody responses in mice deficient in secreted IgM. *J Immunol* 160, 4776-4787.
- Bohannon, C., Powers, R., Satyabhama, L., Cui, A., Tipton, C., Michaeli, M., Skountzou, I., Mittler, R.S., Kleinstein, S.H., Mehr, R., *et al.* (2016). Long-lived antigen-induced IgM plasma cells demonstrate somatic mutations and contribute to long-term protection. *Nat Commun* 7, 11826.
- Bokun, V., Moore, J.J., Moore, R., Smallcombe, C.C., Harford, T.J., Rezaee, F., Esper, F., and Piedimonte, G. (2019). Respiratory syncytial virus exhibits differential tropism for distinct human placental cell types with Hofbauer cells acting as a permissive reservoir for infection. *PLoS One* 14, e0225767.
- Boonnak, K., Slike, B.M., Donofrio, G.C., and Marovich, M.A. (2013). Human FcγRIII cytoplasmic domains differentially influence antibody-mediated dengue virus infection. *J Immunol* 190, 5659-5665.
- Bowen, J.R., Quicke, K.M., Maddur, M.S., O'Neal, J.T., McDonald, C.E., Fedorova, N.B., Puri, V., Shabman, R.S., Pulendran, B., and Suthar, M.S. (2017a). Zika Virus Antagonizes Type I

- Interferon Responses during Infection of Human Dendritic Cells. *PLoS Pathog* 13, e1006164.
- Bowen, J.R., Quicke, K.M., Maddur, M.S., O'Neal, J.T., McDonald, C.E., Fedorova, N.B., Puri, V., Shabman, R.S., Pulendran, B., and Suthar, M.S. (2017b). Zika Virus Antagonizes Type I Interferon Responses during Infection of Human Dendritic Cells. *PLOS Pathogens* 13, e1006164.
- Brady, O.J., and Hay, S.I. (2019). The first local cases of Zika virus in Europe. *Lancet* 394, 1991-1992.
- Brasil, P., Pereira, J.P., Jr., Moreira, M.E., Ribeiro Nogueira, R.M., Damasceno, L., Wakimoto, M., Rabello, R.S., Valderramos, S.G., Halai, U.A., Salles, T.S., *et al.* (2016a). Zika Virus Infection in Pregnant Women in Rio de Janeiro. *N Engl J Med* 375, 2321-2334.
- Brasil, P., Pereira, J.P., Moreira, E.M., Nogueira, R.M., Damasceno, L., Wakimoto, M., Rabello, R.S., Valderramos, S.G., Halai, U.-A., Salles, T.S., *et al.* (2016b). Zika Virus Infection in Pregnant Women in Rio de Janeiro. *The New England Journal of Medicine* 375, 2321-2334.
- Breitbach, M.E., Newman, C.M., Dudley, D.M., Stewart, L.M., Aliota, M.T., Koenig, M.R., Shepherd, P.M., Yamamoto, K., Crooks, C.M., Young, G., *et al.* (2019). Primary infection with dengue or Zika virus does not affect the severity of heterologous secondary infection in macaques. *PLoS Pathog* 15, e1007766.
- Brown, J.A., Singh, G., Acklin, J.A., Lee, S., Duehr, J.E., Chokola, A.N., Frere, J.J., Hoffman, K.W., Foster, G.A., Kryzstof, D., *et al.* (2019). Dengue Virus Immunity Increases Zika Virus-Induced Damage during Pregnancy. *Immunity* 50, 751-762 e755.
- Bruhns, P. (2012). Properties of mouse and human IgG receptors and their contribution to disease models. *Blood* 119, 5640-5649.
- Bruns, A.M., Leser, G.P., Lamb, R.A., and Horvath, C.M. (2014). The innate immune sensor LGP2 activates antiviral signaling by regulating MDA5-RNA interaction and filament assembly. *Mol Cell* 55, 771-781.
- Burakoff, A., Lehman, J., Fischer, M., Staples, J.E., and Lindsey, N.P. (2018). West Nile Virus and Other Nationally Notifiable Arboviral Diseases - United States, 2016. *MMWR Morb Mortal Wkly Rep* 67, 13-17.
- Burke, D.S., Nisalak, A., Johnson, D.E., and Scott, R.M. (1988). A prospective study of dengue infections in Bangkok. *Am J Trop Med Hyg* 38, 172-180.
- Busch, M.P., Kleinman, S.H., Tobler, L.H., Kamel, H.T., Norris, P.J., Walsh, I., Matud, J.L., Prince, H.E., Lanciotti, R.S., Wright, D.J., *et al.* (2008). Virus and antibody dynamics in acute west nile virus infection. *J Infect Dis* 198, 984-993.
- Byts, N., Samoylenko, A., Fasshauer, T., Ivanisevic, M., Hennighausen, L., Ehrenreich, H., and Siren, A.L. (2008). Essential role for Stat5 in the neurotrophic but not in the neuroprotective effect of erythropoietin. *Cell Death Differ* 15, 783-792.
- Cardosa, M.J., Gordon, S., Hirsch, S., Springer, T.A., and Porterfield, J.S. (1986). Interaction of West Nile virus with primary murine macrophages: role of cell activation and receptors for antibody and complement. *J Virol* 57, 952-959.
- Cardosa, M.J., Porterfield, J.S., and Gordon, S. (1983). Complement receptor mediates enhanced flavivirus replication in macrophages. *J Exp Med* 158, 258-263.
- Cardoso, T.F., Jr., Santos, R.S.D., Correa, R.M., Campos, J.V., Silva, R.B., Tobias, C.C., Prata-Barbosa, A., Cunha, A., and Ferreira, H.C. (2019). Congenital Zika infection: neurology can occur without microcephaly. *Arch Dis Child* 104, 199-200.
- Carrington, L.B., and Simmons, C.P. (2014). Human to mosquito transmission of dengue viruses. *Front Immunol* 5, 290.
- Carroll, T., Lo, M., Lanteri, M., Dutra, J., Zarbock, K., Silveira, P., Rourke, T., Ma, Z.M., Fritts, L., O'Connor, S., *et al.* (2017). Zika virus preferentially replicates in the female reproductive tract after vaginal inoculation of rhesus macaques. *PLoS Pathog* 13, e1006537.

- Carson, P.J., Konewko, P., Wold, K.S., Mariani, P., Goli, S., Bergloff, P., and Crosby, R.D. (2006). Long-term clinical and neuropsychological outcomes of West Nile virus infection. *Clin Infect Dis* 43, 723-730.
- Castanha, P.M., Braga, C., Cordeiro, M.T., Souza, A.I., Silva, C.D., Jr., Martelli, C.M., van Panhuis, W.G., Nascimento, E.J., and Marques, E.T. (2016). Placental Transfer of Dengue Virus (DENV)-Specific Antibodies and Kinetics of DENV Infection-Enhancing Activity in Brazilian Infants. *J Infect Dis* 214, 265-272.
- Castanha, P.M.S., Erdos, G., Watkins, S.C., Falo, L.D., Jr., Marques, E.T.A., and Barratt-Boyes, S.M. (2020). Reciprocal immune enhancement of dengue and Zika virus infection in human skin. *JCI Insight* 5.
- Centers for Disease, C., and Prevention (2002). Intrauterine West Nile virus infection--New York, 2002. *MMWR Morb Mortal Wkly Rep* 51, 1135-1136.
- Cervar, M., Blaschitz, A., Dohr, G., and Desoye, G. (1999). Paracrine regulation of distinct trophoblast functions in vitro by placental macrophages. *Cell Tissue Res* 295, 297-305.
- Chanama, S., Anantapreecha, S., A, A.n., Sa-gnasang, A., Kurane, I., and Sawanpanyalert, P. (2004). Analysis of specific IgM responses in secondary dengue virus infections: levels and positive rates in comparison with primary infections. *J Clin Virol* 31, 185-189.
- Chancey, C., Grinev, A., Volkova, E., and Rios, M. (2015). The global ecology and epidemiology of West Nile virus. *BioMed research international* 2015, 376230.
- Chareonsirisuthigul, T., Kalayanarooj, S., and Ubol, S. (2007). Dengue virus (DENV) antibody-dependent enhancement of infection upregulates the production of anti-inflammatory cytokines, but suppresses anti-DENV free radical and pro-inflammatory cytokine production, in THP-1 cells. *J Gen Virol* 88, 365-375.
- Charlier, C., Beaudoin, M.C., Couderc, T., Lortholary, O., and Lecuit, M. (2017). Arboviruses and pregnancy: maternal, fetal, and neonatal effects. *Lancet Child Adolesc Health* 1, 134-146.
- Chaturvedi, U.C., Mathur, A., Chandra, A., Das, S.K., Tandon, H.O., and Singh, U.K. (1980). Transplacental infection with Japanese encephalitis virus. *J Infect Dis* 141, 712-715.
- Chen, J., Liang, Y., Yi, P., Xu, L., Hawkins, H.K., Rossi, S.L., Soong, L., Cai, J., Menon, R., and Sun, J. (2017). Outcomes of Congenital Zika Disease Depend on Timing of Infection and Maternal-Fetal Interferon Action. *Cell Rep* 21, 1588-1599.
- Chin, H., Arai, A., Wakao, H., Kamiyama, R., Miyasaka, N., and Miura, O. (1998). Lyn physically associates with the erythropoietin receptor and may play a role in activation of the Stat5 pathway. *Blood* 91, 3734-3745.
- Chow, K.T., Gale, M., Jr., and Loo, Y.M. (2018). RIG-I and Other RNA Sensors in Antiviral Immunity. *Annu Rev Immunol* 36, 667-694.
- Christianson, G.J., Sun, V.Z., Akilesh, S., Pesavento, E., Proetz, G., and Roopenian, D.C. (2012). Monoclonal antibodies directed against human FcRn and their applications. *MABs* 4, 208-216.
- Clapham, H.E., Cummings, D.A.T., and Johansson, M.A. (2017). Immune status alters the probability of apparent illness due to dengue virus infection: Evidence from a pooled analysis across multiple cohort and cluster studies. *PLoS Negl Trop Dis* 11, e0005926.
- Coffey, L.L., Mertens, E., Brehin, A.C., Fernandez-Garcia, M.D., Amara, A., Despres, P., and Sakuntabhai, A. (2009). Human genetic determinants of dengue virus susceptibility. *Microbes Infect* 11, 143-156.
- Collins, M.H., McGowan, E., Jadi, R., Young, E., Lopez, C.A., Baric, R.S., Lazear, H.M., and de Silva, A.M. (2017). Lack of Durable Cross-Neutralizing Antibodies Against Zika Virus from Dengue Virus Infection. *Emerg Infect Dis* 23, 773-781.
- Collins, M.H., Tu, H.A., Gimblet-Ochieng, C., Liou, G.A., Jadi, R.S., Metz, S.W., Thomas, A., McElvany, B.D., Davidson, E., Doranz, B.J., et al. (2019). Human antibody response to Zika targets type-specific quaternary structure epitopes. *JCI Insight* 4.

- Corbett, K.S., Katzelnick, L., Tissera, H., Amerasinghe, A., de Silva, A.D., and de Silva, A.M. (2015). Preexisting neutralizing antibody responses distinguish clinically inapparent and apparent dengue virus infections in a Sri Lankan pediatric cohort. *J Infect Dis* *211*, 590-599.
- Corry, J., Arora, N., Good, C.A., Sadovsky, Y., and Coyne, C.B. (2017). Organotypic models of type III interferon-mediated protection from Zika virus infections at the maternal-fetal interface. *Proc Natl Acad Sci U S A* *114*, 9433-9438.
- Costa, V.V., Ye, W., Chen, Q., Teixeira, M.M., Preiser, P., Ooi, E.E., and Chen, J. (2017). Dengue Virus-Infected Dendritic Cells, but Not Monocytes, Activate Natural Killer Cells through a Contact-Dependent Mechanism Involving Adhesion Molecules. *MBio* *8*.
- Coyne, C.B., and Lazear, H.M. (2016). Zika virus - reigniting the TORCH. *Nat Rev Microbiol* *14*, 707-715.
- Cross, J.C., Werb, Z., and Fisher, S.J. (1994). Implantation and the placenta: key pieces of the development puzzle. *Science* *266*, 1508-1518.
- D'Ortenzio, E., Matheron, S., Yazdanpanah, Y., de Lamballerie, X., Hubert, B., Piorkowski, G., Maquart, M., Descamps, D., Damond, F., and Leparc-Goffart, I. (2016). Evidence of Sexual Transmission of Zika Virus. *N Engl J Med* *374*, 2195-2198.
- Darman, J., Backovic, S., Dike, S., Maragakis, N.J., Krishnan, C., Rothstein, J.D., Irani, D.N., and Kerr, D.A. (2004). Viral-induced spinal motor neuron death is non-cell-autonomous and involves glutamate excitotoxicity. *J Neurosci* *24*, 7566-7575.
- Davis, L.E., DeBiasi, R., Goade, D.E., Haaland, K.Y., Harrington, J.A., Harnar, J.B., Pergam, S.A., King, M.K., DeMasters, B.K., and Tyler, K.L. (2006). West Nile virus neuroinvasive disease. *Ann Neurol* *60*, 286-300.
- de Alwis, R., Beltramello, M., Messer, W.B., Sukupolvi-Petty, S., Wahala, W.M., Kraus, A., Olivarez, N.P., Pham, Q., Brien, J.D., Tsai, W.Y., *et al.* (2011). In-depth analysis of the antibody response of individuals exposed to primary dengue virus infection. *PLoS Negl Trop Dis* *5*, e1188.
- de Alwis, R., Smith, S.A., Olivarez, N.P., Messer, W.B., Huynh, J.P., Wahala, W.M., White, L.J., Diamond, M.S., Baric, R.S., Crowe, J.E., Jr., *et al.* (2012). Identification of human neutralizing antibodies that bind to complex epitopes on dengue virions. *Proc Natl Acad Sci U S A* *109*, 7439-7444.
- de Araujo, T.V.B., Rodrigues, L.C., de Alencar Ximenes, R.A., de Barros Miranda-Filho, D., Montarroyos, U.R., de Melo, A.P.L., Valongueiro, S., de Albuquerque, M., Souza, W.V., Braga, C., *et al.* (2016). Association between Zika virus infection and microcephaly in Brazil, January to May, 2016: preliminary report of a case-control study. *Lancet Infect Dis* *16*, 1356-1363.
- de Araujo, T.V.B., Ximenes, R.A.A., Miranda-Filho, D.B., Souza, W.V., Montarroyos, U.R., de Melo, A.P.L., Valongueiro, S., de Albuquerque, M., Braga, C., Filho, S.P.B., *et al.* (2018). Association between microcephaly, Zika virus infection, and other risk factors in Brazil: final report of a case-control study. *Lancet Infect Dis* *18*, 328-336.
- de Oliveira, W.K., de Franca, G.V.A., Carmo, E.H., Duncan, B.B., de Souza Kuchenbecker, R., and Schmidt, M.I. (2017). Infection-related microcephaly after the 2015 and 2016 Zika virus outbreaks in Brazil: a surveillance-based analysis. *Lancet* *390*, 861-870.
- Deisenhofer, J. (1981). Crystallographic refinement and atomic models of a human Fc fragment and its complex with fragment B of protein A from *Staphylococcus aureus* at 2.9- and 2.8-Å resolution. *Biochemistry* *20*, 2361-2370.
- Dejnirattisai, W., Jumnainsong, A., Onsirakul, N., Fitton, P., Vasanawathana, S., Limpitikul, W., Puttikhunt, C., Edwards, C., Duangchinda, T., Supasa, S., *et al.* (2010). Cross-reacting antibodies enhance dengue virus infection in humans. *Science* *328*, 745-748.
- Dejnirattisai, W., Supasa, P., Wongwiwat, W., Rouvinski, A., Barba-Spaeth, G., Duangchinda, T., Sakuntabhai, A., Cao-Lormeau, V.M., Malasit, P., Rey, F.A., *et al.* (2016). Dengue virus

- sero-cross-reactivity drives antibody-dependent enhancement of infection with zika virus. *Nat Immunol* *17*, 1102-1108.
- Delaney, A., Mai, C., Smoots, A., Cragan, J., Ellington, S., Langlois, P., Breidenbach, R., Fornoff, J., Dunn, J., Yazdy, M., *et al.* (2018). Population-Based Surveillance of Birth Defects Potentially Related to Zika Virus Infection - 15 States and U.S. Territories, 2016. *MMWR Morb Mortal Wkly Rep* *67*, 91-96.
- Delorme-Axford, E., Donker, R.B., Mouillet, J.F., Chu, T., Bayer, A., Ouyang, Y., Wang, T., Stolz, D.B., Sarkar, S.N., Morelli, A.E., *et al.* (2013). Human placental trophoblasts confer viral resistance to recipient cells. *Proc Natl Acad Sci U S A* *110*, 12048-12053.
- Demir, R., Kayisli, U.A., Seval, Y., Celik-Ozenci, C., Korgun, E.T., Demir-Weusten, A.Y., and Huppertz, B. (2004). Sequential expression of VEGF and its receptors in human placental villi during very early pregnancy: differences between placental vasculogenesis and angiogenesis. *Placenta* *25*, 560-572.
- Demir, R., Seval, Y., and Huppertz, B. (2007). Vasculogenesis and angiogenesis in the early human placenta. *Acta Histochem* *109*, 257-265.
- Diamond, M.S., Shrestha, B., Marri, A., Mahan, D., and Engle, M. (2003a). B cells and antibody play critical roles in the immediate defense of disseminated infection by West Nile encephalitis virus. *J Virol* *77*, 2578-2586.
- Diamond, M.S., Sitati, E.M., Friend, L.D., Higgs, S., Shrestha, B., and Engle, M. (2003b). A critical role for induced IgM in the protection against West Nile virus infection. *J Exp Med* *198*, 1853-1862.
- Dowd, K.A., DeMasos, C.R., Pelc, R.S., Speer, S.D., Smith, A.R.Y., Goo, L., Platt, D.J., Mascola, J.R., Graham, B.S., Mulligan, M.J., *et al.* (2016). Broadly Neutralizing Activity of Zika Virus-Immune Sera Identifies a Single Viral Serotype. *Cell Rep* *16*, 1485-1491.
- Durrant, D.M., Robinette, M.L., and Klein, R.S. (2013). IL-1R1 is required for dendritic cell-mediated T cell reactivation within the CNS during West Nile virus encephalitis. *J Exp Med* *210*, 503-516.
- Dussupt, V., Sankhala, R.S., Gromowski, G.D., Donofrio, G., De La Barrera, R.A., Larocca, R.A., Zaky, W., Mendez-Rivera, L., Choe, M., Davidson, E., *et al.* (2020). Potent Zika and dengue cross-neutralizing antibodies induced by Zika vaccination in a dengue-experienced donor. *Nat Med* *26*, 228-235.
- Eddy, W.E., Gong, K.Q., Bell, B., Parks, W.C., Ziegler, S.F., and Manicone, A.M. (2017). Stat5 Is Required for CD103(+) Dendritic Cell and Alveolar Macrophage Development and Protection from Lung Injury. *J Immunol* *198*, 4813-4822.
- Ehrenstein, M.R., and Notley, C.A. (2010). The importance of natural IgM: scavenger, protector and regulator. *Nat Rev Immunol* *10*, 778-786.
- Errett, J.S., Suthar, M.S., McMillan, A., Diamond, M.S., and Gale, M., Jr. (2013). The essential, nonredundant roles of RIG-I and MDA5 in detecting and controlling West Nile virus infection. *J Virol* *87*, 11416-11425.
- Esashi, E., Wang, Y.H., Perng, O., Qin, X.F., Liu, Y.J., and Watowich, S.S. (2008). The signal transducer STAT5 inhibits plasmacytoid dendritic cell development by suppressing transcription factor IRF8. *Immunity* *28*, 509-520.
- Evans, J.D., Crown, R.A., Sohn, J.A., and Seeger, C. (2011). West Nile virus infection induces depletion of IFNAR1 protein levels. *Viral Immunol* *24*, 253-263.
- Fehr, T., Bachmann, M.F., Bluethmann, H., Kikutani, H., Hengartner, H., and Zinkernagel, R.M. (1996). T-independent activation of B cells by vesicular stomatitis virus: no evidence for the need of a second signal. *Cell Immunol* *168*, 184-192.
- Fernandez Gonzalez, S., Jayasekera, J.P., and Carroll, M.C. (2008). Complement and natural antibody are required in the long-term memory response to influenza virus. *Vaccine* *26 Suppl 8*, I86-93.

- Figueiredo, C.P., Barros-Aragao, F.G.Q., Neris, R.L.S., Frost, P.S., Soares, C., Souza, I.N.O., Zeidler, J.D., Zamberlan, D.C., de Sousa, V.L., Souza, A.S., *et al.* (2019). Zika virus replicates in adult human brain tissue and impairs synapses and memory in mice. *Nat Commun* 10, 3890.
- Fish, E.N., Uddin, S., Korkmaz, M., Majchrzak, B., Druker, B.J., and Platanius, L.C. (1999). Activation of a CrkL-stat5 signaling complex by type I interferons. *J Biol Chem* 274, 571-573.
- Fisher, S., Genbacev, O., Maidji, E., and Pereira, L. (2000). Human cytomegalovirus infection of placental cytotrophoblasts in vitro and in utero: implications for transmission and pathogenesis. *J Virol* 74, 6808-6820.
- Fitzgerald, B., Boyle, C., and Honein, M.A. (2018). Birth Defects Potentially Related to Zika Virus Infection During Pregnancy in the United States. *JAMA*.
- Flipse, J., and Smit, J.M. (2015). The Complexity of a Dengue Vaccine: A Review of the Human Antibody Response. *PLoS Negl Trop Dis* 9, e0003749.
- Fowler, A.M., Tang, W.W., Young, M.P., Mamidi, A., Viramontes, K.M., McCauley, M.D., Carlin, A.F., Schooley, R.T., Swanstrom, J., Baric, R.S., *et al.* (2018). Maternally Acquired Zika Antibodies Enhance Dengue Disease Severity in Mice. *Cell Host Microbe* 24, 743-750 e745.
- Fredericks, A.C., and Fernandez-Sesma, A. (2014). The burden of dengue and chikungunya worldwide: implications for the southern United States and California. *Ann Glob Health* 80, 466-475.
- Furigo, I.C., Melo, H.M., Lyra, E.S.N.M., Ramos-Lobo, A.M., Teixeira, P.D.S., Buonfiglio, D.C., Wasinski, F., Lima, E.R., Higuti, E., Peroni, C.N., *et al.* (2018). Brain STAT5 signaling modulates learning and memory formation. *Brain Struct Funct* 223, 2229-2241.
- Gallichotte, E.N., Widman, D.G., Yount, B.L., Wahala, W.M., Durbin, A., Whitehead, S., Sariol, C.A., Crowe, J.E., Jr., de Silva, A.M., and Baric, R.S. (2015). A new quaternary structure epitope on dengue virus serotype 2 is the target of durable type-specific neutralizing antibodies. *MBio* 6, e01461-01415.
- Gandini, M., Reis, S.R., Torrentes-Carvalho, A., Azeredo, E.L., Freire Mda, S., Galler, R., and Kubelka, C.F. (2011). Dengue-2 and yellow fever 17DD viruses infect human dendritic cells, resulting in an induction of activation markers, cytokines and chemokines and secretion of different TNF-alpha and IFN-alpha profiles. *Mem Inst Oswaldo Cruz* 106, 594-605.
- Garcia, G., Gonzalez, N., Perez, A.B., Sierra, B., Aguirre, E., Rizo, D., Izquierdo, A., Sanchez, L., Diaz, D., Lezcay, M., *et al.* (2011). Long-term persistence of clinical symptoms in dengue-infected persons and its association with immunological disorders. *Int J Infect Dis* 15, e38-43.
- George, J., Valiant, W.G., Mattapallil, M.J., Walker, M., Huang, Y.S., Vanlandingham, D.L., Misamore, J., Greenhouse, J., Weiss, D.E., Verthelyi, D., *et al.* (2017). Prior Exposure to Zika Virus Significantly Enhances Peak Dengue-2 Viremia in Rhesus Macaques. *Sci Rep* 7, 10498.
- Girard, S., Tremblay, L., Lepage, M., and Sebire, G. (2010). IL-1 receptor antagonist protects against placental and neurodevelopmental defects induced by maternal inflammation. *J Immunol* 184, 3997-4005.
- Glasner, D.R., Ratnasiri, K., Puerta-Guardo, H., Espinosa, D.A., Beatty, P.R., and Harris, E. (2017). Dengue virus NS1 cytokine-independent vascular leak is dependent on endothelial glycocalyx components. *PLoS Pathog* 13, e1006673.
- Gordon, A., Gresh, L., Ojeda, S., Katzelnick, L.C., Sanchez, N., Mercado, J.C., Chowell, G., Lopez, B., Elizondo, D., Coloma, J., *et al.* (2019). Prior dengue virus infection and risk of Zika: A pediatric cohort in Nicaragua. *PLoS Med* 16, e1002726.

- Gorman, M.J., Caine, E.A., Zaitsev, K., Begley, M.C., Weger-Lucarelli, J., Uccellini, M.B., Tripathi, S., Morrison, J., Yount, B.L., Dinnon, K.H., 3rd, *et al.* (2018). An Immunocompetent Mouse Model of Zika Virus Infection. *Cell Host Microbe* 23, 672-685 e676.
- Gossner, C.M., Ducheyne, E., and Schaffner, F. (2018). Increased risk for autochthonous vector-borne infections transmitted by *Aedes albopictus* in continental Europe. *Euro Surveill* 23.
- Goubau, D., Schlee, M., Deddouche, S., Puijssers, A.J., Zillinger, T., Goldeck, M., Schuberth, C., Van der Veen, A.G., Fujimura, T., Rehwinkel, J., *et al.* (2014). Antiviral immunity via RIG-I-mediated recognition of RNA bearing 5'-diphosphates. *Nature* 514, 372-375.
- Gouilleux, F., Wakao, H., Mundt, M., and Groner, B. (1994). Prolactin induces phosphorylation of Tyr694 of Stat5 (MGF), a prerequisite for DNA binding and induction of transcription. *EMBO J* 13, 4361-4369.
- Grant, A., Ponia, S.S., Tripathi, S., Balasubramaniam, V., Miorin, L., Sourisseau, M., Schwarz, M.C., Sanchez-Seco, M.P., Evans, M.J., Best, S.M., *et al.* (2016). Zika Virus Targets Human STAT2 to Inhibit Type I Interferon Signaling. *Cell Host Microbe* 19, 882-890.
- Griffin, I., Martin, S.W., Fischer, M., Chambers, T.V., Kosoy, O., Falise, A., Ponomareva, O., Gillis, L.D., Blackmore, C., and Jean, R. (2019). Zika Virus IgM Detection and Neutralizing Antibody Profiles 12-19 Months after Illness Onset. *Emerg Infect Dis* 25, 299-303.
- Guilliams, M., Bruhns, P., Saeys, Y., Hammad, H., and Lambrecht, B.N. (2014). The function of Fc γ receptors in dendritic cells and macrophages. *Nat Rev Immunol* 14, 94-108.
- Guzman, M.G., and Harris, E. (2015). Dengue. *Lancet* 385, 453-465.
- Guzman, M.G., Kouri, G., Valdes, L., Bravo, J., Alvarez, M., Vazques, S., Delgado, I., and Halstead, S.B. (2000). Epidemiologic studies on Dengue in Santiago de Cuba, 1997. *Am J Epidemiol* 152, 793-799; discussion 804.
- Halai, U.A., Nielsen-Saines, K., Moreira, M.L., de Sequeira, P.C., Junior, J.P.P., de Araujo Zin, A., Cherry, J., Gabaglia, C.R., Gaw, S.L., Adachi, K., *et al.* (2017a). Maternal Zika Virus Disease Severity, Virus Load, Prior Dengue Antibodies, and Their Relationship to Birth Outcomes. *Clin Infect Dis* 65, 877-883.
- Halai, U.A., Nielsen-Saines, K., Moreira, M.L., de Sequeira, P.C., Pereira, J.P., Zin, A.A., Cherry, J., Gabaglia, C.R., Gaw, S.L., Adachi, K., *et al.* (2017b). Maternal Zika Virus Disease Severity, Virus Load, Prior Dengue Antibodies, and Their Relationship to Birth Outcomes. *Clin Infect Dis* 65, 877-883.
- Halstead, S.B. (1979). In vivo enhancement of dengue virus infection in rhesus monkeys by passively transferred antibody. *J Infect Dis* 140, 527-533.
- Halstead, S.B. (2003). Neutralization and antibody-dependent enhancement of dengue viruses. *Adv Virus Res* 60, 421-467.
- Halstead, S.B. (2014). Dengue Antibody-Dependent Enhancement: Knowns and Unknowns. *Microbiol Spectr* 2.
- Halstead, S.B., and O'Rourke, E.J. (1977). Antibody-enhanced dengue virus infection in primate leukocytes. *Nature* 265, 739-741.
- Hammaren, H.M., Virtanen, A.T., Raivola, J., and Silvennoinen, O. (2019). The regulation of JAKs in cytokine signaling and its breakdown in disease. *Cytokine* 118, 48-63.
- Harte, P.G., Cooke, A., and Playfair, J.H. (1983). Specific monoclonal IgM is a potent adjuvant in murine malaria vaccination. *Nature* 302, 256-258.
- Hasan, S.S., Sevvana, M., Kuhn, R.J., and Rossmann, M.G. (2018). Structural biology of Zika virus and other flaviviruses. *Nat Struct Mol Biol* 25, 13-20.
- Heald-Sargent, T., and Muller, W. (2017). Zika Virus: A Review for Pediatricians. *Pediatr Ann* 46, e428-e432.
- Henderson, A.D., Aubry, M., Kama, M., Vanhomwegen, J., Teissier, A., Mariteragi-Helle, T., Paoaafaita, T., Teissier, Y., Manuguerra, J.C., Edmunds, J., *et al.* (2020). Zika seroprevalence declines and neutralizing antibodies wane in adults following outbreaks in French Polynesia and Fiji. *Elife* 9.

- Hennighausen, L., and Robinson, G.W. (2008). Interpretation of cytokine signaling through the transcription factors STAT5A and STAT5B. *Genes Dev* 22, 711-721.
- Hermanns, K., Gohner, C., Kopp, A., Schmidt, A., Merz, W.M., Markert, U.R., Junglen, S., and Drosten, C. (2018). Zika virus infection in human placental tissue explants is enhanced in the presence of dengue virus antibodies in-vitro. *Emerg Microbes Infect* 7, 198.
- Hessell, A.J., Hangartner, L., Hunter, M., Havenith, C.E., Beurskens, F.J., Bakker, J.M., Lanigan, C.M., Landucci, G., Forthal, D.N., Parren, P.W., *et al.* (2007). Fc receptor but not complement binding is important in antibody protection against HIV. *Nature* 449, 101-104.
- Hill, S.C., Vasconcelos, J., Neto, Z., Jandondo, D., Ze-Ze, L., Aguiar, R.S., Xavier, J., Theze, J., Mirandela, M., Micoló Candido, A.L., *et al.* (2019). Emergence of the Asian lineage of Zika virus in Angola: an outbreak investigation. *Lancet Infect Dis* 19, 1138-1147.
- Hirsch, A.J., Roberts, V.H.J., Grigsby, P.L., Haese, N., Schabel, M.C., Wang, X., Lo, J.O., Liu, Z., Kroenke, C.D., Smith, J.L., *et al.* (2018). Zika virus infection in pregnant rhesus macaques causes placental dysfunction and immunopathology. *Nat Commun* 9, 263.
- Ho, L.J., Wang, J.J., Shaio, M.F., Kao, C.L., Chang, D.M., Han, S.W., and Lai, J.H. (2001). Infection of human dendritic cells by dengue virus causes cell maturation and cytokine production. *J Immunol* 166, 1499-1506.
- Hoen, B., Carpentier, M., Gaete, S., Tressieres, B., Herrmann-Storck, C., Vingadassalom, I., Huc-Anais, P., Funk, A.L., Fontanet, A., and de Lamballerie, X. (2019). Kinetics of Anti-Zika Virus Antibodies after Acute Infection in Pregnant Women. *J Clin Microbiol* 57.
- Ilag, L.L. (2011). Immunoglobulin M as a vaccine adjuvant. *Med Hypotheses* 77, 473-478.
- Ingman, K., Cookson, V.J., Jones, C.J., and Aplin, J.D. (2010). Characterisation of Hofbauer cells in first and second trimester placenta: incidence, phenotype, survival in vitro and motility. *Placenta* 31, 535-544.
- Ito, M., Mukai, R.Z., Takasaki, T., Kotaki, A., and Kurane, I. (2010). Antibody-dependent enhancement of dengue virus infection in vitro by undiluted sera from monkeys infected with heterotypic dengue virus. *Arch Virol* 155, 1617-1624.
- Jagger, B.W., Miner, J.J., Cao, B., Arora, N., Smith, A.M., Kovacs, A., Mysorekar, I.U., Coyne, C.B., and Diamond, M.S. (2017). Gestational Stage and IFN-lambda Signaling Regulate ZIKV Infection In Utero. *Cell Host Microbe* 22, 366-376 e363.
- Janky, R., Verfaillie, A., Imrichova, H., Van de Sande, B., Standaert, L., Christiaens, V., Hulselmans, G., Hertzen, K., Naval Sanchez, M., Potier, D., *et al.* (2014). iRegulon: from a gene list to a gene regulatory network using large motif and track collections. *PLoS Comput Biol* 10, e1003731.
- Jayasekera, J.P., Moseman, E.A., and Carroll, M.C. (2007). Natural antibody and complement mediate neutralization of influenza virus in the absence of prior immunity. *J Virol* 81, 3487-3494.
- Jendeberg, L., Nilsson, P., Larsson, A., Denker, P., Uhlen, M., Nilsson, B., and Nygren, P.A. (1997). Engineering of Fc(1) and Fc(3) from human immunoglobulin G to analyse subclass specificity for staphylococcal protein A. *J Immunol Methods* 201, 25-34.
- Johnsen, I.B., Nguyen, T.T., Bergstroem, B., Fitzgerald, K.A., and Anthonson, M.W. (2009). The tyrosine kinase c-Src enhances RIG-I (retinoic acid-inducible gene I)-elicited antiviral signaling. *J Biol Chem* 284, 19122-19131.
- Johnson, E.L., and Chakraborty, R. (2012). Placental Hofbauer cells limit HIV-1 replication and potentially offset mother to child transmission (MTCT) by induction of immunoregulatory cytokines. *Retrovirology* 9, 101.
- Jurado, K.A., Simoni, M.K., Tang, Z., Uraki, R., Hwang, J., Householder, S., Wu, M., Lindenbach, B.D., Abrahams, V.M., Guller, S., *et al.* (2016). Zika virus productively infects primary human placenta-specific macrophages. *JCI Insight* 1.

- Kapogiannis, B.G., Chakhtoura, N., Hazra, R., and Spong, C.Y. (2017). Bridging Knowledge Gaps to Understand How Zika Virus Exposure and Infection Affect Child Development. *JAMA Pediatr* 171, 478-485.
- Katzelnick, L.C., Gresh, L., Halloran, M.E., Mercado, J.C., Kuan, G., Gordon, A., Balmaseda, A., and Harris, E. (2017). Antibody-dependent enhancement of severe dengue disease in humans. *Science* 358, 929-932.
- Keeffe, J.R., Van Rompay, K.K.A., Olsen, P.C., Wang, Q., Gazumyan, A., Azzopardi, S.A., Schaefer-Babajew, D., Lee, Y.E., Stuart, J.B., Singapuri, A., *et al.* (2018). A Combination of Two Human Monoclonal Antibodies Prevents Zika Virus Escape Mutations in Non-human Primates. *Cell Rep* 25, 1385-1394 e1387.
- Keller, B.C., Fredericksen, B.L., Samuel, M.A., Mock, R.E., Mason, P.W., Diamond, M.S., and Gale, M., Jr. (2006). Resistance to alpha/beta interferon is a determinant of West Nile virus replication fitness and virulence. *J Virol* 80, 9424-9434.
- Khan, S., Katabuchi, H., Araki, M., Nishimura, R., and Okamura, H. (2000). Human villous macrophage-conditioned media enhance human trophoblast growth and differentiation in vitro. *Biol Reprod* 62, 1075-1083.
- Kim, J., Mohanty, S., Ganesan, L.P., Hua, K., Jarjoura, D., Hayton, W.L., Robinson, J.M., and Anderson, C.L. (2009). FcRn in the yolk sac endoderm of mouse is required for IgG transport to fetus. *J Immunol* 182, 2583-2589.
- Kim, S.Y., Romero, R., Tarca, A.L., Bhatti, G., Kim, C.J., Lee, J., Elsey, A., Than, N.G., Chaiworapongsa, T., Hassan, S.S., *et al.* (2012). Methylome of fetal and maternal monocytes and macrophages at the feto-maternal interface. *Am J Reprod Immunol* 68, 8-27.
- Kliks, S.C., Nimmanitya, S., Nisalak, A., and Burke, D.S. (1988). Evidence that maternal dengue antibodies are important in the development of dengue hemorrhagic fever in infants. *Am J Trop Med Hyg* 38, 411-419.
- Koga, K., Izumi, G., Mor, G., Fujii, T., and Osuga, Y. (2014). Toll-like receptors at the maternal-fetal interface in normal pregnancy and pregnancy complications. *Am J Reprod Immunol* 72, 192-205.
- Koraka, P., Suharti, C., Setiati, T.E., Mairuhu, A.T., Van Gorp, E., Hack, C.E., Juffrie, M., Sutaryo, J., Van Der Meer, G.M., Groen, J., *et al.* (2001). Kinetics of dengue virus-specific serum immunoglobulin classes and subclasses correlate with clinical outcome of infection. *J Clin Microbiol* 39, 4332-4338.
- Kovats, S., Turner, S., Simmons, A., Powe, T., Chakravarty, E., and Alberola-Ila, J. (2016). West Nile virus-infected human dendritic cells fail to fully activate invariant natural killer T cells. *Clin Exp Immunol* 186, 214-226.
- Kraemer, M.U.G., Reiner, R.C., Jr., Brady, O.J., Messina, J.P., Gilbert, M., Pigott, D.M., Yi, D., Johnson, K., Earl, L., Marczak, L.B., *et al.* (2019). Past and future spread of the arbovirus vectors *Aedes aegypti* and *Aedes albopictus*. *Nat Microbiol* 4, 854-863.
- Kramer, L.D., Li, J., and Shi, P.Y. (2007). West Nile virus. *Lancet Neurol* 6, 171-181.
- Lai, C.Y., Tsai, W.Y., Lin, S.R., Kao, C.L., Hu, H.P., King, C.C., Wu, H.C., Chang, G.J., and Wang, W.K. (2008). Antibodies to envelope glycoprotein of dengue virus during the natural course of infection are predominantly cross-reactive and recognize epitopes containing highly conserved residues at the fusion loop of domain II. *J Virol* 82, 6631-6643.
- Lanciotti, R.S., Kosoy, O.L., Laven, J.J., Velez, J.O., Lambert, A.J., Johnson, A.J., Stanfield, S.M., and Duffy, M.R. (2008). Genetic and serologic properties of Zika virus associated with an epidemic, Yap State, Micronesia, 2007. *Emerg Infect Dis* 14, 1232-1239.
- Langerak, T., Mumtaz, N., Tolk, V.I., van Gorp, E.C.M., Martina, B.E., Rockx, B., and Koopmans, M.P.G. (2019). The possible role of cross-reactive dengue virus antibodies in Zika virus pathogenesis. *PLoS Pathog* 15, e1007640.

- Larocca, R.A., Mendes, E.A., Abbink, P., Peterson, R.L., Martinot, A.J., Iampietro, M.J., Kang, Z.H., Aid, M., Kirilova, M., Jacob-Dolan, C., *et al.* (2019). Adenovirus Vector-Based Vaccines Confer Maternal-Fetal Protection against Zika Virus Challenge in Pregnant IFN- α Mice. *Cell Host Microbe* 26, 591-600 e594.
- Latvala, S., Jacobsen, B., Otteneder, M.B., Herrmann, A., and Kronenberg, S. (2017). Distribution of FcRn Across Species and Tissues. *J Histochem Cytochem* 65, 321-333.
- Lazear, H.M., Daniels, B.P., Pinto, A.K., Huang, A.C., Vick, S.C., Doyle, S.E., Gale, M., Jr., Klein, R.S., and Diamond, M.S. (2015a). Interferon- λ restricts West Nile virus neuroinvasion by tightening the blood-brain barrier. *Sci Transl Med* 7, 284ra259.
- Lazear, H.M., and Diamond, M.S. (2016). Zika Virus: New Clinical Syndromes and Its Emergence in the Western Hemisphere. *J Virol* 90, 4864-4875.
- Lazear, H.M., Govero, J., Smith, A.M., Platt, D.J., Fernandez, E., Miner, J.J., and Diamond, M.S. (2016). A Mouse Model of Zika Virus Pathogenesis. *Cell Host Microbe* 19, 720-730.
- Lazear, H.M., Lancaster, A., Wilkins, C., Suthar, M.S., Huang, A., Vick, S.C., Clepper, L., Thackray, L., Brassil, M.M., Virgin, H.W., *et al.* (2013). IRF-3, IRF-5, and IRF-7 coordinately regulate the type I IFN response in myeloid dendritic cells downstream of MAVS signaling. *PLoS Pathog* 9, e1003118.
- Lazear, H.M., Nice, T.J., and Diamond, M.S. (2015b). Interferon- λ : Immune Functions at Barrier Surfaces and Beyond. *Immunity* 43, 15-28.
- Lazear, H.M., Schoggins, J.W., and Diamond, M.S. (2019). Shared and Distinct Functions of Type I and Type III Interferons. *Immunity* 50, 907-923.
- Li, C., Xu, D., Ye, Q., Hong, S., Jiang, Y., Liu, X., Zhang, N., Shi, L., Qin, C.F., and Xu, Z. (2016). Zika Virus Disrupts Neural Progenitor Development and Leads to Microcephaly in Mice. *Cell Stem Cell* 19, 672.
- Li, H.S., Yang, C.Y., Nallaparaju, K.C., Zhang, H., Liu, Y.J., Goldrath, A.W., and Watowich, S.S. (2012). The signal transducers STAT5 and STAT3 control expression of Id2 and E2-2 during dendritic cell development. *Blood* 120, 4363-4373.
- Libraty, D.H., Nisalak, A., Endy, T.P., Suntayakorn, S., Vaughn, D.W., and Innis, B.L. (2002). Clinical and immunological risk factors for severe disease in Japanese encephalitis. *Trans R Soc Trop Med Hyg* 96, 173-178.
- Lim, D.S., Yawata, N., Selva, K.J., Li, N., Tsai, C.Y., Yeong, L.H., Liong, K.H., Ooi, E.E., Chong, M.K., Ng, M.L., *et al.* (2014). The combination of type I IFN, TNF- α , and cell surface receptor engagement with dendritic cells enables NK cells to overcome immune evasion by dengue virus. *J Immunol* 193, 5065-5075.
- Lim, Y.J., Koo, J.E., Hong, E.H., Park, Z.Y., Lim, K.M., Bae, O.N., and Lee, J.Y. (2015). A Src-family-tyrosine kinase, Lyn, is required for efficient IFN- β expression in pattern recognition receptor, RIG-I, signal pathway by interacting with IPS-1. *Cytokine* 72, 63-70.
- Lin, R.J., Chang, B.L., Yu, H.P., Liao, C.L., and Lin, Y.L. (2006). Blocking of interferon-induced Jak-Stat signaling by Japanese encephalitis virus NS5 through a protein tyrosine phosphatase-mediated mechanism. *J Virol* 80, 5908-5918.
- Lindmark, R., Thoren-Tolling, K., and Sjoquist, J. (1983). Binding of immunoglobulins to protein A and immunoglobulin levels in mammalian sera. *J Immunol Methods* 62, 1-13.
- Loo, Y.M., and Gale, M., Jr. (2011). Immune signaling by RIG-I-like receptors. *Immunity* 34, 680-692.
- Lopes Moreira, M.E., Nielsen-Saines, K., Brasil, P., Kerin, T., Damasceno, L., Pone, M., Carvalho, L.M.A., Pone, S.M., Vasconcelos, Z., Ribeiro, I.P., *et al.* (2018). Neurodevelopment in Infants Exposed to Zika Virus In Utero. *N Engl J Med* 379, 2377-2379.
- Lubick, K.J., Robertson, S.J., McNally, K.L., Freedman, B.A., Rasmussen, A.L., Taylor, R.T., Walts, A.D., Tsuruda, S., Sakai, M., Ishizuka, M., *et al.* (2015). Flavivirus Antagonism of Type I Interferon Signaling Reveals Prolidase as a Regulator of IFNAR1 Surface Expression. *Cell Host Microbe* 18, 61-74.

- Lutz, M.B., Schnare, M., Menges, M., Rossner, S., Rollinghoff, M., Schuler, G., and Gessner, A. (2002). Differential functions of IL-4 receptor types I and II for dendritic cell maturation and IL-12 production and their dependency on GM-CSF. *J Immunol* *169*, 3574-3580.
- Lyden, T.W., Robinson, J.M., Tridandapani, S., Teillaud, J.L., Garber, S.A., Osborne, J.M., Frey, J., Budde, P., and Anderson, C.L. (2001). The Fc receptor for IgG expressed in the villus endothelium of human placenta is Fc gamma RIIb2. *J Immunol* *166*, 3882-3889.
- Ma, D., Jiang, D., Qing, M., Weidner, J.M., Qu, X., Guo, H., Chang, J., Gu, B., Shi, P.Y., Block, T.M., *et al.* (2009). Antiviral effect of interferon lambda against West Nile virus. *Antiviral Res* *83*, 53-60.
- Magnani, D.M., Rogers, T.F., Beutler, N., Ricciardi, M.J., Bailey, V.K., Gonzalez-Nieto, L., Briney, B., Sok, D., Le, K., Strubel, A., *et al.* (2017). Neutralizing human monoclonal antibodies prevent Zika virus infection in macaques. *Sci Transl Med* *9*.
- Magnani, D.M., Rogers, T.F., Maness, N.J., Grubaugh, N.D., Beutler, N., Bailey, V.K., Gonzalez-Nieto, L., Gutman, M.J., Pedreno-Lopez, N., Kwal, J.M., *et al.* (2018). Fetal demise and failed antibody therapy during Zika virus infection of pregnant macaques. *Nat Commun* *9*, 1624.
- Maidji, E., McDonagh, S., Genbacev, O., Tabata, T., and Pereira, L. (2006). Maternal antibodies enhance or prevent cytomegalovirus infection in the placenta by neonatal Fc receptor-mediated transcytosis. *Am J Pathol* *168*, 1210-1226.
- Malafa, S., Medits, I., Aberle, J.H., Aberle, S.W., Haslwanter, D., Tsouchnikas, G., Wolfel, S., Huber, K.L., Percivalle, E., Cherpillod, P., *et al.* (2020). Impact of flavivirus vaccine-induced immunity on primary Zika virus antibody response in humans. *PLoS Negl Trop Dis* *14*, e0008034.
- Marchette, N.J., Halstead, S.B., O'Rourke, T., Scott, R.M., Bancroft, W.H., and Vanopruks, V. (1979). Effect of immune status on dengue 2 virus replication in cultured leukocytes from infants and children. *Infect Immun* *24*, 47-50.
- Markham, K., Schuurmans, C., and Weiss, S. (2007). STAT5A/B activity is required in the developing forebrain and spinal cord. *Mol Cell Neurosci* *35*, 272-282.
- Marques, E.T.A., and Drexler, J.F. (2019). Complex Scenario of Homotypic and Heterotypic Zika Virus Immune Enhancement. *mBio* *10*.
- Martin, W.L., West, A.P., Jr., Gan, L., and Bjorkman, P.J. (2001). Crystal structure at 2.8 Å of an FcRn/heterodimeric Fc complex: mechanism of pH-dependent binding. *Mol Cell* *7*, 867-877.
- Martina, B.E., Koraka, P., and Osterhaus, A.D. (2009). Dengue virus pathogenesis: an integrated view. *Clin Microbiol Rev* *22*, 564-581.
- Martines, R.B., Bhatnagar, J., de Oliveira Ramos, A.M., Davi, H.P., Iglezias, S.D., Kanamura, C.T., Keating, M.K., Hale, G., Silva-Flannery, L., Muehlenbachs, A., *et al.* (2016). Pathology of congenital Zika syndrome in Brazil: a case series. *Lancet* *388*, 898-904.
- Martinot, A.J., Abbink, P., Afacan, O., Prohl, A.K., Bronson, R., Hecht, J.L., Borducchi, E.N., Larocca, R.A., Peterson, R.L., Rinaldi, W., *et al.* (2018). Fetal Neuropathology in Zika Virus-Infected Pregnant Female Rhesus Monkeys. *Cell* *173*, 1111-1122 e1110.
- McConkey, C.A., Delorme-Axford, E., Nickerson, C.A., Kim, K.S., Sadovsky, Y., Boyle, J.P., and Coyne, C.B. (2016). A three-dimensional culture system recapitulates placental syncytiotrophoblast development and microbial resistance. *Sci Adv* *2*, e1501462.
- Mead, P.S., Duggal, N.K., Hook, S.A., Delorey, M., Fischer, M., Olzenak McGuire, D., Becksted, H., Max, R.J., Anishchenko, M., Schwartz, A.M., *et al.* (2018). Zika Virus Shedding in Semen of Symptomatic Infected Men. *N Engl J Med* *378*, 1377-1385.
- Mehlhop, E., Ansarah-Sobrinho, C., Johnson, S., Engle, M., Fremont, D.H., Pierson, T.C., and Diamond, M.S. (2007). Complement protein C1q inhibits antibody-dependent enhancement of flavivirus infection in an IgG subclass-specific manner. *Cell Host Microbe* *2*, 417-426.

- Mehlhof, E., Nelson, S., Jost, C.A., Gorlatov, S., Johnson, S., Fremont, D.H., Diamond, M.S., and Pierson, T.C. (2009). Complement protein C1q reduces the stoichiometric threshold for antibody-mediated neutralization of West Nile virus. *Cell Host Microbe* 6, 381-391.
- Meinke, A., Barahmand-Pour, F., Wohrl, S., Stoiber, D., and Decker, T. (1996). Activation of different Stat5 isoforms contributes to cell-type-restricted signaling in response to interferons. *Mol Cell Biol* 16, 6937-6944.
- Melo, A.S.O., Chimelli, L., and Tanuri, A. (2017). Congenital Zika Virus Infection: Beyond Neonatal Microcephaly-Reply. *JAMA Neurol* 74, 610-611.
- Messer, W.B., Yount, B., Hacker, K.E., Donaldson, E.F., Huynh, J.P., de Silva, A.M., and Baric, R.S. (2012). Development and characterization of a reverse genetic system for studying dengue virus serotype 3 strain variation and neutralization. *PLoS Negl Trop Dis* 6, e1486.
- Michlmayr, D., and Lim, J.K. (2014). Chemokine receptors as important regulators of pathogenesis during arboviral encephalitis. *Front Cell Neurosci* 8, 264.
- Miner, J.J., and Diamond, M.S. (2016). Understanding How Zika Virus Enters and Infects Neural Target Cells. *Cell Stem Cell* 18, 559-560.
- Miner, J.J., and Diamond, M.S. (2017). Zika Virus Pathogenesis and Tissue Tropism. *Cell Host Microbe* 21, 134-142.
- Modhiran, N., Watterson, D., Muller, D.A., Panetta, A.K., Sester, D.P., Liu, L., Hume, D.A., Stacey, K.J., and Young, P.R. (2015). Dengue virus NS1 protein activates cells via Toll-like receptor 4 and disrupts endothelial cell monolayer integrity. *Sci Transl Med* 7, 304ra142.
- Montoya, M., Collins, M., Dejnirattisai, W., Katzelnick, L.C., Puerta-Guardo, H., Jadi, R., Schildhauer, S., Supasa, P., Vasanawathana, S., Malasit, P., *et al.* (2018). Longitudinal Analysis of Antibody Cross-neutralization Following Zika Virus and Dengue Virus Infection in Asia and the Americas. *J Infect Dis* 218, 536-545.
- Moreno, G.K., Newman, C.M., Koenig, M.R., Mohns, M.S., Weiler, A.M., Rybarczyk, S., Weisgrau, K.L., Vosler, L.J., Pomplun, N., Schultz-Darken, N., *et al.* (2020). Long-Term Protection of Rhesus Macaques from Zika Virus Reinfection. *J Virol* 94.
- Morrison, J., Laurent-Rolle, M., Maestre, A.M., Rajsbaum, R., Pisanelli, G., Simon, V., Mulder, L.C., Fernandez-Sesma, A., and Garcia-Sastre, A. (2013). Dengue virus co-opts UBR4 to degrade STAT2 and antagonize type I interferon signaling. *PLoS Pathog* 9, e1003265.
- Mulkey, S.B., Vezina, G., Bulas, D.I., Khademian, Z., Blask, A., Kousa, Y., Cristante, C., Pesacreta, L., du Plessis, A.J., and DeBiasi, R.L. (2018). Neuroimaging Findings in Normocephalic Newborns With Intrauterine Zika Virus Exposure. *Pediatr Neurol* 78, 75-78.
- Munoz-Jordan, J.L., Laurent-Rolle, M., Ashour, J., Martinez-Sobrido, L., Ashok, M., Lipkin, W.I., and Garcia-Sastre, A. (2005). Inhibition of alpha/beta interferon signaling by the NS4B protein of flaviviruses. *J Virol* 79, 8004-8013.
- Musso, D., Ko, A.I., and Baud, D. (2019). Zika Virus Infection - After the Pandemic. *N Engl J Med* 381, 1444-1457.
- Nguyen, T.T., and Baumgarth, N. (2016). Natural IgM and the Development of B Cell-Mediated Autoimmune Diseases. *Crit Rev Immunol* 36, 163-177.
- Nielsen-Saines, K., Brasil, P., Kerin, T., Vasconcelos, Z., Gabaglia, C.R., Damasceno, L., Pone, M., Abreu de Carvalho, L.M., Pone, S.M., Zin, A.A., *et al.* (2019). Delayed childhood neurodevelopment and neurosensory alterations in the second year of life in a prospective cohort of ZIKV-exposed children. *Nat Med* 25, 1213-1217.
- Nogueira, M.L., Nery Junior, N.R.R., Estofolete, C.F., Bernardes Terzian, A.C., Guimaraes, G.F., Zini, N., Alves da Silva, R., Dutra Silva, G.C., Junqueira Franco, L.C., Rahal, P., *et al.* (2018). Adverse birth outcomes associated with Zika virus exposure during pregnancy in Sao Jose do Rio Preto, Brazil. *Clin Microbiol Infect* 24, 646-652.
- Nunes, P., Nogueira, R., Coelho, J., Rodrigues, F., Salomao, N., Jose, C., de Carvalho, J., Rabelo, K., de Azeredo, E., Basilio-de-Oliveira, R., *et al.* (2019). A Stillborn Multiple

- Organs' Investigation from a Maternal DENV-4 Infection: Histopathological and Inflammatory Mediators Characterization. *Viruses* 11.
- Nunes, P.C., Paes, M.V., de Oliveira, C.A., Soares, A.C., de Filippis, A.M., Lima Mda, R., de Barcelos Alves, A.M., da Silva, J.F., de Oliveira Coelho, J.M., de Carvalho Rodrigues, F., *et al.* (2016). Detection of dengue NS1 and NS3 proteins in placenta and umbilical cord in fetal and maternal death. *J Med Virol* 88, 1448-1452.
- O'Leary, D.R., Kuhn, S., Kniss, K.L., Hinckley, A.F., Rasmussen, S.A., Pape, W.J., Kightlinger, L.K., Beecham, B.D., Miller, T.K., Neitzel, D.F., *et al.* (2006). Birth outcomes following West Nile Virus infection of pregnant women in the United States: 2003-2004. *Pediatrics* 117, e537-545.
- Ober, R.J., Radu, C.G., Ghetie, V., and Ward, E.S. (2001). Differences in promiscuity for antibody-FcRn interactions across species: implications for therapeutic antibodies. *Int Immunol* 13, 1551-1559.
- Oh, Y., Zhang, F., Wang, Y., Lee, E.M., Choi, I.Y., Lim, H., Mirakhori, F., Li, R., Huang, L., Xu, T., *et al.* (2017). Zika virus directly infects peripheral neurons and induces cell death. *Nat Neurosci* 20, 1209-1212.
- Okutani, Y., Kitanaka, A., Tanaka, T., Kamano, H., Ohnishi, H., Kubota, Y., Ishida, T., and Takahara, J. (2001). Src directly tyrosine-phosphorylates STAT5 on its activation site and is involved in erythropoietin-induced signaling pathway. *Oncogene* 20, 6643-6650.
- Olagnier, D., Peri, S., Steel, C., van Montfoort, N., Chiang, C., Beljanski, V., Slifker, M., He, Z., Nichols, C.N., Lin, R., *et al.* (2014). Cellular oxidative stress response controls the antiviral and apoptotic programs in dengue virus-infected dendritic cells. *PLoS Pathog* 10, e1004566.
- Oliphant, T., Engle, M., Nybakken, G.E., Doane, C., Johnson, S., Huang, L., Gorlatov, S., Mehlhop, E., Marri, A., Chung, K.M., *et al.* (2005). Development of a humanized monoclonal antibody with therapeutic potential against West Nile virus. *Nat Med* 11, 522-530.
- Onorati, M., Li, Z., Liu, F., Sousa, A.M.M., Nakagawa, N., Li, M., Dell'Anno, M.T., Gulden, F.O., Pochareddy, S., Tebbenkamp, A.T.N., *et al.* (2016). Zika Virus Disrupts Phospho-TBK1 Localization and Mitosis in Human Neuroepithelial Stem Cells and Radial Glia. *Cell Rep* 16, 2576-2592.
- Palmeira, P., Quinello, C., Silveira-Lessa, A.L., Zago, C.A., and Carneiro-Sampaio, M. (2012). IgG placental transfer in healthy and pathological pregnancies. *Clin Dev Immunol* 2012, 985646.
- Pantoja, P., Perez-Guzman, E.X., Rodriguez, I.V., White, L.J., Gonzalez, O., Serrano, C., Giavedoni, L., Hodara, V., Cruz, L., Arana, T., *et al.* (2017). Zika virus pathogenesis in rhesus macaques is unaffected by pre-existing immunity to dengue virus. *Nat Commun* 8, 15674.
- Pardi, N., Hogan, M.J., Pelc, R.S., Muramatsu, H., Andersen, H., DeMaso, C.R., Dowd, K.A., Sutherland, L.L., Scarce, R.M., Parks, R., *et al.* (2017). Zika virus protection by a single low-dose nucleoside-modified mRNA vaccination. *Nature* 543, 248-251.
- Patel, B., Longo, P., Miley, M.J., Montoya, M., Harris, E., and de Silva, A.M. (2017). Dissecting the human serum antibody response to secondary dengue virus infections. *PLoS Negl Trop Dis* 11, e0005554.
- Patel, H., Sander, B., and Nelder, M.P. (2015). Long-term sequelae of West Nile virus-related illness: a systematic review. *Lancet Infect Dis* 15, 951-959.
- Paul, L.M., Carlin, E.R., Jenkins, M.M., Tan, A.L., Barcellona, C.M., Nicholson, C.O., Michael, S.F., and Isern, S. (2016). Dengue virus antibodies enhance Zika virus infection. *Clin Transl Immunology* 5, e117.
- Paz-Bailey, G., Rosenberg, E.S., and Sharp, T.M. (2019). Persistence of Zika Virus in Body Fluids - Final Report. *N Engl J Med* 380, 198-199.

- Pedroso, C., Fischer, C., Feldmann, M., Sarno, M., Luz, E., Moreira-Soto, A., Cabral, R., Netto, E.M., Brites, C., Kummerer, B.M., *et al.* (2019). Cross-Protection of Dengue Virus Infection against Congenital Zika Syndrome, Northeastern Brazil. *Emerg Infect Dis* 25, 1485-1493.
- Pentsuk, N., and van der Laan, J.W. (2009). An interspecies comparison of placental antibody transfer: new insights into developmental toxicity testing of monoclonal antibodies. *Birth Defects Res B Dev Reprod Toxicol* 86, 328-344.
- Perez-Guzman, E.X., Pantoja, P., Serrano-Collazo, C., Hassert, M.A., Ortiz-Rosa, A., Rodriguez, I.V., Giavedoni, L., Hodara, V., Parodi, L., Cruz, L., *et al.* (2019). Time elapsed between Zika and dengue virus infections affects antibody and T cell responses. *Nat Commun* 10, 4316.
- Petersen, L.R., Carson, P.J., Biggerstaff, B.J., Custer, B., Borchardt, S.M., and Busch, M.P. (2013). Estimated cumulative incidence of West Nile virus infection in US adults, 1999-2010. *Epidemiol Infect* 141, 591-595.
- Pinto, A.K., Ramos, H.J., Wu, X., Aggarwal, S., Shrestha, B., Gorman, M., Kim, K.Y., Suthar, M.S., Atkinson, J.P., Gale, M., Jr., *et al.* (2014). Deficient IFN signaling by myeloid cells leads to MAVS-dependent virus-induced sepsis. *PLoS Pathog* 10, e1004086.
- Platt, D.J., Smith, A.M., Arora, N., Diamond, M.S., Coyne, C.B., and Miner, J.J. (2018). Zika virus-related neurotropic flaviviruses infect human placental explants and cause fetal demise in mice. *Sci Transl Med* 10.
- Plotkin, S.A. (2010). Correlates of protection induced by vaccination. *Clin Vaccine Immunol* 17, 1055-1065.
- Pridjian, G., Sirois, P.A., McRae, S., Hinckley, A.F., Rasmussen, S.A., Kissinger, P., Buekens, P., Hayes, E.B., O'Leary, D., Kuhn, S., *et al.* (2016). Prospective study of pregnancy and newborn outcomes in mothers with West Nile illness during pregnancy. *Birth Defects Res A Clin Mol Teratol* 106, 716-723.
- Prince, H.E., and Matud, J.L. (2011). Estimation of dengue virus IgM persistence using regression analysis. *Clin Vaccine Immunol* 18, 2183-2185.
- Priyamvada, L., Cho, A., Onlamoon, N., Zheng, N.Y., Huang, M., Kovalenkov, Y., Chokephaibulkit, K., Angkasekwinai, N., Pattanapanyasat, K., Ahmed, R., *et al.* (2016a). B Cell Responses during Secondary Dengue Virus Infection Are Dominated by Highly Cross-Reactive, Memory-Derived Plasmablasts. *J Virol* 90, 5574-5585.
- Priyamvada, L., Quicke, K.M., Hudson, W.H., Onlamoon, N., Sewatanon, J., Edupuganti, S., Pattanapanyasat, K., Chokephaibulkit, K., Mulligan, M.J., Wilson, P.C., *et al.* (2016b). Human antibody responses after dengue virus infection are highly cross-reactive to Zika virus. *Proc Natl Acad Sci U S A* 113, 7852-7857.
- Pudney, J., He, X., Masheeb, Z., Kindelberger, D.W., Kuohung, W., and Ingalls, R.R. (2016). Differential expression of toll-like receptors in the human placenta across early gestation. *Placenta* 46, 1-10.
- Puerta-Guardo, H., Glasner, D.R., and Harris, E. (2016). Dengue Virus NS1 Disrupts the Endothelial Glycocalyx, Leading to Hyperpermeability. *PLoS Pathog* 12, e1005738.
- Pulendran, B. (2015). The Varieties of Immunological Experience; Of Pathogens, Stress, and Dendritic Cells. *Annu Rev Immunol* 33, 563-606.
- Pyzik, M., Rath, T., Lencer, W.I., Baker, K., and Blumberg, R.S. (2015). FcRn: The Architect Behind the Immune and Nonimmune Functions of IgG and Albumin. *J Immunol* 194, 4595-4603.
- Pyzik, M., Sand, K.M.K., Hubbard, J.J., Andersen, J.T., Sandlie, I., and Blumberg, R.S. (2019). The Neonatal Fc Receptor (FcRn): A Misnomer? *Front Immunol* 10, 1540.
- Querec, T., Bennouna, S., Alkan, S., Laouar, Y., Gorden, K., Flavell, R., Akira, S., Ahmed, R., and Pulendran, B. (2006). Yellow fever vaccine YF-17D activates multiple dendritic cell subsets via TLR2, 7, 8, and 9 to stimulate polyvalent immunity. *J Exp Med* 203, 413-424.

- Quicke, K.M., Bowen, J.R., Johnson, E.L., McDonald, C.E., Ma, H., O'Neal, J.T., Rajakumar, A., Wrammert, J., Rimawi, B.H., Pulendran, B., *et al.* (2016a). Zika Virus Infects Human Placental Macrophages. *Cell Host Microbe*.
- Quicke, K.M., Bowen, J.R., Johnson, E.L., McDonald, C.E., Ma, H., O'Neal, J.T., Rajakumar, A., Wrammert, J., Rimawi, B.H., Pulendran, B., *et al.* (2016b). Zika Virus Infects Human Placental Macrophages. *Cell Host Microbe* 20, 83-90.
- Quicke, K.M., Kim, K.Y., Horvath, C.M., and Suthar, M.S. (2019). RNA Helicase LGP2 Negatively Regulates RIG-I Signaling by Preventing TRIM25-Mediated Caspase Activation and Recruitment Domain Ubiquitination. *J Interferon Cytokine Res* 39, 669-683.
- Quicke, K.M., and Suthar, M.S. (2013). The innate immune playbook for restricting West Nile virus infection. *Viruses* 5, 2643-2658.
- Racine, R., and Winslow, G.M. (2009). IgM in microbial infections: taken for granted? *Immunol Lett* 125, 79-85.
- Raghavan, M., Chen, M.Y., Gastinel, L.N., and Bjorkman, P.J. (1994). Investigation of the interaction between the class I MHC-related Fc receptor and its immunoglobulin G ligand. *Immunity* 1, 303-315.
- Rasmussen, S.A., Jamieson, D.J., Honein, M.A., and Petersen, L.R. (2016). Zika Virus and Birth Defects--Reviewing the Evidence for Causality. *N Engl J Med* 374, 1981-1987.
- Rastogi, M., Sharma, N., and Singh, S.K. (2016). Flavivirus NS1: a multifaceted enigmatic viral protein. *Virol J* 13, 131.
- Rathore, A.P.S., Saron, W.A.A., Lim, T., Jahan, N., and St John, A.L. (2019). Maternal immunity and antibodies to dengue virus promote infection and Zika virus-induced microcephaly in fetuses. *Sci Adv* 5, eaav3208.
- Reagan-Steiner, S., Simeone, R., Simon, E., Bhatnagar, J., Oduyebo, T., Free, R., Denison, A.M., Rabeneck, D.B., Ellington, S., Petersen, E., *et al.* (2017). Evaluation of Placental and Fetal Tissue Specimens for Zika Virus Infection - 50 States and District of Columbia, January-December, 2016. *MMWR Morb Mortal Wkly Rep* 66, 636-643.
- Retallack, H., Di Lullo, E., Arias, C., Knopp, K.A., Laurie, M.T., Sandoval-Espinosa, C., Mancia Leon, W.R., Krencik, R., Ullian, E.M., Spatazza, J., *et al.* (2016). Zika virus cell tropism in the developing human brain and inhibition by azithromycin. *Proc Natl Acad Sci U S A* 113, 14408-14413.
- Reyes, L., and Golos, T.G. (2018). Hofbauer Cells: Their Role in Healthy and Complicated Pregnancy. *Front Immunol* 9, 2628.
- Reyes, L., Wolfe, B., and Golos, T. (2017). Hofbauer Cells: Placental Macrophages of Fetal Origin. *Results Probl Cell Differ* 62, 45-60.
- Reyes, Y., Bowman, N.M., Becker-Dreps, S., Centeno, E., Collins, M.H., Liou, G.A., and Bucardo, F. (2019). Prolonged Shedding of Zika Virus RNA in Vaginal Secretions, Nicaragua. *Emerg Infect Dis* 25, 808-810.
- Ribeiro, C.F., Lopes, V.G., Brasil, P., Coelho, J., Muniz, A.G., and Nogueira, R.M. (2013). Perinatal transmission of dengue: a report of 7 cases. *J Pediatr* 163, 1514-1516.
- Ribeiro, C.F., Lopes, V.G.S., Brasil, P., Pires, A.R.C., Rohloff, R., and Nogueira, R.M.R. (2017). Dengue infection in pregnancy and its impact on the placenta. *Int J Infect Dis* 55, 109-112.
- Ribeiro, G.S., Hamer, G.L., Diallo, M., Kitron, U., Ko, A.I., and Weaver, S.C. (2020). Influence of herd immunity in the cyclical nature of arboviruses. *Curr Opin Virol* 40, 1-10.
- Rice, M.E., Galang, R.R., Roth, N.M., Ellington, S.R., Moore, C.A., Valencia-Prado, M., Ellis, E.M., Tufa, A.J., Taulung, L.A., Alfred, J.M., *et al.* (2018). Vital Signs: Zika-Associated Birth Defects and Neurodevelopmental Abnormalities Possibly Associated with Congenital Zika Virus Infection - U.S. Territories and Freely Associated States, 2018. *MMWR Morb Mortal Wkly Rep* 67, 858-867.

- Richner, J.M., Himansu, S., Dowd, K.A., Butler, S.L., Salazar, V., Fox, J.M., Julander, J.G., Tang, W.W., Shresta, S., Pierson, T.C., *et al.* (2017). Modified mRNA Vaccines Protect against Zika Virus Infection. *Cell* **169**, 176.
- Robbiani, D.F., Olsen, P.C., Costa, F., Wang, Q., Oliveira, T.Y., Nery, N., Jr., Aromolaran, A., do Rosario, M.S., Sacramento, G.A., Cruz, J.S., *et al.* (2019). Risk of Zika microcephaly correlates with features of maternal antibodies. *J Exp Med*.
- Robbins, J.R., and Bakardjiev, A.I. (2012). Pathogens and the placental fortress. *Curr Opin Microbiol* **15**, 36-43.
- Robbins, J.R., Skrzypczynska, K.M., Zeldovich, V.B., Kapidzic, M., and Bakardjiev, A.I. (2010). Placental syncytiotrophoblast constitutes a major barrier to vertical transmission of *Listeria monocytogenes*. *PLoS Pathog* **6**, e1000732.
- Rodenhuis-Zybert, I.A., da Silva Voorham, J.M., Torres, S., van de Pol, D., and Smit, J.M. (2015). Antibodies against immature virions are not a discriminating factor for dengue disease severity. *PLoS Negl Trop Dis* **9**, e0003564.
- Rodriguez-Madoz, J.R., Bernal-Rubio, D., Kaminski, D., Boyd, K., and Fernandez-Sesma, A. (2010). Dengue virus inhibits the production of type I interferon in primary human dendritic cells. *J Virol* **84**, 4845-4850.
- Roehrig, J.T., Nash, D., Maldin, B., Labowitz, A., Martin, D.A., Lanciotti, R.S., and Campbell, G.L. (2003). Persistence of virus-reactive serum immunoglobulin m antibody in confirmed west nile virus encephalitis cases. *Emerg Infect Dis* **9**, 376-379.
- Rogers, T.F., Goodwin, E.C., Briney, B., Sok, D., Beutler, N., Strubel, A., Nedellec, R., Le, K., Brown, M.E., Burton, D.R., *et al.* (2017). Zika virus activates de novo and cross-reactive memory B cell responses in dengue-experienced donors. *Sci Immunol* **2**.
- Rosenberg, A.Z., Yu, W., Hill, D.A., Reyes, C.A., and Schwartz, D.A. (2017). Placental Pathology of Zika Virus: Viral Infection of the Placenta Induces Villous Stromal Macrophage (Hofbauer Cell) Proliferation and Hyperplasia. *Arch Pathol Lab Med* **141**, 43-48.
- Sa-Ngasang, A., Anantapreecha, S., A, A.N., Chanama, S., Wibulwattanakij, S., Pattanakul, K., Sawanpanyalert, P., and Kurane, I. (2006). Specific IgM and IgG responses in primary and secondary dengue virus infections determined by enzyme-linked immunosorbent assay. *Epidemiol Infect* **134**, 820-825.
- Saito, T., Owen, D.M., Jiang, F., Marcotrigiano, J., and Gale, M., Jr. (2008). Innate immunity induced by composition-dependent RIG-I recognition of hepatitis C virus RNA. *Nature* **454**, 523-527.
- Sassetti, M., Ze-Ze, L., Franco, J., Cunha, J.D., Gomes, A., Tome, A., and Alves, M.J. (2018). First case of confirmed congenital Zika syndrome in continental Africa. *Trans R Soc Trop Med Hyg* **112**, 458-462.
- Schlieffsteiner, C., Peinhaupt, M., Kopp, S., Logl, J., Lang-Olip, I., Hiden, U., Heinemann, A., Desoye, G., and Wadsack, C. (2017). Human Placental Hofbauer Cells Maintain an Anti-inflammatory M2 Phenotype despite the Presence of Gestational Diabetes Mellitus. *Front Immunol* **8**, 888.
- Schmid, M.A., and Harris, E. (2014). Monocyte recruitment to the dermis and differentiation to dendritic cells increases the targets for dengue virus replication. *PLoS Pathog* **10**, e1004541.
- Schneider, W.M., Chevillotte, M.D., and Rice, C.M. (2014). Interferon-stimulated genes: a complex web of host defenses. *Annu Rev Immunol* **32**, 513-545.
- Schnell, G., Loo, Y.-M., Marcotrigiano, J., and Gale, M. (2012). Uridine Composition of the Poly-U/UC Tract of HCV RNA Defines Non-Self Recognition by RIG-I. *PLoS Pathogens* **8**.
- Serman, T.M., and Gack, M.U. (2019). Evasion of Innate and Intrinsic Antiviral Pathways by the Zika Virus. *Viruses* **11**.
- Seval, Y., Korgun, E.T., and Demir, R. (2007). Hofbauer cells in early human placenta: possible implications in vasculogenesis and angiogenesis. *Placenta* **28**, 841-845.

- Shapiro-Mendoza, C.K., Rice, M.E., Galang, R.R., Fulton, A.C., VanMaldeghem, K., Prado, M.V., Ellis, E., Anesi, M.S., Simeone, R.M., Petersen, E.E., *et al.* (2017). Pregnancy Outcomes After Maternal Zika Virus Infection During Pregnancy - U.S. Territories, January 1, 2016-April 25, 2017. *MMWR Morb Mortal Wkly Rep* 66, 615-621.
- Sharma, N., Kumawat, K.L., Rastogi, M., Basu, A., and Singh, S.K. (2016). Japanese Encephalitis Virus exploits the microRNA-432 to regulate the expression of Suppressor of Cytokine Signaling (SOCS) 5. *Sci Rep* 6, 27685.
- Shim, B.S., Kwon, Y.C., Ricciardi, M.J., Stone, M., Otsuka, Y., Berri, F., Kwal, J.M., Magnani, D.M., Jackson, C.B., Richard, A.S., *et al.* (2019). Zika Virus-Immune Plasmas from Symptomatic and Asymptomatic Individuals Enhance Zika Pathogenesis in Adult and Pregnant Mice. *mBio* 10.
- Silen, M.L., Firpo, A., Morgello, S., Lowry, S.F., and Francus, T. (1989). Interleukin-1 alpha and tumor necrosis factor alpha cause placental injury in the rat. *Am J Pathol* 135, 239-244.
- Silva, M.C., Guerrero-Plata, A., Gilfoy, F.D., Garofalo, R.P., and Mason, P.W. (2007). Differential activation of human monocyte-derived and plasmacytoid dendritic cells by West Nile virus generated in different host cells. *J Virol* 81, 13640-13648.
- Simister, N.E. (1998). Human placental Fc receptors and the trapping of immune complexes. *Vaccine* 16, 1451-1455.
- Simister, N.E., and Story, C.M. (1997). Human placental Fc receptors and the transmission of antibodies from mother to fetus. *J Reprod Immunol* 37, 1-23.
- Simister, N.E., Story, C.M., Chen, H.L., and Hunt, J.S. (1996). An IgG-transporting Fc receptor expressed in the syncytiotrophoblast of human placenta. *Eur J Immunol* 26, 1527-1531.
- Sirohi, D., Chen, Z., Sun, L., Klose, T., Pierson, T.C., Rossmann, M.G., and Kuhn, R.J. (2016). The 3.8 Å resolution cryo-EM structure of Zika virus. *Science* 352, 467-470.
- Sirois, P.A., Pridjian, G., McRae, S., Hinckley, A.F., Rasmussen, S.A., Kissinger, P., Buekens, P., Hayes, E.B., O'Leary, D.R., Swan, K.F., *et al.* (2014). Developmental outcomes in young children born to mothers with West Nile illness during pregnancy. *Birth Defects Res A Clin Mol Teratol* 100, 792-796.
- Smith, K.G., and Clatworthy, M.R. (2010). FcγRIIB in autoimmunity and infection: evolutionary and therapeutic implications. *Nat Rev Immunol* 10, 328-343.
- Sridhar, S., Luedtke, A., Langevin, E., Zhu, M., Bonaparte, M., Machabert, T., Savarino, S., Zambrano, B., Moureau, A., Khromava, A., *et al.* (2018). Effect of Dengue Serostatus on Dengue Vaccine Safety and Efficacy. *N Engl J Med* 379, 327-340.
- Stettler, K., Beltramello, M., Espinosa, D.A., Graham, V., Cassotta, A., Bianchi, S., Vanzetta, F., Minola, A., Jaconi, S., Mele, F., *et al.* (2016). Specificity, cross-reactivity, and function of antibodies elicited by Zika virus infection. *Science* 353, 823-826.
- Stoermer, K.A., and Morrison, T.E. (2011). Complement and viral pathogenesis. *Virology* 411, 362-373.
- Story, C.M., Mikulska, J.E., and Simister, N.E. (1994). A major histocompatibility complex class I-like Fc receptor cloned from human placenta: possible role in transfer of immunoglobulin G from mother to fetus. *J Exp Med* 180, 2377-2381.
- Suthar, M.S., Brassil, M.M., Blahnik, G., and Gale, M., Jr. (2012a). Infectious clones of novel lineage 1 and lineage 2 West Nile virus strains WNV-TX02 and WNV-Madagascar. *J Virol* 86, 7704-7709.
- Suthar, M.S., Diamond, M.S., and Gale, M., Jr. (2013). West Nile virus infection and immunity. *Nature reviews Microbiology* 11, 115-128.
- Suthar, M.S., Ma, D.Y., Thomas, S., Lund, J.M., Zhang, N., Daffis, S., Rudensky, A.Y., Bevan, M.J., Clark, E.A., Kaja, M.K., *et al.* (2010). IPS-1 is essential for the control of West Nile virus infection and immunity. *PLoS Pathog* 6, e1000757.

- Suthar, M.S., Ramos, H.J., Brassil, M.M., Netland, J., Chappell, C.P., Blahnik, G., McMillan, A., Diamond, M.S., Clark, E.A., Bevan, M.J., *et al.* (2012b). The RIG-I-like receptor LGP2 controls CD8(+) T cell survival and fitness. *Immunity* 37, 235-248.
- Tabata, T., Petitt, M., Puerta-Guardo, H., Michlmayr, D., Harris, E., and Pereira, L. (2018). Zika Virus Replicates in Proliferating Cells in Explants From First-Trimester Human Placentas, Potential Sites for Dissemination of Infection. *J Infect Dis* 217, 1202-1213.
- Tabata, T., Petitt, M., Puerta-Guardo, H., Michlmayr, D., Wang, C., Fang-Hoover, J., Harris, E., and Pereira, L. (2016). Zika Virus Targets Different Primary Human Placental Cells, Suggesting Two Routes for Vertical Transmission. *Cell Host Microbe* 20, 155-166.
- Takada, A., Feldmann, H., Ksiazek, T.G., and Kawaoka, Y. (2003). Antibody-dependent enhancement of Ebola virus infection. *J Virol* 77, 7539-7544.
- Tanabe, Y., Nishibori, T., Su, L., Arduini, R.M., Baker, D.P., and David, M. (2005). Role of STAT1, STAT3, and STAT5 in IFN- α Responses in T Lymphocytes. *The Journal of Immunology* 174, 609-613.
- Tang, H., Hammack, C., Ogden, S.C., Wen, Z., Qian, X., Li, Y., Yao, B., Shin, J., Zhang, F., Lee, E.M., *et al.* (2016). Zika Virus Infects Human Cortical Neural Progenitors and Attenuates Their Growth. *Cell Stem Cell* 18, 587-590.
- Taylor, A., Foo, S.S., Bruzzone, R., Dinh, L.V., King, N.J., and Mahalingam, S. (2015). Fc receptors in antibody-dependent enhancement of viral infections. *Immunol Rev* 268, 340-364.
- Teixeira, F.M.E., Pietrobon, A.J., Oliveira, L.M., Oliveira, L., and Sato, M.N. (2020). Maternal-Fetal Interplay in Zika Virus Infection and Adverse Perinatal Outcomes. *Front Immunol* 11, 175.
- Toniolo, P.A., Liu, S., Yeh, J.E., Moraes-Vieira, P.M., Walker, S.R., Vafaizadeh, V., Barbuto, J.A., and Frank, D.A. (2015). Inhibiting STAT5 by the BET bromodomain inhibitor JQ1 disrupts human dendritic cell maturation. *J Immunol* 194, 3180-3190.
- Toth, F.D., Mosborg-Petersen, P., Kiss, J., Aboagye-Mathiesen, G., Zdravkovic, M., Hager, H., Aranyosi, J., Lampe, L., and Ebbesen, P. (1994). Antibody-dependent enhancement of HIV-1 infection in human term syncytiotrophoblast cells cultured in vitro. *Clin Exp Immunol* 96, 389-394.
- Toti, P., Arcuri, F., Tang, Z., Schatz, F., Zambrano, E., Mor, G., Niven-Fairchild, T., Abrahams, V.M., Krikun, G., Lockwood, C.J., *et al.* (2011). Focal increases of fetal macrophages in placentas from pregnancies with histological chorioamnionitis: potential role of fibroblast monocyte chemotactic protein-1. *Am J Reprod Immunol* 65, 470-479.
- Tsai, T.T., Chuang, Y.J., Lin, Y.S., Chang, C.P., Wan, S.W., Lin, S.H., Chen, C.L., and Lin, C.F. (2014). Antibody-dependent enhancement infection facilitates dengue virus-regulated signaling of IL-10 production in monocytes. *PLoS Negl Trop Dis* 8, e3320.
- Tzaban, S., Massol, R.H., Yen, E., Hamman, W., Frank, S.R., Lapierre, L.A., Hansen, S.H., Goldenring, J.R., Blumberg, R.S., and Lencer, W.I. (2009). The recycling and transcytotic pathways for IgG transport by FcRn are distinct and display an inherent polarity. *J Cell Biol* 185, 673-684.
- Ubol, S., Phuklia, W., Kalayanarooj, S., and Modhiran, N. (2010). Mechanisms of immune evasion induced by a complex of dengue virus and preexisting enhancing antibodies. *J Infect Dis* 201, 923-935.
- van der Linden, V., Pessoa, A., Dobyns, W., Barkovich, A.J., Junior, H.V., Filho, E.L., Ribeiro, E.M., Leal, M.C., Coimbra, P.P., Aragao, M.F., *et al.* (2016). Description of 13 Infants Born During October 2015-January 2016 With Congenital Zika Virus Infection Without Microcephaly at Birth - Brazil. *MMWR Morb Mortal Wkly Rep* 65, 1343-1348.
- Van Rompay, K.K.A., Coffey, L.L., Kapoor, T., Gazumyan, A., Keesler, R.I., Jurado, A., Peace, A., Agudelo, M., Watanabe, J., Usachenko, J., *et al.* (2020). A combination of two human

- monoclonal antibodies limits fetal damage by Zika virus in macaques. *Proc Natl Acad Sci U S A* *117*, 7981-7989.
- Vaughn, D.W., Green, S., Kalayanarooj, S., Innis, B.L., Nimmannitya, S., Suntayakorn, S., Endy, T.P., Raengsakulrach, B., Rothman, A.L., Ennis, F.A., *et al.* (2000). Dengue viremia titer, antibody response pattern, and virus serotype correlate with disease severity. *J Infect Dis* *181*, 2-9.
- Vazquez, S., Cabezas, S., Perez, A.B., Pupo, M., Ruiz, D., Calzada, N., Bernardo, L., Castro, O., Gonzalez, D., Serrano, T., *et al.* (2007). Kinetics of antibodies in sera, saliva, and urine samples from adult patients with primary or secondary dengue 3 virus infections. *Int J Infect Dis* *11*, 256-262.
- Wahala, W.M., and Silva, A.M. (2011). The human antibody response to dengue virus infection. *Viruses* *3*, 2374-2395.
- Wang, J.P., Liu, P., Latz, E., Golenbock, D.T., Finberg, R.W., and Libraty, D.H. (2006). Flavivirus activation of plasmacytoid dendritic cells delineates key elements of TLR7 signaling beyond endosomal recognition. *J Immunol* *177*, 7114-7121.
- Watanabe, S., Itoh, T., and Arai, K. (1996). JAK2 is essential for activation of c-fos and c-myc promoters and cell proliferation through the human granulocyte-macrophage colony-stimulating factor receptor in BA/F3 cells. *J Biol Chem* *271*, 12681-12686.
- Weflen, A.W., Baier, N., Tang, Q.J., Van den Hof, M., Blumberg, R.S., Lencer, W.I., and Massol, R.H. (2013). Multivalent immune complexes divert FcRn to lysosomes by exclusion from recycling sorting tubules. *Mol Biol Cell* *24*, 2398-2405.
- Wheeler, A.C., Ventura, C.V., Ridenour, T., Toth, D., Nobrega, L.L., Silva de Souza Dantas, L.C., Rocha, C., Bailey, D.B., Jr., and Ventura, L.O. (2018). Skills attained by infants with congenital Zika syndrome: Pilot data from Brazil. *PLoS One* *13*, e0201495.
- Wichmann, O., Gascon, J., Schunk, M., Puente, S., Siikamaki, H., Gjorup, I., Lopez-Velez, R., Clerinx, J., Peyerl-Hoffmann, G., Sundoy, A., *et al.* (2007). Severe dengue virus infection in travelers: risk factors and laboratory indicators. *J Infect Dis* *195*, 1089-1096.
- Widman, D.G., Young, E., Nivarthi, U., Swanstrom, J.A., Royal, S.R., Yount, B.L., Debbink, K., Begley, M., Marcet, S., Durbin, A., *et al.* (2017). Transplantation of a quaternary structure neutralizing antibody epitope from dengue virus serotype 3 into serotype 4. *Sci Rep* *7*, 17169.
- Wilson, J.R., de Sessions, P.F., Leon, M.A., and Scholle, F. (2008). West Nile virus nonstructural protein 1 inhibits TLR3 signal transduction. *J Virol* *82*, 8262-8271.
- World Health Organization (2019). Zika Epidemiology Update
- Wrarmert, J., Koutsonanos, D., Li, G.M., Edupuganti, S., Sui, J., Morrissey, M., McCausland, M., Skountzou, I., Hornig, M., Lipkin, W.I., *et al.* (2011). Broadly cross-reactive antibodies dominate the human B cell response against 2009 pandemic H1N1 influenza virus infection. *J Exp Med* *208*, 181-193.
- Wrarmert, J., Onlamoon, N., Akondy, R.S., Perng, G.C., Polsrila, K., Chandele, A., Kwissa, M., Pulendran, B., Wilson, P.C., Wittawatmongkol, O., *et al.* (2012). Rapid and massive virus-specific plasmablast responses during acute dengue virus infection in humans. *J Virol* *86*, 2911-2918.
- Wu, Y., Liu, Q., Zhou, J., Xie, W., Chen, C., Wang, Z., Yang, H., and Cui, J. (2017). Erratum: Zika virus evades interferon-mediated antiviral response through the co-operation of multiple nonstructural proteins in vitro. *Cell Discov* *3*, 17014.
- Xiao, W., Ando, T., Wang, H.Y., Kawakami, Y., and Kawakami, T. (2010). Lyn- and PLC-beta3-dependent regulation of SHP-1 phosphorylation controls Stat5 activity and myelomonocytic leukemia-like disease. *Blood* *116*, 6003-6013.
- Xie, X., Kum, D.B., Xia, H., Luo, H., Shan, C., Zou, J., Muruato, A.E., Medeiros, D.B.A., Nunes, B.T.D., Dallmeier, K., *et al.* (2018). A Single-Dose Live-Attenuated Zika Virus Vaccine with

- Controlled Infection Rounds that Protects against Vertical Transmission. *Cell Host Microbe* 24, 487-499 e485.
- Xu, K., Song, Y., Dai, L., Zhang, Y., Lu, X., Xie, Y., Zhang, H., Cheng, T., Wang, Q., Huang, Q., *et al.* (2018). Recombinant Chimpanzee Adenovirus Vaccine AdC7-M/E Protects against Zika Virus Infection and Testis Damage. *J Virol* 92.
- Xu, Z., Zan, H., Pone, E.J., Mai, T., and Casali, P. (2012). Immunoglobulin class-switch DNA recombination: induction, targeting and beyond. *Nat Rev Immunol* 12, 517-531.
- Yockey, L.J., Jurado, K.A., Arora, N., Millet, A., Rakib, T., Milano, K.M., Hastings, A.K., Fikrig, E., Kong, Y., Horvath, T.L., *et al.* (2018). Type I interferons instigate fetal demise after Zika virus infection. *Sci Immunol* 3.
- Yockey, L.J., Varela, L., Rakib, T., Khoury-Hanold, W., Fink, S.L., Stutz, B., Szigeti-Buck, K., Van den Pol, A., Lindenbach, B.D., Horvath, T.L., *et al.* (2016). Vaginal Exposure to Zika Virus during Pregnancy Leads to Fetal Brain Infection. *Cell* 166, 1247-1256 e1244.
- Yu, C.L., Jin, Y.J., and Burakoff, S.J. (2000). Cytosolic tyrosine dephosphorylation of STAT5. Potential role of SHP-2 in STAT5 regulation. *J Biol Chem* 275, 599-604.
- Zeldovich, V.B., Clausen, C.H., Bradford, E., Fletcher, D.A., Maltepe, E., Robbins, J.R., and Bakardjiev, A.I. (2013). Placental syncytium forms a biophysical barrier against pathogen invasion. *PLoS Pathog* 9, e1003821.
- Zimmerman, M.G., Bowen, J.R., McDonald, C.E., Pulendran, B., and Suthar, M.S. (2019a). West Nile Virus Subverts T Cell Stimulatory Capacity of Human Dendritic Cells. *bioRxiv*.
- Zimmerman, M.G., Bowen, J.R., McDonald, C.E., Young, E., Baric, R.S., Pulendran, B., and Suthar, M.S. (2019b). STAT5: a Target of Antagonism by Neurotropic Flaviviruses. *J Virol* 93.
- Zimmerman, M.G., Quicke, K.M., O'Neal, J.T., Arora, N., Machiah, D., Priyamvada, L., Kauffman, R.C., Register, E., Adekunle, O., Swieboda, D., *et al.* (2018). Cross-Reactive Dengue Virus Antibodies Augment Zika Virus Infection of Human Placental Macrophages. *Cell Host Microbe* 24, 731-742 e736.
- Zust, R., Toh, Y.X., Valdes, I., Cerny, D., Heinrich, J., Hermida, L., Marcos, E., Guillen, G., Kalinke, U., Shi, P.Y., *et al.* (2014). Type I interferon signals in macrophages and dendritic cells control dengue virus infection: implications for a new mouse model to test dengue vaccines. *J Virol* 88, 7276-7285.